Initial Piloted Simulation Evaluation of the Reference-H High-Speed Civil Transport Design During Takeoff and Recovery From Limit Flight Conditions

Louis J. Glaab
Lockheed Martin Engineering & Sciences Company, Hampton, Virginia

The NASA STI Program Office . . . in Profile

Since its founding, NASA has been dedicated to the advancement of aeronautics and space science. The NASA Scientific and Technical Information (STI) Program Office plays a key part in helping NASA maintain this important role.

The NASA STI Program Office is operated by Langley Research Center, the lead center for NASA's scientific and technical information. The NASA STI Program Office provides access to the NASA STI Database, the largest collection of aeronautical and space science STI in the world. The Program Office is also NASA's institutional mechanism for disseminating the results of its research and development activities. These results are published by NASA in the NASA STI Report Series, which includes the following report types:

- TECHNICAL PUBLICATION. Reports of completed research or a major significant phase of research that present the results of NASA programs and include extensive data or theoretical analysis. Includes compilations of significant scientific and technical data and information deemed to be of continuing reference value. NASA counterpart of peer-reviewed formal professional papers, but having less stringent limitations on manuscript length and extent of graphic presentations.

- TECHNICAL MEMORANDUM. Scientific and technical findings that are preliminary or of specialized interest, e.g., quick release reports, working papers, and bibliographies that contain minimal annotation. Does not contain extensive analysis.

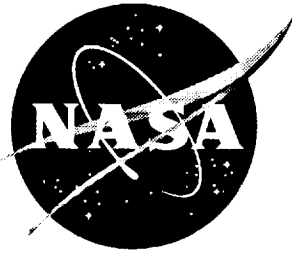- CONTRACTOR REPORT. Scientific and technical findings by NASA-sponsored contractors and grantees.

- CONFERENCE PUBLICATION. Collected papers from scientific and technical conferences, symposia, seminars, or other meetings sponsored co-sponsored by NASA.

- SPECIAL PUBLICATION. Scientific, technical, or historical information from NASA programs, projects, and mission often concerned with subjects having substantial public interest.

- TECHNICAL TRANSLATION. English language translations of foreign scienti and technical material pertinent to NASA's mission.

Specialized services that complement the STI Program Office's diverse offerings inc creating custom thesauri, building custom databases, organizing and publishing research results . . . even providing video:

For more information about the NASA ST Program Office, see the following:

- Access the NASA STI Program Home Page at *http://www.sti.nasa.gov*

- Email your question via the Internet to help@sti.nasa.gov

- Fax your question to the NASA STI Help Desk at (301) 621-0134

- Telephone the NASA STI Help Desk at (301) 621-0390

- Write to:
  NASA STI Help Desk
  NASA Center for AeroSpace Informati
  7121 Standard Drive
  Hanover, MD 21076-1320

NASA/CR-1999-209523

Initial Piloted Simulation Evaluation of the Reference-H High-Speed Civil Transport Design During Takeoff and Recovery From Limit Flight Conditions

Louis J. Glaab
Lockheed Martin Engineering & Sciences Company, Hampton, Virginia

December 1999

Summary

An initial assessment of a proposed High-Speed Civil Transport (HSCT) was conducted in the fall of 1995 at the NASA Langley Research Center. This configuration, known as the Industry Reference-H (Ref.-H), was designed by the Boeing Aircraft Company as part of their work in the High Speed Research program. It included a conventional tail, a cranked-arrow wing, four mixed-flow turbofan engines, and capacity for transporting approximately 300 passengers. The purpose of this assessment was to evaluate and quantify operational aspects of the Reference-H configuration from a pilot's perspective with the additional goal of identifying design strengths as well any potential configuration deficiencies. Results from this study are to be applied to refine the Reference-H configuration so it will serve as a reference design for future High Speed Civil Transport configurations.

This study was aimed at evaluating the Ref.-H configuration at many points of the aircraft's envelope to determine the suitability of the vehicle to accomplish typical mission profiles as well as emergency or envelope-limit conditions. Pilot-provided Cooper-Harper ratings and comments constituted the primary vehicle evaluation metric. Incidents of nacelle, tail, or wingtip ground strikes during takeoff and landing, repeated occurrence of control saturation or rate limiting during a particular task, or unfavorable propulsive influences on the vehicle's flight characteristics were also of particular interest. The analysis included simulated real-time piloted evaluations, performed in a 6 degree of freedom motion base cockpit simulator, combined with extensive batch analysis. The assessment was performed using the NASA Langley Visual-Motion Simulator and incorporated the third major release of the simulation data base (known as Ref.-H cycle 2B).

The model of the control system was based upon industry-provided control laws for the longitudinal and lateral/directional axes as well as control surface allocation and mixing logic. The control surface actuator models used in the assessment included the effect of hinge moments upon actuator dynamics. Quasi-static aeroelastic (QSE) aerodynamics were also modeled in the aerodynamic data base.

A total of five pilots completed the assessment maneuver set. They evaluated 55 different maneuvers and provided commentary on those and five additional demonstration maneuvers. Maneuvers included in the evaluation set consisted of normal operational scenarios, such as takeoffs and landings, as well as emergency conditions. Various Federal Aviation Administration mandated certification maneuvers were also included in the maneuver set.

Data recorded included Cooper-Harper ratings and comments from the 5 participating research pilots, video and audio recordings of all real-time piloted research simulation sessions, as well as real-time data for post-session analysis. A takeoff noise assessment was also conducted. The ability of the vehicle to meet its mission requirements was based on a combination of Cooper-Harper ratings combined with pilot comments, real-time data, and batch analysis of the vehicle.

This report documents results from a sub-set of the evaluation maneuvers which dealt with takeoff and recovery from low-speed limit flight tasks. A total of 11 maneuvers were contained in this maneuver sub-set. Results are summarized regarding the Reference-H configuration's ability to perform all aspects of the maneuvers evaluated.

Results indicate that the Reference-H configuration exhibited satisfactory stability and control over most of the operational envelope considered in this report. Only minor deficiencies were encountered for the takeoff maneuvers considered. However, some significant potential short comings of the configuration were apparent for the recovery from limit flight tasks. These inadequacies involved nose-down pitch control authority and several aspects of lateral/directional stability and control. Other results of the assessment include a demonstration of a decrease in runway environment noise if a programmed lapse rate takeoff maneuver was employed in which

throttles and flaps are automatically reconfigured. No problems were encountered performing either the standard or advanced noise-abatement procedures.

Introduction

An initial assessment of a proposed High-Speed Civil Transport (HSCT) configuration was conducted in the fall of 1995 at the NASA Langley Research Center. The configuration, known as the Industry Reference H (Ref.-H), included a conventional aft-tail, a cranked-arrow wing, four mixed-flow turbofan engines, and capacity for approximately 300 passengers. The assessment was performed by five pilots who evaluated 55 different maneuvers and provided commentary on those and five additional demonstration maneuvers. The maneuvers chosen for evaluation included the more demanding emergency-type maneuvers, such as emergency descents, engine failure scenarios, and stalls, as well as routine maneuvers such as takeoffs, climbs, turns, descents, and approaches and landings. The purpose of the assessment was to evaluate and quantify operational aspects of the Reference-H configuration from a pilot's perspective with the additional goal of identifying potential configuration deficiencies, rather than to critique a particular control, display, or guidance concept. Results from this study are to be applied to refine the Reference-H configuration so it will serve as a reference design for future High Speed Civil Transport configurations. Operational aspects of the configuration were assessed and quantified through a combination of Cooper-Harper pilot ratings and comments combined with real-time data and extensive batch analysis. Identifying potential configuration deficiencies were of primary concern, rather than to critique a particular control, display, or guidance concept. While the flight dynamics of the simulated vehicle were inextricably linked with aspects of the control system, the evaluation pilots were urged, to the best of their ability, to look beyond the present development level of the flight control laws and to identify deficiencies associated with the vehicle aerodynamics, control surfaces, and landing gear configuration. For this reason, incidents of nacelle, tail, or wingtip ground strikes during takeoff and landing, repeated occurrence of control saturation or rate limiting during a particular task, or unfavorable propulsive influences on the vehicle's flight characteristics were of particular interest.

The assessment was completed using the third major release of the simulation data (known as Ref.-H cycle 2B). This simulation data-base included detailed models of the Ref.-H aerodynamics, mass and inertia, landing gear, control system elements, and propulsion systems. The aerodynamics model included the effects of airframe bending under flight loads (quasi-static aeroelastic effects). Although the Cycle-2B data-base represented the latest most comprehensive representation of the Ref.-H vehicle, several modifications were incorporated to improve and enhance the value of the current study. These modifications included improvements in low-speed lateral/directional stability parameters as well as enhanced tire cornering and engine failure models.

The control system employed was based upon industry-provided control laws for the longitudinal and lateral/directional axes as well as control surface allocation and mixing logic. It was the latest release of the candidate control systems, which are undergoing continuous development. The control surface actuator models used in the assessment included the effect of hinge moments upon actuator dynamics.

This report documents results from a sub-set of the evaluation maneuvers which dealt with takeoff and recovery from low-speed limit flight tasks. A total of 11 maneuvers were contained in this maneuver sub-set. Results are summarized regarding the Reference-H configuration's ability to perform all aspects of the maneuvers evaluated.

Symbols and Abbreviations

α Aircraft angle of attack, degrees, positive nose up

β Aircraft sideslip angle, degrees, positive nose left

$C_{l\beta}$	Body-axis lateral stability derivative	r	Body axis yaw rate, positive nose right, deg/sec
$C_{n\beta}$	Body-axis directional stability derivative	SX_{OBS}	Distance aircraft traveled from brake release to climbing to an altitude of 35 feet
$C_{l\delta_a}$	Rolling moment due to aileron deflection	SX_{LO}	Distance aircraft traveled from brake release to lift-off, feet
$C_{n\delta_a}$	Yawing moment due to aileron deflection	tmu	Landing gear tire sideforce coefficient of friction
δ_e	Elevator deflection, positive trailing-edge down, degrees	T_{rot}	Time when aircraft reached rotation speed, sec.
δ_h	Horizontal tail deflection, positive trailing-edge down, degrees	V	Commanded velocity, kts.
$\dot{\gamma}$	Commanded rate of change of flight path angle, deg/sec	V_{mcg}	Minimum control speed on ground, kts.
I_{xx}	Body x-axis aircraft moment of inertia, slug-ft^2	V_1	Takeoff decision speed, kts.
I_{xz}	Body axis product of inertia, slug-ft^2	V_2	Engine out safety speed, kts.
I_{zz}	Body z-axis aircraft moment of inertia, slug-ft^2	V_{35}	Speed at obstacle height, kts.
M	Mach number	V_c	Commanded climb speed, kts.
p	Body axis roll rate, deg/sec, positive right wing down	V_{ef}	Engine failure, kts.
q	Body axis pitch rate, deg/sec, positive nose up	$V_{dot\ inertial}$	Inertial rate of acceleration, kts.
Q_{dot}	Pitch rate acceleration, positive nose-up, degrees/sec^2	V_{lo}	Lift-off speed, kts.
θ_{max}	Maximum pitch attitude achieved before lift-off	$V_{min-dem}$	Minimum required demonstration speed, kts.
		V_{mu}	Minimum un-stick speed, kts.
R	Tire load divided by tire rated load	V_r	Takeoff rotation speed, kts.

Equations

$C_{n\beta}$-dynamic:

$$C_{n_{\beta_{dyn}}} = C_{n_\beta} * \cos(\alpha) - (I_z / I_x) * C_{l_\beta} * \sin(\alpha)$$

LCDP:

$$LCDP = (C_{n_\beta} + (I_{xz} / I_x) * C_{l_\beta}) - (C_{l_\beta}$$
$$+ (I_{xz} / I_x) * C_{n_\beta}) * \{NUM / DENOM\}$$
where:
$$NUM = C_{n_{\delta_a}} + (I_{xz} / I_x) * C_{l_{\delta_a}}$$
$$DENOM = C_{l_{\delta_a}} + (I_{xz} / I_x) * C_{n_{\delta_a}}$$

Abbreviations

AEO	All Engines Operating condition
ALT	Altitude of CG above ground level, ft
ALTLG	Altitude of landing gear above ground level, ft
ANOPP	Aircraft Noise Prediction Program
ARI	Aileron to Rudder Interconnect
CGI	Computer Generated Image
CHR	Cooper-Harper Rating
C.L.	Centerline noise, units are EPNdB
CRT	Cathode ray tube display
DAC	Digital to Analog Converter
DCPILOT	Pilot's longitudinal stick input, fraction of max.
DELEV	Elevator deflection, positive trailing-edge down, degrees
DRUD	Combined rudder deflection of all three segments, positive trailing-edge left, degrees
EADI	Electronic Attitude Director Indicator
EPNdB	Effective Perceived Noise Level, dB
FAA	Federal Aviation Administration
FAR	Federal Aviation Regulation
GW	Gross weight
HQ	Handling Quality Ratings
HSCT	High Speed Civil Transport
HSI	Horizontal situation indicator
HUD	Heads Up Display
IAS	Indicated airspeed, kts.
LaRC	Langley Research Center
lef	Symmetric leading-edge flap deflection, positive down, degrees
LCDP	Lateral Control Divergence Parameter
M13	Mass case M13 (GW=649,914 lbs)
MFC	Mass MFC (GW=384,862 lbs)
MFTF	Mixed Flow Turbo Fan
NASA	National Aeronautics and Space Administration
OEO	One Engine Out condition
PCFN #4	Percent net thrust of left-outboard engine
PF	Pilot Flying

PIO	Pilot Induced Oscillation
PLR	Program Lapse Rate
PNF	Pilot Not Flying
RHA	Reference-H assessment
QERR	Pitch rate error, deg/sec
QSE	Quasi-static aeroelastic aerodynamic modeling
RFLF	Recovery From Limit Flight
RTO	Rejected Takeoff
SDB	Structural Dynamics Branch
S.L.	Sideline noise, units are EPNdB
tef	Symmetric trailing-edge flap deflection, positive down, degrees
TOFL	Takeoff filed length, feet.
QSE	Quasi-Static Elastic

Cockpit Simulator

The current investigation was performed using the Langley Visual Motion Simulator (VMS), which is a hydraulically operated, 6-legged synergistic motion base cockpit simulator (see Figure 1). Six computed leg positions were used to drive the motion base. The transformation equations used to compute the leg extensions, the filter characteristics used to smooth the computed drive signals from the DAC outputs, and the performance limits of the VMS are given in references ref 1 and ref 2. The washout system used to present the motion-cue commands to the motion base was the coordinated adaptive washout of references ref 3 and ref 4 with some adjustment of the parameter values to improve base response for this study.

The interior of the simulator was configured to be that of a transport with typical pilot information displays found in current transport type aircraft. A CGI system generated the out-of-the-window visual scenes which were displayed to the pilots using color monitors viewed through beam splitters and infinity optics mirrors. Forward and side window views were generated using this system. Both the pilot and copilot were provided duplicate sets of heads-down pilot information displays, which included an EADI, HSI and engine data displays. They were presented to the pilot and copilot using a total of six standard CRT devices mounted symmetrically in the instrument panel. The HUD was the primary instrument used for the takeoff procedure with the EADI providing additional auxiliary information. The HUD image was presented to the pilot and copilot through the use of a video mixer, which combined the HUD image and forward CGI view to produce a combined image. The combined image was then displayed on the forward window view. Other traditional round dial mechanical instruments were also employed in this study and included pressure altitude, vertical speed, and turn rate and side-slip indicators. The total instrumentation provided to the pilot on the instrument panel is shown in Figure 2. The pilot's controls consisted of a side-stick controller, rudder pedals, and engine throttle levers.

The Ref.-H mathematics model was driven by a real-time digital simulation system using a Convex computer. The dynamics of the simulated airplane were calculated using six-degree-of-freedom nonlinear equations of motion and were computed at an iteration rate of 80 frames per second.

Control laws

The simulation model used in the RHA test employed custom-designed control systems that featured flight-path rate command/flight-path and airspeed hold (gamma-dot/V, or $\dot{\gamma}/V$) in the longitudinal axis, and a roll rate/sideslip command and bank angle hold system in the lateral-directional axes (p/β). These systems were developed by Boeing and McDonnell-Douglas, respectively, as part of their work in the HSR program and were implemented in the Langley simulation model. These control laws were designed to provide (1)

5

stabilization and control authority over several flight regimes and (2) rudimentary autoflap/autothrottle capability sufficient to perform the various tasks in the RHA tests. Since these control systems can not necessarily reflect the ultimate final control law set selected for potential production HSCT aircraft, comments from the evaluating pilots regarding these control laws were welcomed. The pilots were reminded, however, that evaluation of these control laws was not the main focus of the RHA test. Extensive improvements that were made to the p/β control system during the NASA Ames control law downselect simulation conducted in October-November '95 were not able to be incorporated into this simulation, so the version of the lateral/directional laws used in this investigation were functional, although not fully developed. The control laws used in the piloted assessment are described in appendix B.

Simulated vehicle

The vehicle simulated is referred to as the industry standard Reference-H configuration, or Ref.-H and is illustrated in Figure 3. It was designed to transport approximately 300 passengers over a distance of 6,000 nautical miles at a cruising speed of Mach 2.4. Reference ref 5 describes the Cycle-2B data base, which was the third major data release regarding the Ref.-H vehicle. It was preceded by Cycle-1 and Cycle-2A. Each subsequent release contained information and data developed after the previous release. As such, the fidelity and value of the simulation model increased with each subsequent data release. Cycle-2B will be superseded by Cycle-3 which is due for release in mid-1996. Required modifications to the Cycle-2B data are presented below.

Selected vehicle geometric parameters, control surface definitions and mass characteristics are listed in Table 1 though Table 3, respectively. The control surface allocation strategy as well as definition of the control laws are defined in Appendix B. To summarize the control allocation strategy, the four leading-edge flaps were deployed symmetrically as camber-changing devices; half of the eight trailing-edge flaps were used

as symmetric flaps and half were used as flaperons providing both roll control and camber changing effects. Trailing-edge flap segments 1, 3, 6, and 8 where employed as flaperons and 2, 4, 5, and 7 were used only as flaps. The elevator and stabilizer segments were used as pitch control devices and commands to the elevator and stabilizer were geared in a ratio of 2:1, respectively. The rudder was separated into three segments with all three segments being driven together as one surface for this portion of the Ref.-H assessment providing directional control.

Landing gear modifications

As a result of some initial testing and evaluation of the Ref.-H simulation during cross-wind ground-handling maneuvers the amount of skid angle needed to track the runway centerline became an issue. Pilot comments indicated that the large amounts of skid angle, as much as 5 to 6 degrees in a 35 kt cross-wind with aircraft speeds above 100 kts, were unrealistic compared with the pilot's operational experience with similar aircraft and could cause problems maintaining the aircraft within the runway bounds. A modification to the cornering force model was obtained from the NASA LaRC Structural Dynamics Branch (SDB) and incorporated into the simulation model. This modification was based on extensive work performed on the Space Shuttle main gear tire model. It also included data from a candidate 50x20-20 HSCT tire tested at the NASA LaRC Landing Loads Facility.

The SDB model differed significantly from the model contained in the Ref.-H Cycle-2B release. While the Ref.-H Cycle-2B model employed a tire sideforce coefficient that was a function of aircraft speed and cornering angle, the SDB model used a tire sideforce coefficient that was a function of normal load and cornering angle. Basically the SDB model was speed insensitive while the Ref.-H Cycle-2B model was not. Also, the Ref.-H Cycle-2B model assumed that the total sideforce generated by the tire was linear in normal load at a given speed, whereas the SDB model provided a variable sideforce coefficient based on normal force.

A comparison of the sideforce coefficient for the two models is provided in Figure 4 where

sideforce coefficient is plotted against tire skid angle for various combinations of speed and tire load. For the Ref.-H configured in the M13 mass case a nominal load factor per tire is approximately 0.7 for the main centerline unit and 0.5 for the outboard main gear units. Nominal load factor, R, is the actual load on the tire divided by the rated load of the tire. In this case the rated load is 57,000 lbs. As can be seen from Figure 4, similar results are obtained from the two different models at speeds below 50 kts. This agreement rapidly deteriorates as speed is increased. Typical tire skid angles encountered during the Ref.-H assessment were about 2 degrees for the 35 kt aborted takeoff maneuver. From Figure 4 it can be seen that for an R=0.7 condition the SDB model at 150 kts and the M13 mass case specifies 2 degrees of skid angle, whereas the Ref.-H Cycle-2B model would have required a skid angle of approximately 5.0 degrees.

Aerodynamic modifications

This section provides details regarding the aerodynamic modifications to the Cycle-2B aerodynamic data-base as documented in reference ref 5 , which were implemented just prior to commencement of the piloted evaluations supporting the NASA LaRC Fall 1995 Ref.-H assessment project. All simulated research flights were performed with this aerodynamic modification selected.

As a result of performing initial batch analysis using the Ref.-H Cycle-2B aerodynamic data-base significant discrepancies between existing data obtained from the NASA LaRC 30x60 wind-tunnel (Test-71) results and the Ref.-H Cycle-2B aerodynamic data-base were identified. These discrepancies involved the low-speed lateral/directional stability derivatives, $C_{l\beta}$, and $C_{n\beta}$, as modeled in the Ref.-H Cycle-2B release.

The data used for evaluating the Cycle-2B data base were obtained from Test-71 which used a 4.6% sting mounted Ref.-H model, that was tested at a Reynolds number of approximately 1.94 million. Sting induced effects were quantified through the use of a "dummy" sting, employed during the sting interference error analysis portion of the wind-

tunnel experiment, to specifically determine the exact effect the sting mounting system had on the resulting data. Wind-tunnel blockage and wall effect magnitudes have previously been found to be of little significance due to the tunnel's large test section area as compared with the size of the model. As a result of the sting interference analysis and lack of wall effects, Test-71 data is believed to represent realistic free-air conditions.

Accurate modeling of $C_{l\beta}$, and $C_{n\beta}$ is essential in order to obtain accurate HQ ratings from a piloted simulation. Figure 5 and Figure 6 present $C_{l\beta}$, and $C_{n\beta}$ as a function of angle of attack for data from the Test-71, Cycle-2B, and Cycle-2B modified data-bases. From these figures the differences between the Test-71 and unmodified Cycle-2B data sets are apparent. The lack of agreement in $C_{l\beta}$ was caused through improper modeling of leading-edge flap deflection effects. Unmodified Cycle-2B aerodynamics did not include the affect of leading-edge flap deflection on the lateral directional stability derivatives. Also evident in Figure 5 and Figure 6 is a general lack of agreement involving $C_{n\beta}$ at higher angles of attack (i.e. angles of attack greater than 10 degrees). Since a large portion of the NASA LaRC Ref.-H assessment task list involved maneuvers with the leading-edge flaps deflected combined with the vehicle frequently maneuvering at high angles of attack, an effort was made to resolve these problems to improve the quality of the NASA LaRC Ref.-H assessment. This information was forwarded to personnel at the Boeing Aircraft Company who endeavored to develop a last-minute modification to the Cycle-2B data-base. The resulting modification was subsequently installed, evaluated, and verified in the NASA LaRC Ref.-H simulation.

As can be seen from Figure 5 and Figure 6 a distinct improvement in the agreement between the Test-71 and modified Cycle-2B data is apparent. The aerodynamic modification of the Cycle-2B data produced values of both $C_{l\beta}$ and $C_{n\beta}$ which were much closer to values predicted from the Test-71 results. The zero flap deflection $C_{n\beta}$ is very accurately reproduced by the Cycle-2B data although

7

some differences were still evident for C_{l_β}.

This data is presented to provide information regarding the basic airframe characteristics since none of the NASA LaRC Ref.-H assessment maneuvers involved sub-sonic operation with zero leading- and trailing-edge flaps. The flap deflected case is representative of the takeoff/powered approach flight condition, which is the vehicle configuration for all of Block-1, 2a, 2b, and part of Block-4 maneuvers. Matching results for this condition is obviously a high priority. As can be seen in, Figure 6 the unmodified data would have been unacceptable with values of C_{l_β} off by a factor

of 3 at angles of attack around 10 degrees. Although substantial differences still exist for C_{n_β}, the effect of the aerodynamic modification improved the aerodynamic simulation and provided a larger range of angle of attack where improved agreement exists.

Overall, the selection of the modified Cycle-2B aerodynamics enhanced the value of the NASA LaRC 1995 Ref.-H assessment project. Use of the modified Cycle-2B aerodynamics is highly recommended for any Ref.-H simulation experiments since these modifications will be incorporated into the Cycle-3 release.

Propulsion

The Ref.-H design included two mixed flow turbofan GE21/F15-A17 engines under each wing, capable of producing approximately 53,200 lb. of thrust per engine at a mass flow rate of 780 lbs/sec while operating at sea level static conditions. Each engine was equipped with a down-stream mixer nozzle with a 50% aspiration ratio. The axisymmetric engine inlet included a translating centerbody spike to adjust the location of the shock wave at cruising speeds.

The engine model included in the RHA Cycle-2B simulation allowed for varying levels of detail of engine and inlet operations. At the highest complexity level, the engine inlet simulation reacted to flight conditions that could cause an inlet unstart in supersonic flight on one or more of the four engines being simulated. In general, the inlet was sensitive to small changes in freestream velocity angles - that is, a sudden and non-trivial change in either sideslip angle or angle of attack would

cause the outboard engine inlets to unstart at cruise conditions. The RHA test explored the impact of this sensitivity; one task was designed to simulate a "ripple" unstart in which an inboard engine failure causes the neighboring outboard engine to unstart. Several engine failures in subsonic flight were also evaluated.

The outboard engines were located 31.2 feet from the centerline of the aircraft and were canted inward at 2.4 degrees and downward 3.25 degrees relative to the centerline of the aircraft. The inboard engines were located 17.4 feet from the centerline and were canted inward 1.0 degree and downward 5.7 degrees.

Engine failure modification

One minor error in the engine simulation section of the Cycle-2B data release was identified during engine-out batch analysis. This error involved the amount of thrust generated by the failed engine. A relatively small amount of positive thrust was observed for a failed engine which was not an expected result. An investigation into the anomaly revealed that the failed engine thrust results were based on data assuming the engine was operating in a normal fashion at the engine-failed mass flow rate. Since thrust was a function of mass flow rate, and other parameters, and since there was still substantial mass flow rate existing for a failed engine, a resulting positive thrust was generated.

A simplistic engine failure model was developed and incorporated into the simulation to produce more realistic amounts of thrust in the event of an engine failure. Table 4 lists the amount of engine thrust for a given Mach number and altitude. Values of thrust contained in Table 4 were similar to the ram drag values for flight-idle thrust levels specified in reference ref 5. The dynamic operation of the modified engine failure element proceeded such that at the instant an engine failure was initiated the amount thrust from the failed engine would blend from the last non-failed time step thrust level to the levels listed in Table 4 using a first order lag filter with a 1.0 second time constant.

Description of Test Procedure

Before a pilot could begin a maneuver element block a briefing was provided which detailed the objectives of that maneuver element. Rating metrics, procedures, and other salient information were included in the briefing. Actual flight cards (see Appendix C) were carried by the PNF in the cockpit. The task description and rating criteria of each flight card was provided to the pilot in a separate binder to assist the rating process. A Cooper-Harper rating scale, shown in Figure 7, was also provided to the pilot. See Appendix D for biographies of the five pilots participating in this study.

Maneuvers were flown by the individual research pilots accompanied by at least one crew member. The research engineer responsible for the development and overseeing of the particular maneuver being evaluated always occupied the right hand seat. For this study, the PNF manipulated the throttles during manual thrust operation maneuvers. The PNF also conducted the research session and recorded pilot ratings and noted some comments for reference during research sessions. A micro-cassette recorder was employed to record the pilot's comments and ratings during the rating portion of each maneuver. Tapes from the micro-cassette recorder were subsequently transcribed and reviewed. The rear cockpit jump-seat was used if a third crew-member was present to observe the test procedures. Consistent crew orientation provided increased cockpit efficiency and standardization of the resulting pilot evaluations and performance.

Each research session was limited to a maximum of 2 hours to avoid possible pilot fatigue that could be encountered during long simulation sessions. Pilot fatigue can effect pilot performance and pilot perceptions that could skew the resulting Cooper-Harper ratings as well as the quantitative results. Subject research pilots were only exposed to 2 separate research simulation sessions per day again in an effort to avoid possible pilot fatigue.

During research sessions pilots studied the flight card before attempting the selected task. The research engineer briefed him on the procedure for the selected task as well as answering any questions the pilot had. Pilots were permitted to evaluate a maneuver as many times as they wished before providing pilot ratings and comments. Most pilots usually only needed less than two or three attempts of any maneuver before they were prepared to provide Cooper-Harper ratings and pilot comments for all ratable segments. After each maneuver attempt, a "score card" was presented to the PF and PNF, using a CRT on instrument panel, to display various salient information regarding the pilot's performance. The "score card" was only visible when the simulation was in reset mode. Once the simulation was placed in operate mode the "score card" was replaced with the appropriate instrument display. The information displayed by the "score card" provided the PF and PNF with information regarding the pilot's actual performance of the maneuver, compared with the specified adequate and desired bounds listed on the flight cards, and greatly facilitated the rating process.

Presentation of Results

Results for block 1 simulation flights are presented in two main sections which are takeoff and recovery from limit flight as listed in Table 5. Each main section presents and discusses each individual maneuver in the order presented in Table 5. Information describing each maneuver is presented along with a discussion of results and a condensed version of the pilot's comments. Both main sections provide introductory information pertinent to all maneuvers in that particular section.

Section 1 - Takeoff tasks

Introduction to takeoff task maneuvers. The takeoff assessment block of maneuvers evaluated a series of normal as well as various emergency operational states. Two different noise abatement procedures were considered as well as rejected takeoffs due to engine failure and a one engine out (OEO) takeoff maneuver. Additionally, a maneuver designed to determine the minimum control speed on the ground, V_{mcg}, was included. Execution of these maneuvers permitted an evaluation of the Ref.-H vehicle in this portion of the low-speed operating envelope.

As previously stated, two different noise abatement takeoff procedures were employed in the 1995 LaRC Ref.-H assessment. One

procedure was referred to as the Standard Noise Abatement procedure (Task 2010) and is considered to be the procedure that the Ref.-H would use if it were in service today. It adheres to all safety of flight and noise abatement regulations currently established for subsonic transports. The other noise abatement procedure evaluated was referred to as the Program Lapse Rate (PLR) procedure (Task 2030) which features thrust and symmetric leading- and trailing-edge flap deflections under direct computer control. Operation of the vehicle in this manner has been identified in references ref 6 through ref 9 as a way to drastically reduce jet noise, without sacrificing flight safety. It decreases the reliance of this class of vehicle on jet noise suppressers and was included in the task list since it may be a viable noise abatement procedure at the time the Ref.-H vehicle enters service. The PLR procedure embodies several operations not currently permitted by current FAA regulations. FAA approval of automatic thrust and symmetric leading- and trailing-edge flap operation along with the ability to accelerate to and operate at 250 kts. (app. V_2+49 kts) would have to be obtained in order to include this exact maneuver in the certification process.

Engine failure emergency maneuvers included rejected takeoffs (RTO's), one engine out (OEO) continued takeoffs and the V_{mcg} demonstration maneuver. All rejected takeoff maneuvers (Tasks 1050 to 1052) simulated an engine failure just prior to reaching V_1. A cross-wind component was incorporated with the RTO maneuvers to determine if the Ref.-H vehicle had enough control authority from combined nose-gear and rudder deflection to handle this type of emergency maneuver. The OEO continued takeoff maneuver (Task 7035) simulated a takeoff with an engine failure occurring just after the aircraft had passed the decision speed, V_1. The last takeoff maneuver was the V_{mcg} demonstration maneuver, which was included to determine the minimum controllable speed on the ground with an engine failure. It assumes that no cornering forces are available from the nose gear and is required to demonstrate that the aircraft is controllable with an engine failed during the rotation portion of the maneuver. To examine the worst possible scenario, the lightest takeoff weight

was used for this maneuver which was the MFC mass case. V_{mcg} is required to occur below the specified rotation speed, V_r, for that aircraft weight. The first pilot to perform the tests sequence evaluated a series of engine failure speeds until the aircraft was just able to kept within the required limits. In this case required performance was +/- 30 ft lateral distance from the runway centerline. Once V_{mcg} was determined, all the other pilots were asked to just evaluate the maneuver at that engine failure speed.

Prior to commencement of the takeoff maneuver block a series of analysis were conducted to determine appropriate takeoff reference speeds. The aircraft was configured with leading-edge flaps set to 30 degrees and trailing-edge flaps set to 10 degrees with the M13 mass case. It was determined that a $V_1=166$ kts combined with a $V_r=174$ kts produced a balanced field length of 9,389 ft. Figure 8 presents results for an OEO takeoff and an RTO takeoff to illustrate the merit of the V_1, V_r selection. The data presented in Figure 8 are for runs which produced results that were the closest to the statistical mean for tasks 7035 and 1050. In Figure 8 altitude and airspeed are presented as a function of distance from brake release. Engine failure location and obstacle height are also indicated in the figure. As can be seen in this figure the distance required to accelerate to V_1, experience an engine failure, and then bring the aircraft to a stop was 8,831 ft. The distance required to accelerate the aircraft to V_1, experience an engine failure, and continue the takeoff to the obstacle height was 9,389 ft. The differences in distance between the RTO and OEO takeoff maneuvers was approximately equal to the distance traveled by the aircraft at the V_1 decision speed for 2 seconds, which is part of the FAA certification requirements.

Table 6 presents results of a statistical analysis calculated for all the takeoff maneuvers performed by the 5 research pilots. The mean and standard deviation of distance to lift-off (SX_{LO}), speed at lift-off (V_{lo}), pitch attitude at lift-off (θ_{max}), distance to clear a 35 ft obstacle (SX_{OBS}), speed at the obstacle (V_{35}), and the number of samples are presented for the three continued takeoff maneuvers.

Maximum pitch attitude was specified to be 11.61 degrees for fully extended main landing gears and 10.22 degrees for fully compressed main landing gears. Minimum lift-off speed, V_{mu}, was calculated to be 182 kts for the fully extended main landing gear case. FAA regulations require that lift-off speeds for the all engines operating case be $1.1 * V_{mu} = 200$ kts and $1.05 * V_{mu} = 191$ kts for the one engine out case. From Table 6 it can be seen that the requirements on minimum lift-off speed are very close to being satisfied. A slight increase of V_r or slight decrease of target pitch rate or target pitch attitude may be required. It should also be noted that pilots would frequently need to arrest the rotation rate during the OEO takeoff maneuvers to capture the designated lift-off pitch attitude, which is different than conventional takeoffs that employ a smooth, continuous pitch rotation to capture climb attitudes. V_2 is defined from the V_{35} of task 7035 and is 201 kts. From Table 6 it can be seen that the lift-off speeds for task 7035 (OEO takeoff) were lower than the other two tasks. This results because the pilots were able to achieve a higher pitch attitude before lift-off due to the lower level of acceleration of the OEO takeoff task illustrating the fact that pilots often didn't have sufficient time to rotate the aircraft to the 10.5 degrees pitch attitude, for the normal operating maneuvers, before becoming airborne. Note that the distance required to clear the 35 ft. obstacle for task 7035 defines the takeoff field length of 9,389 ft. which would permit this aircraft to operate from many major airports.

Part of the FAA safety of flight regulations require a four-engined aircraft to be able to maintain 3% climb gradient with an engine failed. To determine the application of this requirement to the Ref.-H vehicle a static trim analysis was performed. Figure 9 presents the amount of thrust required to maintain either a 3% climb gradient with one engine failed or a 4% climb gradient with all engines operating as a function of indicated airspeed. Data are presented for an aircraft configuration with automatic flaps, as employed for task 2030, and with leading-edge flaps set to 30 degrees and trailing-edge flaps set to 10 degrees (lef=30/tef=10), as employed for tasks 2010 and 7035. From this figure it can be seen that the

minimum speed at which the aircraft can maintain a 3% climb gradient with a failed engine is approximately 184 kts for the automatic flap case and 182 kts for the fixed flap case. Since this speed is below the V_2 speed, determined from the OEO takeoff evaluation, V_2 remained at 201 kts. Also shown in Figure 9 is the task 2030 (PLR) first cutback thrust level of 75%. One of the requirements imposed on the PLR procedure was that the thrust level never be allowed to go below the OEO 3% climb gradient thrust curve until the aircraft's altitude was greater than 400 ft. This is an interpretation of the FAA safety of flight regulations pertaining to all aircraft. It is applied here in an effort to demonstrate the relative flight safety of this maneuver. Also on Figure 9 is the amount of thrust required to maintain a 4% climb gradient with all engines operating for both flap scenarios. One obvious feature of Figure 9 is that the optimized automatic flap schedule requires more thrust than the lef=30/tef=10 flap setting. This is completely counter-intuitive since the automatic flap schedule was implemented to optimize performance. This discrepancy will be resolved before the next Ref.-H assessment project. The data shown in Figure 9 are required to determine the amount of thrust cutback for the standard acoustic procedure (task 2010) and also as a check of the amount of thrust that should be automatically selected during the transition to the speed hold portion of the PLR maneuver.

The cutback thrust level used for task 2010 was based on the amount of thrust required to maintain a 4% climb gradient plus a 3% increase of thrust to account for turbulence effects. As a result of incorrectly using the automatic flap deflections to determine the thrust required for the lef=30/tef=10 case, the thrust level for task 2010 was 55%. The amount of error resulted in roughly a 4.5% secondary climb gradient instead of a 4.0% climb gradient. Figure 9 also illustrates the benefit of operating at a higher speed as is shown by almost a 10% decrease of thrust required for flight at 250 kts. as compared to flight at 219 kts. This level of thrust reduction significantly reduces the amount of noise produced and offsets the apparent increase in ground observer noise due to the lower trajectory.

HUD guidance was provided to the pilots to help them perform consistent and accurate rotations. Velocity-vector guidance was provided for the airborne section of the takeoff maneuver as shown in Figure 10. Rotation guidance included information regarding rotation rate and rotation rate acceleration as well as target pitch attitude. Incorporation of this system was intended to standardize the rotation task and provide adherence to consistent, specified, performance parameters such as steady state pitch rate and pitch rate accelerations. The desired rotation rate was generated based on the time the aircraft reached the rotation speed, V_r, and employed a 1.5 deg/sec-sq. pitch acceleration, a 3.0 deg/sec steady-state pitch rate, and a 2.5 deg/sec-sq. deceleration. Additionally, the target lift-off pitch attitude was displayed to the pilot (10.5 degrees). Desired pitch rate control was +/-0.6 deg/sec 90% of the time and adequate was +/- 1.2 deg/sec 90% of the time.

Once the aircraft was airborne an automatic HUD reconfiguration occurred. It removed some elements visible during the rotation task such as the tail scrape bar, target pitch attitude indicator, and pitch rate error brackets and reduced the size of the pitch attitude reference marker. The automatic HUD reconfiguration also added a velocity-vector guidance marker. The velocity-vector guidance marker presented longitudinal and lateral guidance information to the pilot during the airborne phases of the takeoff maneuver. The pilots task was to place the commanded velocity vector on top of the velocity vector guidance symbol. Details regarding the generation of the velocity-vector guidance symbol motions can be found in Appendix A. The airborne HUD configuration is shown in Figure 11. Pilot performance limits are also displayed on the figure. For task 2010 the velocity vector guidance symbol provided guidance to accelerate to and maintain the desired climb speed, V_c. The lower limit of its travel was a 3% climb gradient. This resulted in the lowest climb gradient the pilot would be commanded to fly be no lower than 3%, which occurred mostly during task 7035 (One Engine Out takeoff). For task 2030 (PLR acoustic takeoff) the velocity vector guidance indicator was constrained to remain on the 4% climb gradient which simplified the longitudinal

takeoff task significantly. Lateral guidance was a combination of lateral distance from the runway centerline, track angle, bank angle, and roll rate. Following the lateral velocity vector guidance symbol commanded the pilot to adjust the velocity vector to follow the extended runway centerline and was the same for all takeoff maneuvers.

Pilot ratings were obtained for all takeoff maneuvers except the V_{mcg}, which was a demonstration maneuver. Takeoff maneuvers were broken into segments to provide a more accurate and detailed pilot assessment of the maneuvers. Definition of the maneuver rating segments employed are listed in Table 7.

A portion of the NASA LaRC Ref.-H assessment project was to evaluate the aircraft's ability to meet anticipated takeoff noise restrictions expected to be in place when the HSCT enters service early in the next century. This was accomplished through the application of the NASA LaRC developed aircraft noise prediction program (ANOPP), which is described in reference ref 10. Trajectory data from the real-time piloted simulation was combined with acoustic engine data which formed the input to ANOPP. ANOPP, in turn, can generate noise predictions for any user specified microphone location. The source noise model employed accounted for jet-mixing noise only. No corrections, such as jet shielding, airframe reflective noise, etc., were applied to the data. Although 15 dB of jet-noise suppression was assumed in the thrust simulation model, noise results are presented for the unsupressed mixed flow turbo fan (MFTF) engine designated the GE21/F15-A17. The figure of merit employed for the noise evaluation facet of the Ref.-H assessment project was the amount of jet-noise suppression required to satisfy specified noise regulations. One of the takeoff noise metrics was sideline noise (S.L.) and is defined as the maximum level of noise, in units of effective perceived noise level (EPNdB), along a line parallel to and displaced 1,476 ft to the side of the runway centerline extending from the point adjacent to were the aircraft becomes airborne. The other takeoff noise metric was centerline noise (C.L.) which is the noise at a fixed point along the extended runway centerline and located at 21,325 ft. from brake release. The units of centerline noise are also EPNdB. The

anticipated noise requirement specifies a reduction of sideline noise of 1 EPNdB, a reduction of centerline noise of 5 EPNdB, and a reduction of approach noise of 1 EPNdB with respect to existing FAA FAR Part-36 Stage-3 noise regulations. See Figure 12 for an illustration of the noise measurement system. The permissible amount of noise is a function aircraft weight. Takeoff noise levels, for the anticipated noise requirement are, based on the M13 mass case for takeoff, C.L.=99.1 and S.L.=100.7 EPNdB. The approach noise limit, based on the MFC case, is 102.2 EPNdB.

Maneuver 1: Acoustic profile takeoff. The acoustic profile takeoff maneuver was designed to replicate, as closely as possible, the noise abatement takeoff procedure which would be used today if the Ref.-H aircraft were to be certified or in actual airline operation. As such, the leading- and trailing-edge flaps remained in a fixed position and engine thrust levels remained a manual task. Approximate reference airspeeds were calculated based on Ref.-H Cycle-1 and Cycle-2B data as previously outlined. The reference airspeeds of V_1 (takeoff decision speed, 166 kts), V_r (rotation speed, 174), V_2 (one engine out takeoff obstacle speed, 201 kts), and V_C (commanded climb speed, V_{35} AEO+10=219 kts) were considered to be of sufficient accuracy to perform the evaluation. A manual thrust cutback was performed at 700 ft. altitude where net thrust was reduced to 55% of max. by the PNF. The rate of thrust reduction was adjusted so as to not cause the pilot to command a low-g condition during the cutback pushover.

Generally task 2010 was not difficult to perform. However some aspects of the maneuver were evaluated to be less than desired. One aspect which received some negative comments was the pitch rotation guidance system. Pilots were unused to dealing with guidance during the rotation phase of the takeoff maneuver. They indicated that the system could be improved through changes in display format and logic to be more acceptable. Overall, pilots frequently had difficulty staying within desired limits and even exceeded adequate bounds as shown in Figure 13. Analysis of the data indicates this was probably caused by a combination of control

system and aircraft limitations. As shown in Figure 13 almost full elevator deflection was used between 1 to 2 seconds after rotation initialization, which indicates the aircraft was operating near its maximum capabilities possibly causing some control response anomalies. Some elevator rate limiting was also apparent for the task 7035 example at about 1.0 seconds from rotation initialization which is indicated by the steep straight line of elevator deflection. It should be noted that the $\dot\gamma / V$ control system was not originally designed to support on-ground aircraft operations. It was modified to provide adequate functionality for the Ref.-H assessment project and should be re-evaluated prior to future applications of this control system. Additionally, the Vortex Fence, which was designed to provide added nose-up pitching moment, was not functioning properly for the takeoff maneuvers of the Ref.-H assessment project. Figure 13 also shows that although a 3.0 deg/sec steady state pitch rate was specified, pilot performance frequently went below 2.4 deg/sec as is indicated by the pitch rate falling below desired performance at time equal to 2.0 seconds.

Lift-off pitch attitude, which was defined as the maximum pitch attitude attained before lift-off, was usually in the desired range and was less than +/-0.5 degrees from the specified target. Once airborne pilots generally had little difficulty following the velocity vector guidance which provided information to accelerate to and maintain the desired climb speed and also track the extended runway centerline. Problems were encountered however during the single manual thrust cutback. During this portion of the maneuver thrust was required to be reduced gradually so as to not cause a rapid pitch-over by the pilot to maintain airspeed, resulting in a normal acceleration excursion. Generally normal acceleration was kept above 0.8 g which should avoid any potential passenger discomfort. Another minor problem encountered was some velocity-vector guidance jumpiness due to turbulence even though the guidance system employed complementary filtered airspeed.

Figure 14 presents the amount of noise suppression required to meet the anticipated noise restrictions. The shaded areas represent the amount of effective noise suppression

required for the Ref.-H aircraft to satisfy the anticipated noise restriction employing an optimistic estimate for approach noise. From Figure 14 it can be seen that a large amount of noise suppression was required to meet the anticipated noise regulations if the standard acoustic procedure (Task 2010) was flown. Also note that the amount of noise suppression is being driven by sideline noise requirements not centerline noise. The amount of suppression required for task 2010 is approximately 20 dB. Currently, the Cycle-2B data base only assumes 15 dB and produces a situation where the aircraft would not be able to meet the anticipated noise requirement

Pilot ratings are listed in Table 8 for all takeoff related maneuvers. From this table it can be seen that task 2010 was rated a middle to high level one for all segments of the procedure when combined. The segment receiving the worst rating was segment 2 for the longitudinal case where 3 of the 5 pilots rated it a CHR of 4 reflecting some difficulty performing the rotation for lift-off task within desired boundaries. Another segment which received some level 2 ratings was segment #3, also for the longitudinal case, where 2 of the 5 pilots rated it a CHR of 4 resulting from increased pilot workload during the thrust cutback portion of the maneuver combined with turbulence induced problems maintaining airspeed throughout the airborne segment.

Maneuver 2: Programmed Lapse Rate (PLR) acoustic takeoff procedure. The PLR acoustic takeoff procedure incorporated automatic changes of leading- and trailing-edge flap deflection and thrust level and as a consequence greatly reduced the noise produced by the aircraft during takeoff. It was included as a result of the potentially significant reductions in the amount of noise suppression required for certification and the possibility that a similar maneuver could be employed for HSCT commercial operations. The PLR maneuver was designed to take advantage of all possible changes in FAA regulations regarding automated systems and procedures which may be available to a HSCT aircraft when it enters service. All exceptions to the current regulations have been previously evaluated using other HSCT piloted simulations and have

been initially determined to pose little or no safety of flight problems or concerns.

The significant features of the PLR procedure are; 1) direct computer control of thrust level and symmetric leading- and trailing-edge flap deflections; 2) a smooth low-altitude (i.e. alt. < 50 ft.) initial thrust reduction which maintains thrust above the OEO 3% climb level; 3) a low initial climb gradient which produces an accelerating climb that reaches an advantageous aerodynamic performance speed ($V_c = V_2 + 49 = 250$ kts) prior to passing over the centerline microphone position; 4) a secondary thrust cutback to maintain best aerodynamic performance speed prior to passing over the centerline microphone position. All of these features of the PLR procedure will, of course, need to be accepted by the FAA in order to employ this procedure. However, indications to date are encouraging and that no significant pilot concerns regarding the PLR procedure have been observed and, in most cases, pilots actually preferred the PLR procedure over the Standard Acoustic procedure. A comparison of the two procedures is provided in Figure 15, which shows thrust, leading- and trailing-edge flap deflections, altitude and airspeed as a function of distance from brake release.

All pilot's guidance and tasks were the same as the standard acoustic takeoff maneuver except that the longitudinal velocity-vector guidance only displayed the desired constant climb gradient instead of airspeed error information as was shown in Figure 11. Leading- and trailing-edge flaps were automatically adjusted, in an attempt to produce optimum aerodynamic performance, and were scheduled based on Mach number.

From Figure 14 and Figure 16 it can be seen that a large amount of noise suppression is required to meet the anticipated noise regulations if the Standard Acoustic procedure (Task 2010) was flown. Also note that the amount of noise suppression was being driven by sideline noise requirements and not centerline noise. One of the merits of the PLR procedure (task 2030) is that it is very effective at reducing sideline noise due to the low-altitude thrust cutback which results in reduced amounts of noise suppression required as can be seen in Figure 16. Additionally, since a higher climb speed was used for the PLR procedure, a lower

amount of thrust was required to maintain a 4% climb gradient as was shown on Figure 9. This resulted in a limited increase of C.L. noise due to the much lower C.L. microphone crossing altitude of the PLR procedure. From Figure 16 it can also be seen that the required amount of jet noise suppression is still determined by sideline noise even though sideline noise was reduced approximately 8 EPNdB as a result of the PLR procedure.

Pilot ratings for task 2030 are listed in Table 8. Task 2030 received identical ratings for segment #1 which is to be expected because no differences between maneuvers 2010 and 2030 are encountered during this segment. One difference of pilot ratings observed for the two takeoff maneuvers was the longitudinal portion of segment #2. Pilots felt that the rotation segment was easier to perform as a result of not having to rapidly increase pitch attitude immediately after lift-off to follow the velocity vector guidance to capture the climb speed. Although segment #2 ended at lift-off, pilots tended to rate segment #2 of task 2030 better than the same segment of task 2010 as a result of increased work load immediately after lift-off. Future applications of this maneuver will extend segment #2 to the obstacle height. Lateral ratings for segment #2 were again identical for both takeoff maneuvers. Longitudinal ratings for segment #3 were slightly lower for task 2030 as is shown in Table 8 by two of the pilots rating 2030 a CHR of 3 instead of a CHR of 4. Pilot comments frequently indicated that maneuver 2030 was preferable to 2010 since there were no large pitch transients caused by large changes of flight path angle and that following a constant gamma was easy given the $\dot{\gamma} / V$ control system. Lateral CHR ratings for segment #3 were slightly higher for maneuver 2030 than 2010. Pilot comments supporting the small increase in CHR rating for maneuver 2030 indicated that, since the longitudinal task was much easier for maneuver 2030, the pilots were able to focus more attention on the lateral task and observed a slight tendency to S-turn across the runway centerline if the guidance was followed too closely. This was a minor problem with the takeoff guidance system and will be improved for future applications.

Maneuvers 3, 4, 5: Rejected takeoff maneuver (Cross-winds 0, 15, 35 kts). The rejected takeoff maneuver (RTO) was performed with an engine failure occurring at a speed which would require the pilot to abort the takeoff. The engine failure speed was specified to be slightly lower than the decision speed, V_1 (166 kts). Pilots were aware however, at the beginning of the run, of the pending engine failure. In addition, the level of cross-wind was varied to determine its effect on the combined pilot and aircraft performance. The pilots task for the RTO maneuvers was to accelerate the aircraft up to the engine failure point then apply maximum braking to bring the aircraft to a complete stop. Desired performance was to keep the aircraft within +/-10 feet and adequate performance was +/-27 feet. The only significant guidance available to the pilot was the velocity vector which was used to track the runway centerline. Cross-winds evaluated were 0, 15, and 35 kts. perpendicular to the runway. The engine failed was always the upwind engine (engine #4) which added to the aircraft's weather-vaning tendency.

Figure 17 presents indicated airspeed, distance from runway centerline, rudder deflection, and nose gear steering angle as a function of distance from brake release for representative rejected takeoff maneuvers for each of the cross-winds evaluated. Some interesting observations regarding this maneuver were that the effect of increased cross-wind caused the aircraft to accelerate slower and decelerate quicker as a result of constantly operating at large side-slip and skid angles. Accelerate/stop distances were decreased approximately 300 feet due to the 35 kt cross-wind. Another observation was that pilots had little trouble maintaining the aircraft within the desired boundaries of +/-10 ft. from runway centerline. Maximum rudder deflection was only approximately 20 degrees for the 35 kt cross-wind case and maximum nose-gear steering angles were on the order of 5 to 6 degrees. Overall, the aircraft exhibited ample control authority and performance to perform this maneuver within desired boundaries for cross-winds up to 35 kts.

The effect of cross-wind increased the difficulty of the maneuver somewhat but not enough to increase the Cooper-Harper ratings

by a full unit. CHR ratings for this maneuver were generally CHR of 3,4 with one pilot rating the maneuver a CHR of 1. The average CHR rating was 2.8 indicating overall level 1 performance. Pilots generally needed several runs to become familiar to the simulated task although no pilots needed more than 2 or 3 attempts to complete any one maneuver. Pilot A did not need any additional attempts as indicated by his CHR of 1. Results also indicate that if the pilot had not been briefed to expect an engine failure larger errors, and subsequently lower CHR numbers, may have resulted. Overall the aircraft was able to be brought to a complete stop in about 8,200 ft. for the zero cross-wind scenario. The aircraft had adequate nose-gear steering and rudder authority to compensate for the weather-vaning and engine out condition as is shown in Figure 17. Some pilots also employed differential braking to help steer the aircraft at higher speeds. Pilot comments also indicated that the nose-gear steering had too much authority at higher speeds and that the gearing should be reduced from the +/-15 degrees of authority as is employed by other airline transport aircraft. A solution to this problem could easily be rectified through incorporation of speed sensitive nose-wheel steering gains to soften the aircraft's response to rudder inputs at elevated speeds as is currently employed on other jet transport aircraft.

Maneuver 6: One-engine-out (OEO) takeoff maneuver. The OEO takeoff maneuver was designed to evaluate the aircraft's ability to continue a takeoff after an outboard engine failed. The location of the engine failure was placed immediately after the aircraft reached the decision speed, V_1, which resulted in the pilot being required to continue the takeoff. The HUD guidance selected was the same as the acoustic profile takeoff maneuver and commanded the pilot intercept and maintain the desired climb airspeed (V_c=219 kts) after lift-off. For this maneuver the pilot had the additional task of centering the side-slip indicator using rudder pedal inputs. Some differences in the guidance system were observable by the pilot during this maneuver as compared to the standard acoustic takeoff. One difference involved the lower limit of the velocity-vector guidance system. The lower

limit was set to a 3% climb gradient and prevented the guidance system from commanding too low of a climb gradient while attempting to accelerate to and maintain airspeed. During normal operations the aircraft had sufficient excess power to accelerate at a climb gradient above 3% and the guidance system provide airspeed guidance only. However, when the aircraft was operating at a low speed with an engine failed the available acceleration was less than what was being commanded by the velocity-vector guidance system and resulted in short periods of time, immediately after lift-off, when it would be commanding the pilot to follow the minimum climb gradient instead. Once sufficient aerodynamic performance was achieved at higher airspeeds, the velocity-vector guidance system would again provide airspeed guidance as was done for the standard acoustic takeoff task. Another difference in the HUD guidance involved the control of side-slip angle through the use of rudder pedal inputs combined with information from the side-slip indicator. Obviously, during normal takeoff operations, there was no need to control side-slip angle since it was always at or near zero. During the OEO takeoff task, however, the pilot had to actively control side-slip angle. The side-slip indicator presented complementary filtered side-slip angle.

Pilots had little difficulty performing the OEO takeoff maneuver up to the point of rotation initialization. Once rotation was begun, and the nose wheel lifted from the runway, pilots had some difficulty keeping the aircraft within desired bounds as is shown in Figure 18, which presents indicated airspeed, lateral distance from runway centerline, rudder deflection, and pilots rudder pedal inputs as a function of distance from brake release for three different pilots ratable runs. The ratable runs were the ones which the pilots determined to be of sufficient quality to permit pilot rating evaluation. The data in Figure 18 stops at lift-off for each of the three examples. In this figure it can be seen that, once the aircraft began the rotation maneuver, significant lateral error was built-up. Note also that maximum rudder deflection was not used.

Once airborne the aircraft exhibited ample control authority to handle the asymmetric thrust situation. One benefit of the closely-packed engines, typical of HSCT

configurations, was that the amount of yawing moment produced due a failed engine is relatively small. Figure 19 provides information regarding the amount of rudder and differential aileron deflection for the entire OEO takeoff maneuver along with altitude and airspeed. From Figure 19 it can be seen that the rudder deflection required is only about 10 to 15 degrees immediately after lift-off and decreases to a steady-state value of approximately 8 degrees once the aircraft reaches climb speed. Differential aileron deflection is also small compared to the maximum amount available. Overall, the Ref.-H aircraft had adequate control authority to perform the OEO takeoff maneuver.

Pilot comments regarding the OEO takeoff maneuver identified that it was a little more difficult to perform than the normal operation takeoff maneuvers (tasks 2010 and 2030). See Table 8 for the CHR ratings for all takeoff maneuvers. Segment #1 of the task was rated an average lateral CHR of 3.8 with 3 of the 5 pilots delivering level 2 ratings. This level of rating could be due to the over-sensitive nose-wheel steering system combined with the engine failure and could be reduced with speed sensitive steering as was mentioned for the RTO tasks. During segment #2 pilots commented that there were a lack of visual queues or guidance to maintain the aircraft within the desired boundaries, even though the aircraft had enough control authority, as was shown in Figure 18. As a result, pilots rated the lateral portion of segment #2 an average CHR of 4.2 with 4 of the 5 pilots rating it level 2. Improvements in guidance and/or other visual queues could improve this rating. The longitudinal portion of segment #2 was also rated slightly worse than the same segment for tasks 2010 and 2030. Pilot comments reflected problems regarding the increased work load, introduced by the lateral task resulting from the asymmetric thrust, and rated this segment an average longitudinal CHR of 3.6. Pilot comments for the airborne segment of this maneuver indicated that the longitudinal portion was not much different than task 2010 and actually pointed out that it was slightly easier to perform than task 2010, however those comments weren't reflected in the CHR ratings. Average longitudinal CHR ratings for airborne segments of task 2010 and 7035 were all approximately the same. Pilots rated the

lateral portion of the task an average CHR of 3.8 with 3 of the 5 pilots providing level 2 ratings. Comments regarding this portion of the maneuver indicated that it was not too difficult to perform once the proper amount of rudder pedal bias was determined. Overall, the maneuver was rated a low level 2, which was acceptable given the fact that this is an emergency maneuver. Additional pilot comments regarding the HUD display and guidance logic suggested that the guidance system could be improved although offered no specific options for doing so.

Maneuver 7: VMCG (minimum control speed, ground, task 7030). Task 7030 was designed and executed to determine the minimum controllable rotation airspeed, in the event of an engine failure, for the Ref.-H on the ground. Nose gear cornering forces were zeroed out for this maneuver and the MFC mass case was selected. This maneuver was intended to verify that the V_{mcg} speed was below the rotation speed for the lowest possible takeoff weight. The first pilot to complete task 7030 was asked to perform the maneuver for a series of engine failure speeds and maintain the aircraft to within +/-30 feet of runway centerline. Once the minimum engine failure speed was identified that produced the maximum permissible lateral excursion, that speed was identified as the V_{mcg} speed with the other 4 pilots just demonstrating the maneuver with the engine failure occurring at the V_{mcg} speed. V_{mcg} was determined to be 127 kts. Figure 20 presents percent net thrust from engine #4, rudder deflection, aircraft heading and track angle, and lateral distance from runway centerline as a function of time for a representative demonstration of task 7030. From Figure 20 it can be seen that the pilot/control system combination required less than a second to develop full rudder deflection to counter the asymmetric thrust of the failed engine. Once the engine was failed, aircraft heading increased until the airspeed reached approximately 150 kts where sufficient rudder control was available to counter the asymmetric thrust condition and arrest the increase of aircraft heading error. The maximum lateral excursion occurred, however, when the aircraft's track angle was re-aligned with the runway centerline, which lagged

17

behind the aircraft heading due to landing gear skidding. The rotation speed employed for the takeoff maneuver set was 174 kts which was determined for the aircraft with the M13 mass case. The minimum takeoff weight, and worst condition scenario, was assumed to be when the aircraft was configured in the MFC mass case due to its low inertia and reduced V_r. V_{LO} speed for the MFC mass case would be approximately 143 kts with a V_r of approximately 128 kts. Therefore, a V_{mcg} speed of 127 kts correlates well with an expected rotation speed, for the MFC mass case, of 128 kts.

Section 2 - Recovery from limit flight tasks

Introduction to recovery from limit flight tasks. All commercial transport aircraft are required to demonstrate that a specific margin exists between normal operation flight speeds and stall speeds. Generally, minimum approach speed is dictated by the stall speed. Given the fact that cranked-arrow wing configurations such as the Ref.-H do not stall in the manner of conventional swept-wing transport designs, a series of minimum speed/maximum angle of attack demonstration maneuvers were formulated to verify that controlled flight exists at the minimum speeds required . All of the recovery from limit flight (RFLF) tasks involved the pilot maneuvering the aircraft to a low speed high angle of attack situation, then attempting to recover to wings level flight at the recovered angle of attack to verify the aircraft's capability to safely operate at these conditions. Maneuvers 5010, 5020, 5040, and 5050 were included in this element.

Some modifications of the initial RFLF flight cards were required based on preliminary evaluations performed by the NASA LaRC project pilot. One problem that was encountered involved the airspeed readout on the HUD, which was tied to the commanded velocity vector and would be almost unreadable at the high angle of attack conditions experienced during these maneuvers. Combining difficult readability of the digital airspeed on the HUD with the sometimes rapid rate of airspeed decay proved to make

the maneuver difficult to perform consistently when recovery was specified based on airspeed. Another problem experienced was a discrepancy regarding the minimum airspeed. Tasks 5040 and 5050 were the turning RFLF maneuvers and initially specified a minimum speed of 180 kts, which was even faster than the approach speed (Initial development of the flight cards was performed by personnel in other elements of the HSR program). As a result of the minimum speed anomaly in the flight cards combined with problems reading airspeed, the recovery initiation was based on angle of attack which was readily observable on the HUD.

Determination of the maximum demonstration angle of attack was based on preliminary evaluation runs of tasks 5010 and 5020 in conjunction with a calculation of $V_{min-dem}$ for approach. Task 5010 was initially performed with minimum thrust combined with the MFC mass case and required the pilot to decelerate to 110 kts before initiating the recovery. Task 5020 was performed with maximum thrust and the M13 mass case and required the pilot to decelerate to 156 kts before initiating the recovery. From these runs it was observed that the angle of attack achieved when the aircraft reached the recovery airspeed was approximately 21 degrees for both tasks. Calculation of $V_{min-dem}$, based on an approach speed goal of 160 kts and a maximum landing weight of 402,000 lbs., produced a $V_{min-dem}$ of 123 kts at an angle of attack of approximately 20 degrees. It was therefore determined that the maximum demonstration angle of attack of 21 degrees would be satisfactory. The 21 degree maximum angle of attack demonstration would also permit a takeoff V_{2-min} speed as low as 187 kts for the 649,914 lbs. M13 mass case. The assumed recovered angle attack was based on an initial stability analysis of the vehicle which indicated that directional stability with zero ARI would exists at angles of attack below 13 degrees.

All RFLF maneuvers were performed with fixed thrust levers and required the pilot to attempt to maintain a 3 kt/sec deceleration rate until recovery is called for by the PNF. Limitations involving the capability of the cockpit motion base to provide realistic motion

cues for the RFLF maneuvers resulted in these tasks being flown fixed-base. Figure 21 shows angle of attack, rate of speed change, and bank angle for a representative turning RFLF maneuver.

Results for RFLF maneuvers. An analysis of pilot performance was performed where the maximum and minimum sideslip angles as well as maximum angle of attack were determined for all RFLF maneuvers attempted. This data is presented in Figure 22 and serves the purpose of illustrating the widely ranging performance experienced for this set of maneuvers. Angles of attack of 30 degrees were assumed to have reached an unrecoverable angle of attack condition and were beyond the point of meaningful aerodynamic data. As can be seen from Figure 22, only small amounts of sideslip developed for most of the non-turning RFLF maneuvers (tasks 5010 and 5020). Figure 22 also shows that a wide scatter of maximum angles of attack were achieved through the course of the maneuver evaluations. The variations of maximum angle of attack were largely due to inconsistencies in the rate of deceleration during the maneuver entry phase. The increased amount of sideslip developed for the turning RFLF maneuvers was caused by the lateral maneuvering required during the recovery segment of the maneuver which taxed the independent directional control system capabilities to keep sideslip near zero.

Controlling the rate of airspeed decay was complicated by the $\dot{\gamma}/V$ control system combined with the aircraft's back-sided aerodynamic characteristics in this flight regime along with a lack of adequate rate of airspeed decay information available to the pilots. Only analog and digital airspeed indicators were provided. The $\dot{\gamma}/V$ control system hampered the maneuver entry through its attempts to maintain a constant flight path angle, as airspeed was decreased, by raising the nose of the aircraft. A characteristic of the Ref.-H vehicle, for takeoff speeds less than approximately 250 kts and approach speeds less than 180 kts, was that it requires more thrust to fly slower as a result of rapidly increasing drag. This leads to an unstable situation where the rate of speed decrease continues to grow as the pilot approaches the maximum demonstration angle of attack. If the

pilot did not monitor the rate of airspeed decay, a rapid loss of airspeed developed resulting in a higher than desired maximum angle of attack. Sideslip excursions were much more prevalent for the turning RFLF maneuvers (tasks 5040 and 5050) which required the pilot to level the aircraft's wings as part of the recovery process. Figure 22 shows the amount of sideslip developed varied for a given maximum angle of attack. It was determined that the variation in the amount of sideslip angle was dependent on how aggressive the pilot attempted to level the wings of the aircraft. A discussion of variations of maximum sideslip angle for the turning RFLF maneuvers will be provided later.

As stated previously, the rate of airspeed decay had a significant effect on the maximum angle of attack achieved during a piloted simulation RFLF maneuver. Figure 23 demonstrates the effect of stall entry speed on maximum angle of attack and presents angle of attack, rate of airspeed decay, pilot longitudinal stick input (DCPILOT), and elevator deflection angle (DELEV) as a function of time for two attempts of task 5010. In one attempt (951250 Run 028) the pilot did not maintain the proper rate of airspeed decay which results in the aircraft attaining a higher than desired maximum angle of attack and eventually departing. From Figure 23 it can be seen that the rate of airspeed decay reached almost 15 kts/sec at the time the pilot attempted to recover. In the other maneuver attempt (951205 Run 030) the same pilot maintained the proper rate of airspeed decay as angle of attack was increased to 21 degrees and performed a nominal recovery to below 13 degrees angle of attack. Control system problems, however, were not just limited to hampering airspeed decay rate as is shown during the recovery portion of both maneuver attempts by the uncommanded re-increase of angle of attack when the pilot releases the nose-down stick input. This is shown at approximately T=62 seconds and T=76 seconds for Run 28 and Run 30 and is characterized by a rapid movement of the elevator from the full nose-down position to the full nose up position at or near its rate limit when the pilot relaxes his nose down command. This control system problem was probably caused by a stick position differentiator in the control system which fed in a large nose-up elevator command when the

19

pilot relaxed his nose-down stick input after developing a desired rate of nose down recovery. Other problems were also observed which involved the inner-loop stability of the $\dot{\gamma} / V$ control system.

Figure 24 presents information regarding the aircraft's ability to recover from a high angle of attack situation. Pitch rate acceleration and indicated airspeed are plotted as a function of angle of attack. Data are presented for assumed level flight with quasi-static elastic (QSE) aerodynamics, automatic flaps based on Mach number, minimum thrust, and the MFC mass case. Mach number was determined from the angle of attack at an altitude of 10,000 ft. The aircraft was trimmed in pitch. Nose-down pitch rate authority was then calculated by applying full nose-down control, i.e. δ_h=15 and δ_e=30 degrees. One set of data was calculated assuming the pilot kept the thrust at minimum during the recovery and the other assumes full thrust was commanded, and developed, at the instant of recovery. Modeling thrust effects in this manner simulates a situation where the pilot has allowed the aircraft to get to a low airspeed situation, while maintaining minimum thrust, followed by commanding, and developing, full thrust before initiating the pitch recovery and is considered to be a worse case scenario.

The required pitch rate acceleration, as specified in reference ref 11, of -4 deg/sec-sq. is included on this figure to illustrate the point at which the aircraft satisfies this requirement. From Figure 24 it can be seen that for the scenario with minimum thrust, which closely represents the conditions experienced for tasks 5010 and 5040, satisfies the pitch rate acceleration requirement up to approximately 19 to 20 degrees angle of attack. This corresponds to approximately an airspeed of 123 kts which just barely meets the minimum speed required. If full thrust was being produced at the moment of pitch recovery initialization, then the nose-down pitch acceleration capability of the Ref.-H vehicle was reduced significantly. The aircraft can meet the -4 deg/sec-sq. pitch acceleration criteria up to only 18 degrees angle of attack which corresponds to a speed of 130 kts. Therefore, the aircraft does not meet the nose-down pitch acceleration criteria under all possible scenarios and a strong case could be

made to limit the maximum angle of attack to 18 degrees. It should be noted that the engine package had an average effective moment arm of approximately 8 ft which could be reduced to zero with a thrust axis change of 10 degrees. Given the fact that it would take a finite amount of time for the engines to develop full thrust, however, the vehicle would respond more like the minimum thrust case initially. The Ref.-H vehicle demonstrated barely desired nose-down pitch control for maneuvers 5010, 5040, which were flown with constant minimum thrust and the MFC mass case based on analysis of batch results. A similar analysis performed with the M13 mass case and maximum thrust produced required pitch rate acceleration up to angles of attack higher than 27 degrees.

The data in Figure 24 were obtained for ideal RFLF conditions. Variables that affect the maximum pitch rate acceleration capability at a given angle of attack, such as airspeed, pitch rate, pitch rate acceleration, rate of change of angle of attack, etc., were all set to zero. As a result, Figure 24 presents the best possible vehicle performance. Results from actual real-time piloted evaluations were usually far below what would be expected from Figure 24. Figure 25 presents data for a representative run for task 5010. Angle of attack, elevator and stabilizer positions, pitch rate, and pitch rate acceleration are illustrated in this figure. From Figure 25 it can be seen that the maximum amount of pitch rate acceleration generated during the recovery was achieved when the elevator and horizontal tail reached their position limits, which is indicated by the vertical line labeled "Recovery" on the figure. At this point the vehicle was only producing approximately -2.4 deg/sec-sq. pitch rate acceleration. The low amount of pitch rate acceleration was due to a combination of parameters. At the point of recovery, the aircraft reached a slightly higher angle of attack of approximately 22 degrees, airspeed was almost 10 kts. below the 1-g trim speed as is shown in Figure 26, and a pitch rate of approximately -1.2 deg/sec was already established. All of these had a significant impact on the amount of pitch rate acceleration available. From Figure 24 it can be seen that a decrease of 1.0 degree/sec-sq. pitch rate acceleration was due to the increased angle of attack. The 10 kts. airspeed decrease of the

real-time data reduced dynamic pressure, and pitch rate acceleration, by an additional 15%. Analysis of the effect of pitch rate on pitch rate acceleration indicate that pitch rate acceleration was decreased approximately 0.1 deg/sec-sq. for each deg/sec of pitch rate. The combination of the angle of attack, airspeed, and pitch rate error analysis produced a predicted pitch rate acceleration of approximately -2.4 deg/sec-sq. which was demonstrated by the data in Figure 25.

During the course of pilot evaluations pilots frequently had trouble recovering from the turning RFLF maneuvers. A lateral/directional stability analysis was conducted to determine if any aerodynamic problems associated with the Ref.-H vehicle were responsible for the problems encountered during recovery from high angle of attack turning flight. Figure 27 shows body-axis directional stability, $C_{n\beta}$, and body-axis lateral stability, $C_{l\beta}$ as a function of angle of attack. As was the case with the data from Figure 24, data are presented using QSE aerodynamics, automatic flaps based on Mach number, and the MFC mass case. Mach number was determined from the pitch-trimmed angle of attack at an altitude of 10,000 ft. From Figure 27 it can be seen that directional stability becomes unstable for angles of attack above 14 degrees. However lateral stability remains stable up to approximately 22 degrees angle of attack. The differences between the angles of attack where the stability derivatives becomes unstable poses a question about which one to base the maximum angle of attack limit on.

Figure 28 presents two commonly used stability and control parameters which quantify an aircraft's high angle of attack capabilities. One is referred to as $C_{n\beta}$-dynamic and the other is the lateral control divergence parameter (LCDP) and are defined as:

$$C_{n_{\beta_{dyn}}} = C_{n_{\beta}} * cos\,(\alpha) - (I_z \quad I_x) * C_{l_{\beta}} * sin\,(\alpha)$$

and

$$LCDP = (C_{n_{\beta}} + (I_{xz} \quad I_x) * C_{l_{\beta}}) - (C_{l_{\beta}}$$
$$+ (I_{xz} \quad I_x) * C_{n_{\beta}}) * \{NUM / DENOM\}$$
where:
$$NUM = C_{n_{\delta a}} + (I_{xz} \quad I_x) * C_{l_{\delta a}}$$
$$DENOM = C_{l_{\delta a}} + (I_{xz} \quad I_x) * C_{n_{\delta a}}$$

Both involve combinations of $C_{n\beta}$ and $C_{l\beta}$, along with the vehicles inertia properties to provide a more comprehensive analysis of the stability and control characteristics than independent analysis of $C_{n\beta}$ and $C_{l\beta}$. As was the case with the data from Figure 24, and Figure 27, data are presented using QSE aerodynamics, automatic flaps based on Mach number, and the MFC mass case. Mach number was determined from the pitch-trimmed angle of attack for an altitude of 10,000 ft. $C_{n\beta}$-dynamic represents the vehicles un-augmented stability and its ability to maintain constant flight. It becomes unstable around 21 degrees angle of attack. This implies that flight above 21 degrees angle of attack would be difficult and require a stability augmentation system. The LCDP parameter quantifies the closed-loop lateral control characteristics of the vehicle. It defines the aircraft response to lateral control inputs. A negative LCDP indicates that the aircraft's nose would move in an opposite direction than intended by the pilot due to sideslip buildup. A positive LCDP would indicate that the aircraft would roll in the intended direction. This analysis was performed with an aileron to rudder interconnect (ARI) equal to 0.0 and 1.0. As can be seen from Figure 28 the incorporation of an ARI increased the useable angle of attack range up to approximately 19 degrees which was a 5.5 degree increase from the zero ARI case. The directional control system used for the Ref.-H assessment attempted to control complementary filtered sideslip angle, and consequently, to specifically assign a single usable value of effective ARI to the system was difficult. However, it was observed that lateral maneuvering in the region where the LCDP, with ARI=1, was either marginally stable or unstable resulted in undesirable flying qualities and frequent aircraft departures.

During the course of the Ref.-H assessment turning RFLF maneuvers were performed which

21

resulted in varying results. Some pilots had no difficulty performing the turning stall maneuvers whereas some pilots would encounter great difficulty performing the same maneuver. An attempt was made to determine the differences and reasons behind the discrepancies. The analysis of the LCDP parameter indicated a problem would exist for lateral maneuvering flight above 18 to 19 degrees angle of attack. This was substantiated through a review and analysis of the real-time piloted data. Figure 29a presents angle of attack, pilot stick inputs (longitudinal and lateral), and roll angle as a function of time for two attempts of task 5050. One of the attempts resulted in a complete departure of the vehicle (951129 Run 027) and the other a normal recovery (951201 Run 097). Figure 29b presents the additional information of sideslip angle and rudder deflection along with angle of attack for the same conditions as Figure 29a to provide complementary information.

From these figures it can be seen that even though the pilot initiated recovery at only 18 degrees angle of attack for the 951129 Run 027 attempt, a large PIO developed. Examining the pilot stick inputs shows that for the 951129 Run 027 data an aggressive lateral input to level the wings was issued by the pilot simultaneously with a nose-down command at around 51 seconds into the maneuver. This immediately caused sideslip to buildup rapidly even though the rudder was moving at its rate limit to oppose the sideslip buildup as is shown in Figure 29b. The pilot initially was able to begin to reduce angle of attack but the lateral PIO which developed caused him to become distracted and not continue to force the nose down, and just fought the lateral PIO. Eventually, at time equal to about 65 seconds, the stick was released completely resulting in a longitudinal departure of the vehicle. Conversely, the maneuver attempt which resulted in a nominal recovery, 951201 Run 097, involved the pilot issuing a larger nose-down pitch command initially followed by a delayed, and much smaller, lateral control input as shown in Figure 29a. As can also be seen in Figure 29a, the pilot was able to smoothly reduce bank angle and level the wings. Figure 29b shows that for the nominal recovery run sideslip angle was limited to approximately 5 degrees requiring only 10 to 12 degrees of rudder deflection. Overall, the

effect of the recovery method significantly changed the resulting time history data and directly influenced the pilot ratings.

The resulting CHR ratings for the RFLF maneuvers are listed in Table 9. As can be seen in Table 9 the non-turning RFLF maneuvers where rated high level 1/low to mid level 2 for the longitudinal portions of the task. Some of the longitudinal ratings were influenced by the $\dot{\gamma}/V$ control system. Pilots commented that the longitudinal control system introduced problems regarding the control of airspeed decay during RFLF maneuver entries and also produced uncommanded nose-up elevator deflections during maneuver recoveries. These traits are considered to be highly undesirable for this class of maneuvers.

As pointed out in the discussion of Figure 24 to Figure 26, the effective pitch rate acceleration experienced by the pilots during the RFLF recoveries ranged from -2.0 to -3.0 deg/sec-sq. due to non-ideal recovery conditions. Only 2 of the 5 pilots commented that the aircraft had any nose-down control power deficiencies for the non-maximum thrust RFLF maneuvers (tasks 5010, 5040, and 5050). The maximum thrust RFLF maneuver, task 5020, was performed with the M13 mass case and had ample control power available. The 2 pilots that did mention nose-down control power as an issue only indicated minor deficiencies existed, which could indicate that a -4.0 deg/sec-sq. pitch acceleration capability may not be required for this class of aircraft. Lateral ratings for the non-turning RFLF maneuvers were generally level 1 with one pilot rating the lateral portion of task 5020 a CHR of 4. This reflects the fact that few lateral difficulties were encountered performing these maneuvers. Ratings for the turning RFLF maneuvers were considerably higher than the non-turning with CHR ratings well into the level 2 range with some level 3 ratings. Pilots frequently had difficulty controlling the vehicle during recovery from turning flight at high angles of attack. These difficulties correlated well with the stability and control analysis performed using $C_{n\beta-dynamic}$ and LCDP parameters. Individual pilot recovery techniques employed during the recoveries of the turning RFLF maneuvers had a large effect on the resulting aircraft response.

Limited lateral control inputs were required for flight at angles of attack above 18 to 19 degrees.

Summary of results

An initial assessment of the Ref.-H configuration has been conducted with the goal of quantifying the vehicle's capability to meet all envisioned requirements through an application of real-time piloted simulation techniques combined with extensive batch analysis. A total of 5 research pilots participated in the study that evaluated 60 different maneuvers spanning the anticipated operational envelope of the Ref.-H configuration. A subset of the 60 evaluation maneuvers were contained in the Block 1 maneuver sub-set that focused on takeoff and recovery from limit flight conditions. Results of which are documented in this report. Results are summarized as follows:

1) The Block 1 maneuver set was found to be very useful for this initial Ref.-H assessment project. The maneuvers selected exposed a number of problems and deficiencies in various components of the simulation math model that must be addressed before final Ref.-H evaluations can be made. Confirmation of various Ref.-H design strategies were also obtained.

2) Minor HQ and performance deficiencies of the Ref.-H configuration were observed for the takeoff maneuvers element. These deficiencies involved inconsistent rotation performance and resulted from a combination of the modified $\dot{\gamma}/V$ control system and marginal longitudinal control power. It should be noted that the version of the $\dot{\gamma}/V$ control system used for the Ref.-H assessment was not initially designed with takeoff rotations in mind. It was modified to perform adequately during real-time simulation evaluation runs. Modifications made to the $\dot{\gamma}/V$ system should be re-examined thoroughly prior to any future applications of this control system. A slightly larger elevator/horizontal tail could alleviate the minor problems associated with takeoff rotations as well as proper functioning of the

vortex fence. The vortex fence was not active during takeoff operations due to an unchecked simulation implementation error. Further simulation runs made with the vortex fence operating correctly decreased horizontal tail/elevator deflections approximately 10 to 20%.

3) As a result of the vehicle tail scrape limit, lift-off speed, V_{mu}, determined minimum rotation speed with leading/trailing edge flaps set to 30°/10°. However the Ref.-H vehicle was still capable of operating from a 10,000 foot long runway. Although improvements could be made to the Ref.-H vehicle to shorten the takeoff field length through alleviation of the tail scrape angle limit, such as different flap settings, and or increased gear lengths, etc., only non-essential improvements in takeoff performance would result.

4) The $\dot{\gamma}/V$ and p/β control systems worked adequately for the Ref.-H assessment project. Some interpretation of results as well as detailed analysis of the real-time data were required in order to assess the Ref.-H configuration only. As a result of the full-flight envelope evaluation feature of the Ref.-H assessment project, various enhancements of the longitudinal $\dot{\gamma}/V$ and lateral-directional p/β control systems were identified.

5) It was determined that the advanced PLR takeoff procedure was required to meet the anticipated noise regulations. No HQ problems were encountered performing either the standard or PLR acoustic takeoff procedures. Pilots' comments generally indicated that the PLR procedure posed no serious problems and could be a viable takeoff procedure. Noise results indicated that the standard acoustic takeoff procedure required excessive amounts of noise suppression to decrease sideline noise to acceptable levels. Sideline noise also determined the amount of noise suppression required for the PLR procedure.

6) The target maximum demonstration angle of attack selected for the Ref.-H assessment project was 21 degrees. This value was based on preliminary evaluations of the RFLF maneuvers along with a $V_{min-dem}$

23

required calculation. Control system anomalies combined with less than adequate pilot guidance frequently produced maximum angles of attack higher than 21 degrees. Pilots could generally perform the maneuvers, however, some aircraft departures were experienced especially for the turning RFLF tasks. Subsequent analysis of the real-time piloted data combined with a detailed evaluation of stability and control parameters suggests that the maximum angle of attack limit for the Ref.-H, as it is modeled in Cycle-2B, be set to 18 or 19 degrees. This conclusion is based on lateral directional and longitudinal stability and control limitations. The nose-down pitch acceleration capability of the Ref.-H vehicle during the recovery portion tasks 5010, 5040, and 5050 of the RFLF maneuvers was marginal based on an analysis of batch results when compared with a proposed -4.0 deg/sec-sq. pitch rate acceleration requirement. Results from real-time piloted evaluations produced nose-down pitch rate acceleration results significantly below batch analysis predictions due to non-ideal recovery conditions. Pilots frequently experienced nose-down pitch rate accelerations that were only approximately 60% of the specified requirements. Pilot comments, however, did not indicate the lack of

effective nose-down pitch rate acceleration was a large concern and generally felt comfortable with the demonstrated performance, which indicates that the -4.0 deg/sec-sq. nose-down pitch rate criteria may be too high for this class of vehicle.

7) It should be noted that initial preliminary results from the latest NASA LaRC 14x22/Ref.-H wind-tunnel test indicates the low-speed lateral/directional stability and control parameters are significantly underestimated, even in the Cycle-2B modified data release and will be improved in Cycle-3. The improvements involve more accurate modeling of leading- and trailing-edge flap effects for deflections consistent with high angle of attack operations, and could easily place the angle of attack limit well beyond the required angle of attack. $V_{min-dem}$ requirements for approach require approximately a 20 degree angle of attack. Any increases in lateral/directional capability would not significantly raise the suggested angle of attack limit due to limits imposed by the longitudinal nose-down control power available.

Tables

Table 1
Reference-H vehicle geometric parameters

Aerodynamic Parameter	Wing (reference)	Horizontal tail (exposed)	Vertical Tail (exposed)
Area, ft^2	7,100	700	410
Span, ft	129.64	29.56	18.43
Reference chord (MAC), ft	86.02	26.38	25.05
Aspect ratio	2.214	1.248	0.8285
L.E. Sweep, deg.	76.0/68.5/48.0	54.23	52.59
Taper ratio	0.0694	0.2642	0.2398

Table 2
Reference-H control surface span and deflection range

Control surface	Span (ft)	Deflection range (degrees)
Stabilizer	29.56	-15 to +15
Elevator (both halves)	29.56	-30 to +30
Outboard flaperon (#1 and #8)	14.73	-40 to +40
Outboard flap (#2 and #7)	13.78	-40 to +40
Inboard flaperon (#3 and #6)	7.04	-40 to 40
Inboard flap (#4 and #5)	8.97	-40 to +40
Outboard L.E. flap (#1 and #4)	34.58	0 to +50
Inboard L.E. flap (#2 and #3)	13.96	0 to +50
Rudder (lower segment)	7.16	-30 to 30
Rudder (mid. segment)	5.00	-30 to 30
Rudder (upper segment)	6.69	-30 to 30
Vortex fence	8.82	0 to +90

Table 3
Reference-H mass properties

Mass case	G.W. (lbs)	I_{xx} (slg-ft2)	I_{yy} (slg-ft2)	I_{zz} (slg-ft2)	I_{xz} (slg-ft2)	C.G. (%mac)
MFC	384,862	3,185,260	43,953,900	46,653,700	155,467	53.2
M13	649,914	4,552,820	51,814,400	55,762,300	448,324	48.1

Table 4
Engine out thrust table for modified engine failure option
(all thrust units are lbs.)

Mach	H=0	H=2,000 ft	H=4,000 ft
0.0	0	0	0
0.1	-1429.9	-1329.5	-1234.9
0.2	-3011.8	-2800.3	-2601.0
0.3	-4901.1	-4556.9	-4232.6
0.4	-6878.9	-6396.0	-5940.7

Table 5

Listing of NASA LaRC Ref.-H assessment maneuvers

#	Task#	Priority	MTE	Flight Card Name

Block 1

Familiarization

#	Task#	Priority	MTE	Flight Card Name
1	2010	5	100	Standard acoustic takeoff
2	4020	31	301	Nominal Approach & Landing

Takeoff

#	Task#	Priority	MTE	Flight Card Name
3	2010	5	100	Standard acoustic takeoff
4	2030	4	102	Acoustic Program Lapse Rate (PLR) takeoff
5	1050	6	005	Refused Takeoff
6	1051	6	005	Refused Takeoff - 15 kt x-wind
7	1052	6	005	Refused Takeoff - 35 kt x-wind
8	7035	19	100	One Engine Out Takeoff
9	7030	19	602	VMCG

Recovery from Limit Flight Envelope

#	Task#	Priority	MTE	Flight Card Name
10	5020	9	401	Stall at Max Takeoff Power, M13 mass case
11	5010	7	400	Stall at Idle Power, MFC mass case
12	5040	10	403	Turning Stall at Idle Power, MFC mass case
13	5050	11	404	Turning Stall at Thrust for Level Flight, MFC mass case

Block 2A

Approach, Landing, Go-Around

#	Task#	Priority	MTE	Flight Card Name
14	4020	31	301	Nominal Approach & Landing
15	4025	31	301	Nominal Approach & Landing with flight director
16	4050	32	303	Precision Landing Flare, Touchdown, and Derotation
17	4062	16	304	Lateral Offset Landing - Moderate Turbulence
18	4066	16	304	Lateral Offset Landing - Category 1 / Moderate Turbulence
19	4072	17	305	Vertical Offset Landing - Moderate Turbulence
20	4076	17	305	Vertical Offset Landing - Category 1 / Moderate Turbulence
21	4080	14	306	Go-Around (100')
22	4085	14	307	Go-Around with Minimum Altitude Loss

Block 2B

Approach and Landing, Weather/Failures

#	Task#	Priority	MTE	Flight Card Name
23	4020	31	301	Nominal Approach & Landing
24	4090	2	313	Crosswind Landing - 15 kt
25	4095	2	313	Crosswind Landing - 35 kt
26	4100	29	313	Landing in Cat IIIa Conditions
27	4110	30	313	Landing with Jammed Control
28	7050	18	606	Dynamic V_{MCL-2}
29	7095	23	313	Manual Thrust Landing
30	7110	24	313	Unaugmented Landing - Single axis failed
31	7100	25	313	Unaugmented Landing
32	7090	23	609	All Engine out Landing

Block 3

Operations after Failure, Upsets

33	7060	1	610	Engine Unstart
34	6050	26	504	Inadvertent Speed Increase, High speed
35	6060	12	505	Simulated 2-axis Gust Upset, High speed
36	7010	21	600	Directional Control with 1 Engine out
37	7020	22	601	Lateral Control with 1 Engine Out
38	7040	20	604	Dynamic V_{MCA}

Trajectory Management

39	3030	15	210	Profile Climb
40	5070	3	409	Emergency Descent

Block 4 (Lower Priority Tasks)

Upset Recovery, Engine-Out Stalls

41	5060	8	408	Diving Pull-out
42	6040	13	503	C.G. Shift, High Speed
43	7070	27	608	Engine-out Stall
44	7080	28	609	Engine-out Turning Stall

Climb, Cruise, Descent

45	3020	39	201	Climb Trans. to Level Flight - Transonic
46	3022	39	201	Climb Trans. to Level Flight - Supersonic
47	3040	40	211	Level Flight Trans. to Climb
48	3050	38	220	Profile Descent
49	3060	41	221	Level Flight Trans. to Descent - Supersonic
50	3062	41	221	Level Flight Trans. to Descent - Transonic
51	3070	37	230	Transonic Accel
52	3072	37	230	Supersonic Accel
53	3074	37	230	Transonic Decel
54	3076	37	230	Subsonic Decel
55	3080	36	240	Heading Change - Transonic Climb
56	3082	36	240	Heading Change - Initial Cruise
57	3084	36	240	Heading Change - Final Cruise
58	3086	36	240	Heading Change - Transonic Descent
59	3088	36	240	Heading Change - TCA Descent

Misc.

60	4012	35	300	Configuration Change, Moderate Turbulence

Count 60

Table 6

Takeoff performance data for the Ref.-H assessment project

(Leading-edge flaps set to 30 and trailing-edge flaps set to 10 degrees. M13 mass case)

	2010 (Mean)	2010 (SDEV)	2030 (Mean)	2030 (SDEV)	7035 (Mean)	7035 (SDEV)
SX_{LO} (ft)	6486	143	6880	68	6794	246
V_{LO} (kts)	198	2.2	199	1.0	190	2.7
θ_{max} (deg)	10.2	0.36	10.0	0.24	10.6	0.53
SX_{OBS} (ft)	7942	413	9077	1089	9389	560
V_{35} (kts)	209	5.0	213	6.6	201	3.5
Number of samples	14		11		13	

Table 7

Definition of takeoff maneuver pilot rating segments

Segment#	Name	Cooper-Harper rating	Definition
1	On runway pre-rotation	Lateral only	Aircraft speed less than V_1 for continued takeoff maneuvers. Note that rejected takeoff maneuvers only had one segment even though aircraft speed sometimes exceeded V_r during decelerations.
2	Rotation for lift-off	Lateral and Longitudinal	Aircraft speed greater than or equal to V_1 for continued takeoff maneuvers and aircraft landing gear altitude less than 1.0 feet.
3	Airborne	Lateral and Longitudinal	Landing gear height greater than 1.0 feet

Table 8

Cooper-Harper ratings for the Takeoff maneuvers

(Column labels A,B,C,D,E refer to ratings provided from pilots A,B,C,D,E, respectively)

Longitudinal CHR ratings

Task I.D.	A	B	C	D	E	avg	σ	
2010								segment 1
2030								
1050								
1051								
1052								
7035								
2010	2	4	4	4	3	3.40	0.89	segment 2
2030	1	3	3	4	3	2.80	1.10	
1050								
1051								
1052								
7035	4	3	3	4	4	3.60	0.55	
2010	1	3	4	4	3	3.00	1.22	segment 3
2030	1	3	3	3	3	2.60	0.89	
1050								
1051								
1052								
7035	2	3	4	4	3	3.20	0.84	

Lateral CHR ratings

Task I.D.	A	B	C	D	E	avg	σ	
2010	1	2	4	3	3	2.60	1.14	segment 1
2030	1	2	4	3	3	2.60	1.14	
1050	1	3	3	4	3	2.80	1.10	
1051	1	3	3	4	3	2.80	1.10	
1052	1	3	3	4	3	2.80	1.10	
7035	4	5	4	3	3	3.80	0.84	
2010	2	2	3	2	4	2.60	0.89	segment 2
2030	1	2	3	2	4	2.40	1.14	
1050								
1051								
1052								
7035	4	5	3	5	4	4.20	0.84	
2010	1	2	3	2	3	2.20	0.84	segment 3
2030	1	2	4	3	3	2.60	1.14	
1050								
1051								
1052								
7035	4	5	4	3	3	3.80	0.84	
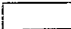
Level 1 CHR = ☐   Level 2 CHR = ▨   Level 3 CHR = ▧

Table 9

Cooper-Harper ratings for the Recovery From Limit Flight (RFLF) maneuvers

(Column labels A,B,C,D,E refer to ratings provided from pilots A,B,C,D,E, respectively)

Longitudinal CHR ratings

Task I.D.	A	B	C	D	E	avg	σ
5020	-	3	5	3	3	3.50	1.00
5010	-	-	3	5	3	3.67	1.15
5040	-	4	3	5	3	3.75	0.96
5050	-	4		5	4	5.25	1.89

Lateral CHR ratings

Task I.D.	A	B	C	D	E	avg	σ
5020	-	2	2	2	4	2.50	1.00
5010	-	-	3	3	2	2.67	0.58
5040	-	4		6	4	5.50	1.91
5050	-	4		6	3	5.25	2.22

Level 1 CHR = ☐   Level 2 CHR = ☐   Level 3 CHR = ▧

References

ref 1 Dieudonne, James E.; Parrish, Russell V. ; and Bardusch, Richard E. : An Actuator Extension Transformation for a Motion Simulator and an Inverse Transformation Applying Newton-Raphson's Method. NASA TN D-7067, 1972.

ref 2 Parrish, Russell V.; Dieudonne, James E.; Martin, Dennis J., Jr.; and Copeland, James L.: Compensation Based on Linearized Analysis for a Six-Degree-of-Freedom Motion Simulator. NASA TN D-7349, 1973.

ref 3 Parrish, Russel V.; Dieudonne, James E.; Boles, Roland L. and Dennis J., Jr.: Coordinated Adaptive Washout for Motion Simulators. J. Aircraft, vol 12, no 1, Jan. 1975, pp. 44-50.

ref 4 Martin, D. J., Jr.: A Digital Program for Motion Washout on Langley's Six-Degree-of-Freedom Motion Simulator. NASA CR-145219, 1977.

ref 5 Dornefeld, G. M.; Lanier, J. K.; Milligan, K. H.; Parker, J. M.; Phillips, B. A.; Stephens, A. T.: *High Speed Civil Transport Reference H-Cycle 2B Simulation Data Base*. NASA Contract NAS1-20220.

ref 6 Grantham, William D.; Smith Paul M.; and Deal Perry L.: *A Simulator Study for the Development and Evaluation of Operating Procedures on a Supersonic Cruise Research Transport To Minimize Airport-Community Noise*. NASA TP-1742, 1980.

ref 7 Olson, E. D.: *Advanced Takeoff Procedures for High-Speed Civil Transport Community Noise Reduction*. SAE Technical Paper Series 921939, Aerotech '92, Anaheim, CA. October 5-8, 1992.

ref 8 Glaab, Louis J.; Riley, Donald R.; Brandon, Jay M.; Person, Lee H.; Glaab, Patricia C.: *Piloted Simulation Study of the Effect of High-Lift Aerodynamics on the Takeoff Noise of a Representative High-Speed Civil Transport*. NASA/TP-1999-209696, 1999.

ref 9 Riley, Donald R.; Glaab, Louis J.; Brandon, Jay M.; Person, Lee H.; Glaab, Patricia C.: *Piloted Simulation Study of a Dual Thrust-Cutback Procedure for Reducing HSCT Takeoff Noise Levels*. NASA/TP-1999-209698, 1999.

ref 10 Zorumski, William E.: *Aircraft Noise Prediction Program Theoretical Manual*. NASA TM-83199, 1982.

ref 11 Ogburn, Marilyn E.; et. al.: *High-Angle-of-Attack Nose-Down Pitch Control Requirements for Relaxed Static Stability Combat Aircraft*. NASA High-Angle-of-Attack Technology Conference, NASA Langley Research Center, Hampton, VA, October 30-November 1, 1990. NASA CP-3149, 1992, Volume I, Part 2, Paper No. 24.

Figures
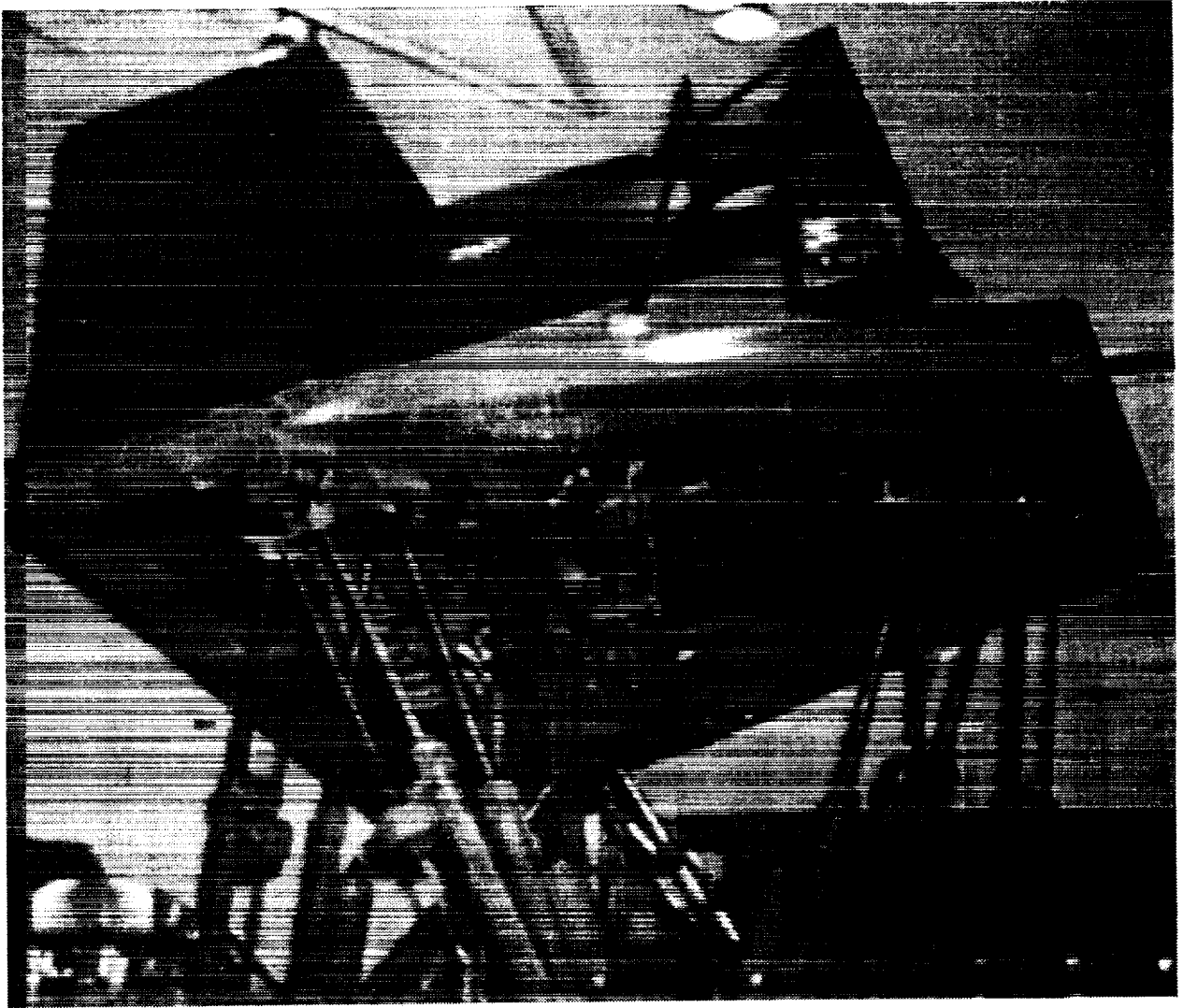
Figure 1. NASA Langley six-degree-of-freedom Visual/Motion Simulator.
(L 75-07570)

32
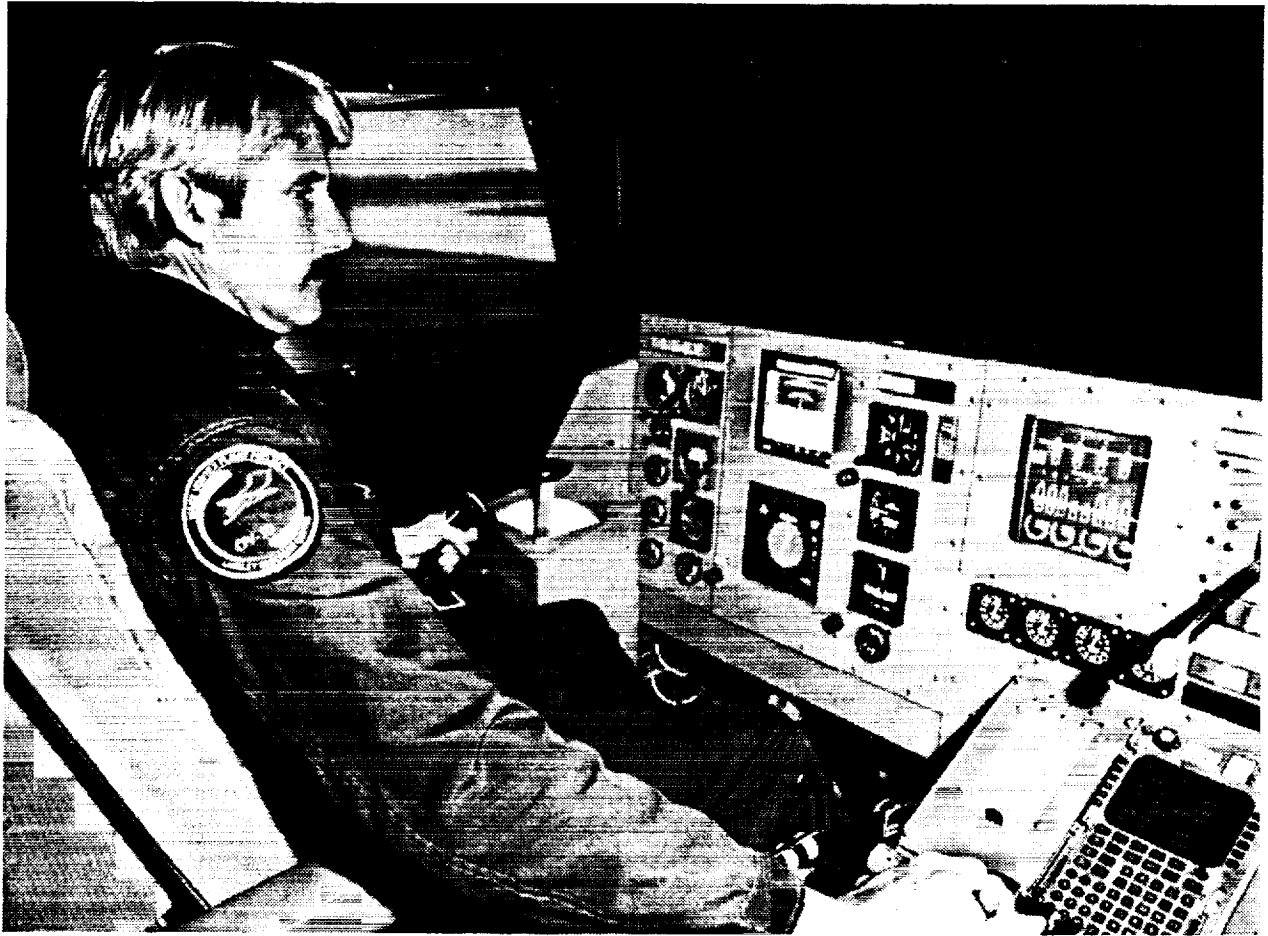
Figure 2. Interior view of NASA LaRC six-degree-of-freedom Visual/Motion Simulator.

129' 8"

311' 2"
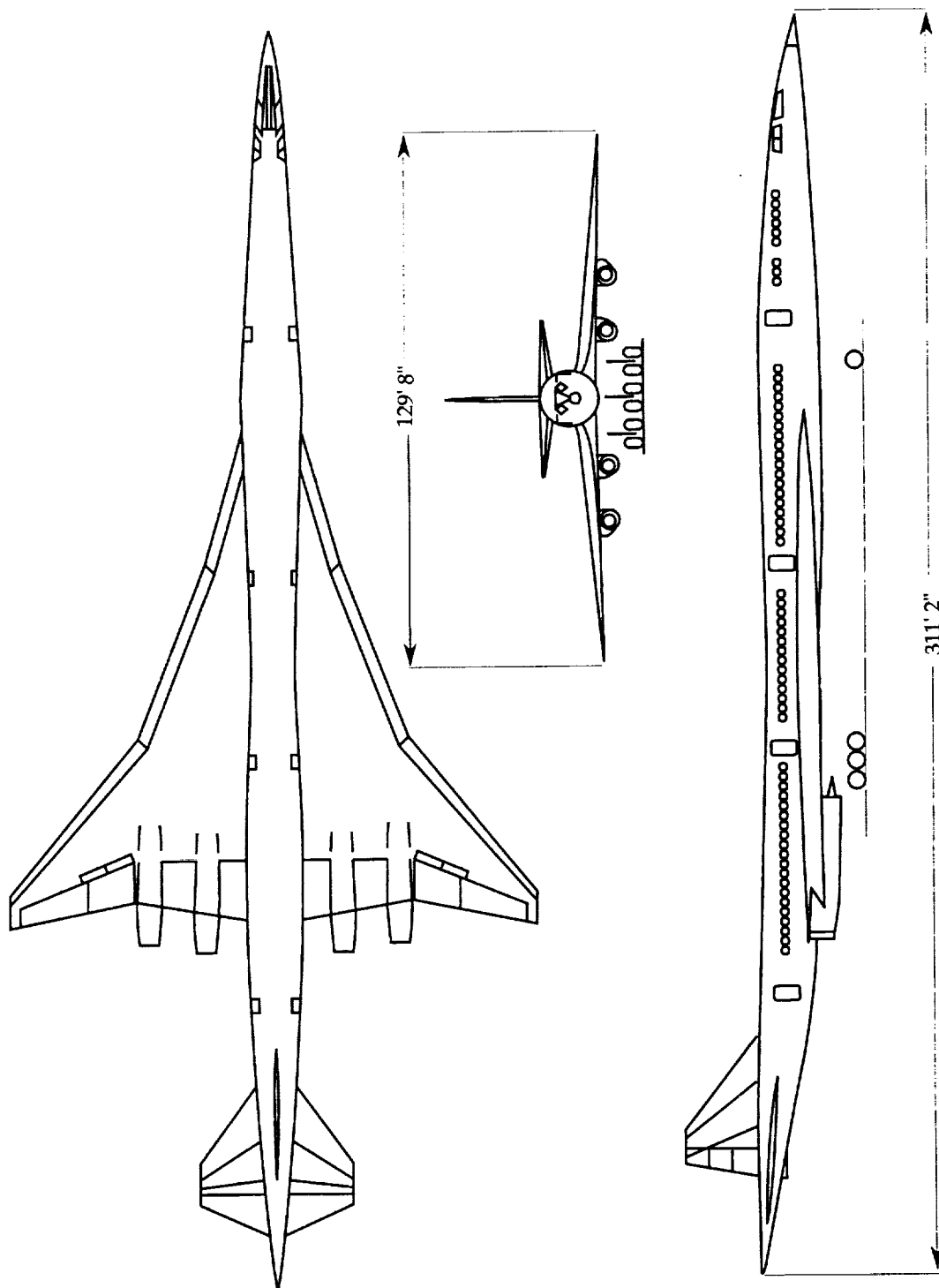
a) Three view drawing of Reference-H configuration.

Figure 3. Views of the Refernce-H configuration

34
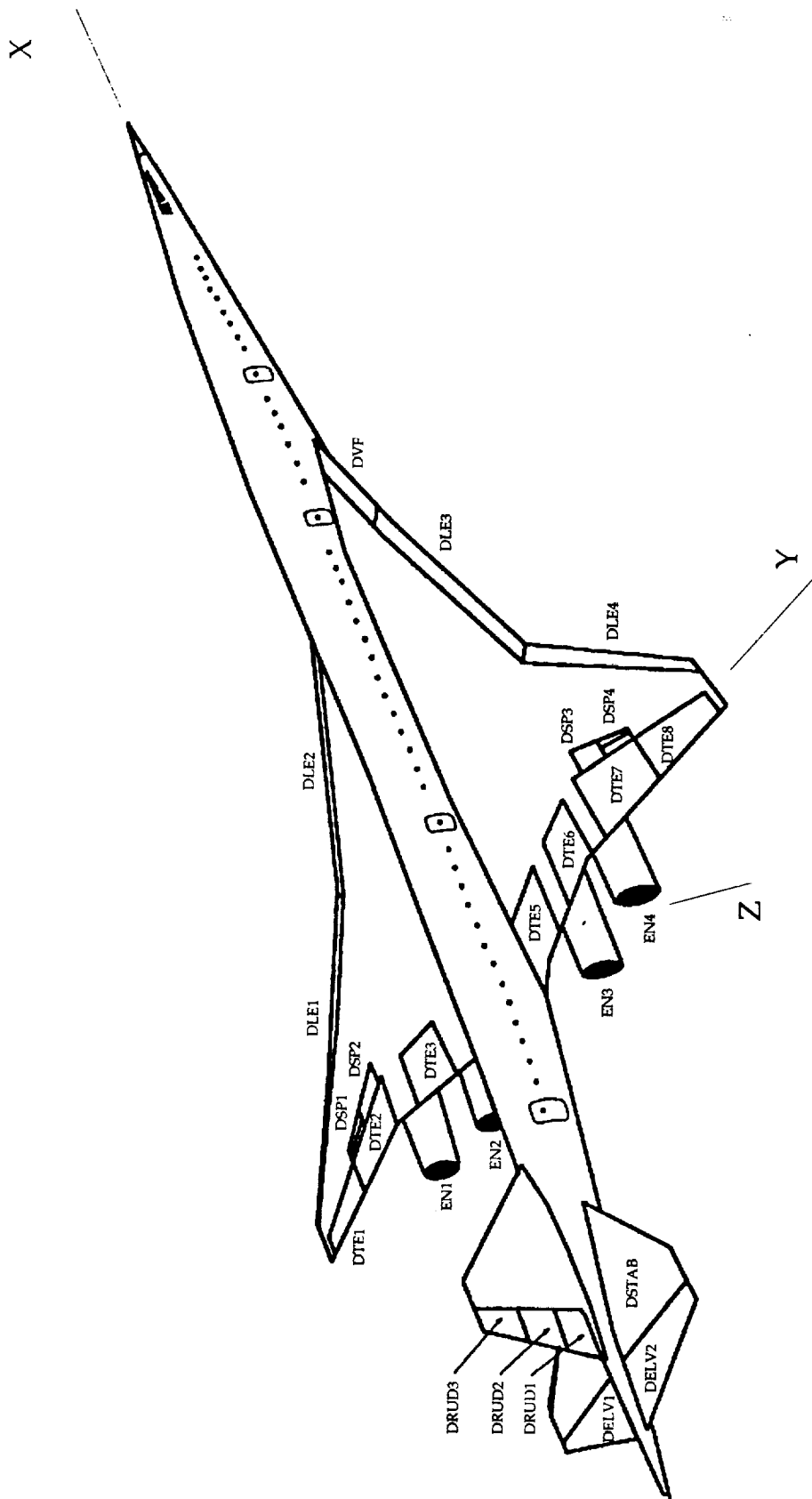
b) Three-quarter rear view of Reference-H configuration showing control surface identifications as axis system employed.

Figure 3 concluded

35
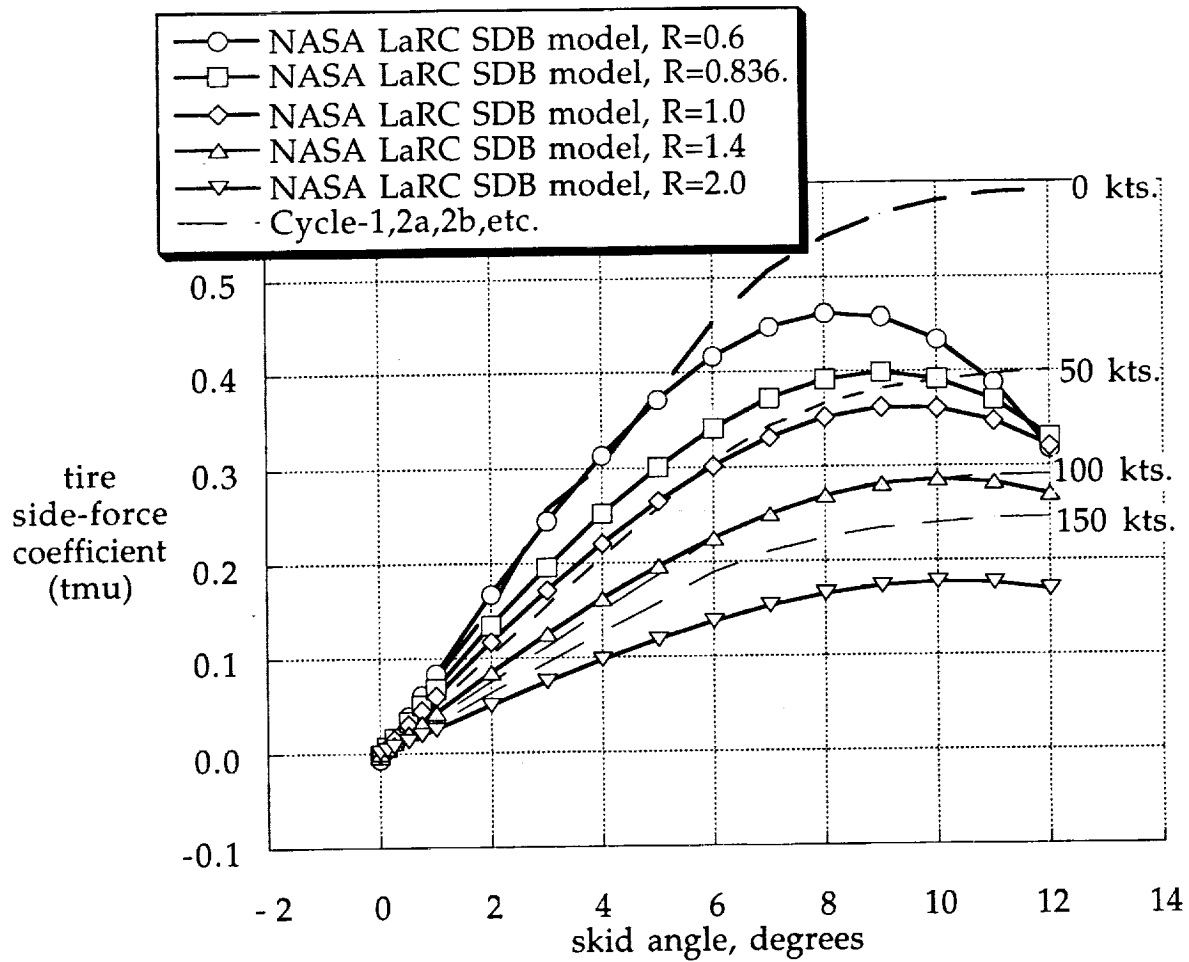
Figure 4. Comparison of Ref.-H Cycle-1, 2A, 2B tire cornering model with the NASA LaRC SDB cornering model.
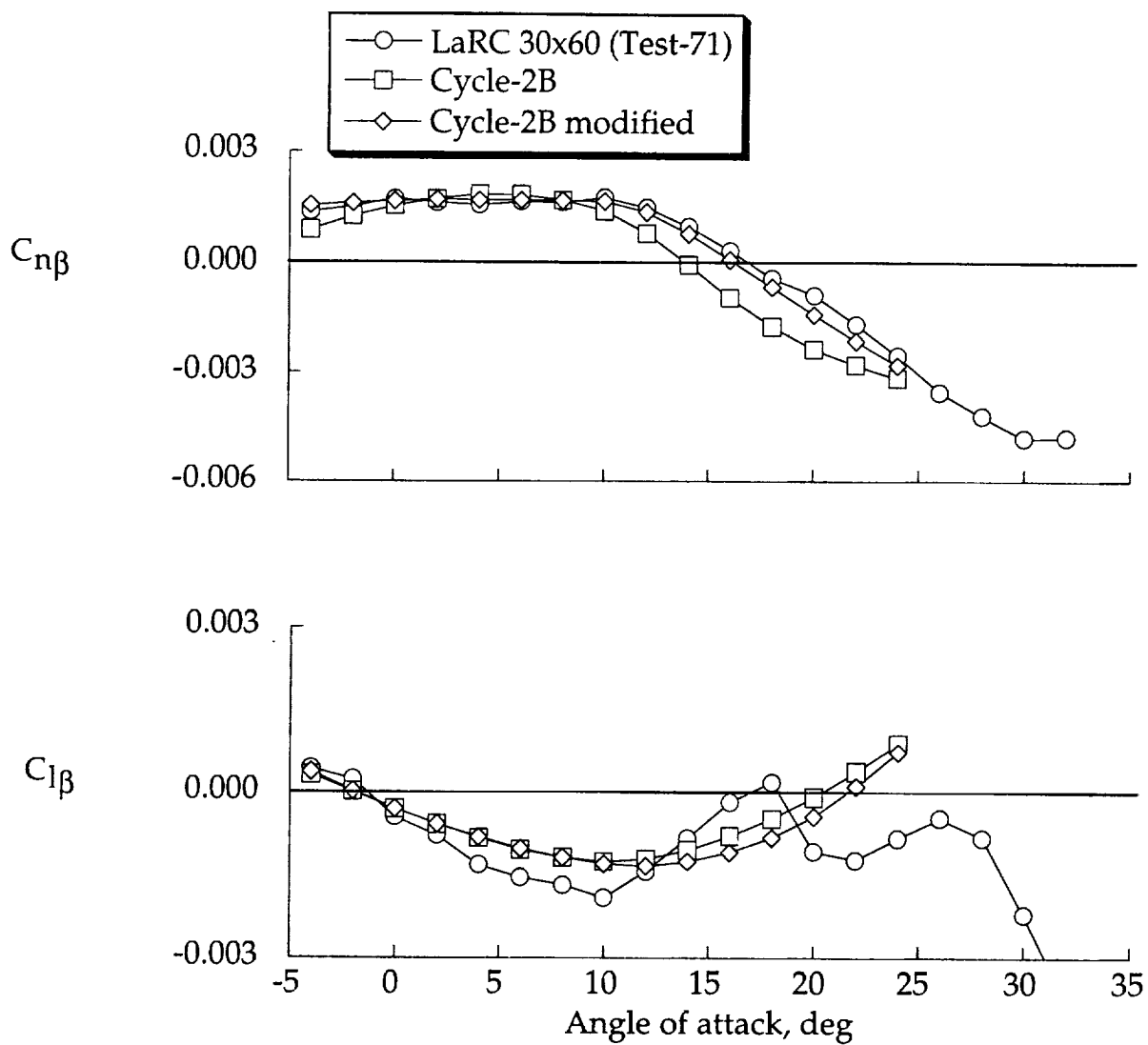
Figure 5. Body axis $C_{n\beta}$ and $C_{l\beta}$ as a function of angle of attack. All control surfaces set to zero. Cycle-2B data was obtained with the aircraft positioned out of ground-effect, M=0.3, with rigid aerodynamics selected
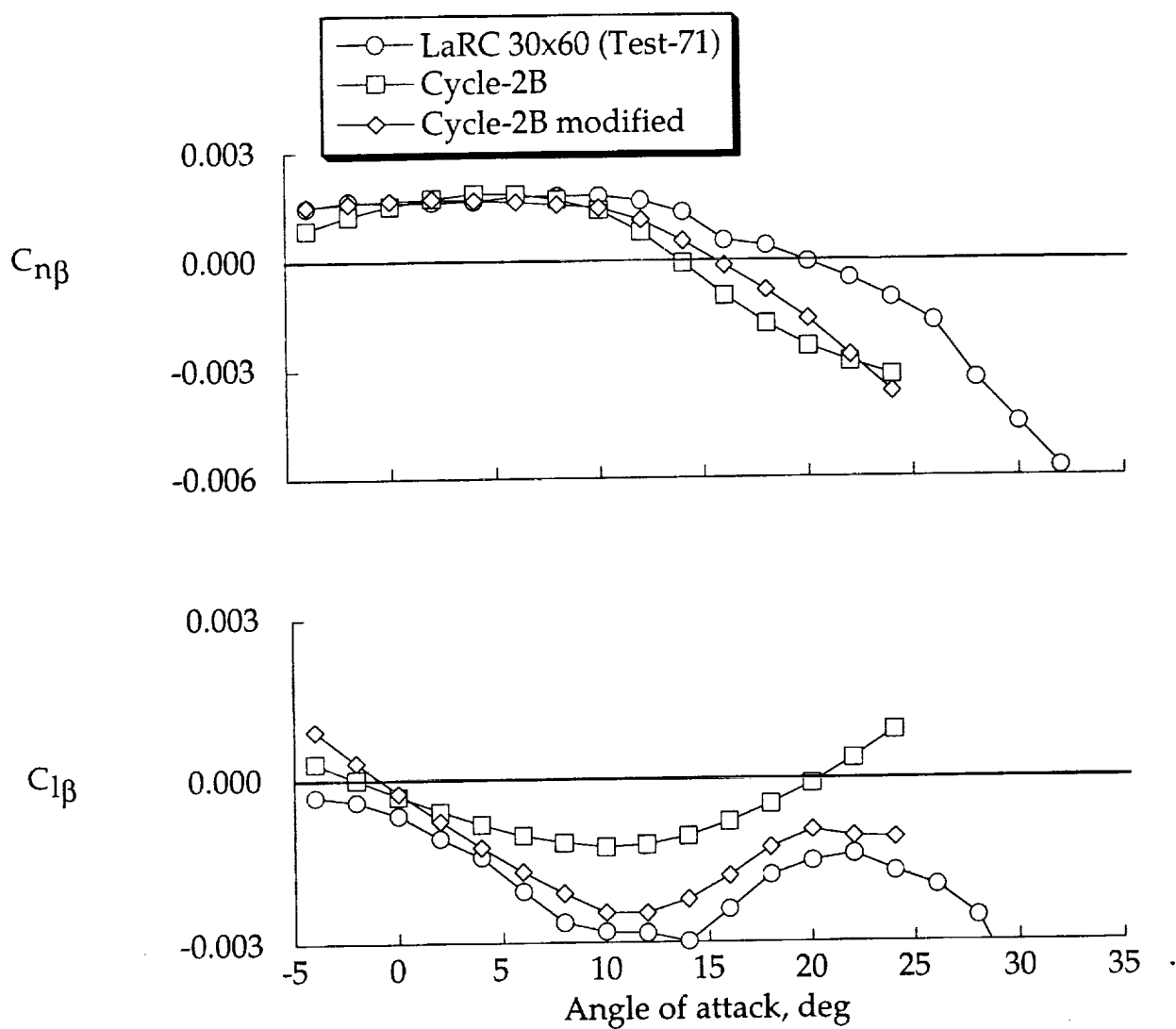
Figure 6. Body axis $C_{n\beta}$ and $C_{l\beta}$ as a function of angle of attack. Leading-edge flaps set to 30 degrees, and trailing-edge flaps set to 10 degrees. All other control surfaces set to zero. Cycle-2B data was obtained with the aircraft positioned out of ground-effect, M=0.3, with rigid aerodynamics selected

ADEQUACY FOR SELECTED TASK
OR
REQUIRED OPERATION*

AIRCRAFT
CHARACTERISTICS

DEMAND ON THE PILOT
IN SELECTED TASK
OR REQUIRED OPERATION*

CHR
RATING

FLYING
QUALITY
LEVEL

AIRCRAFT CHARACTERISTICS	DEMAND ON THE PILOT IN SELECTED TASK OR REQUIRED OPERATION*	CHR RATING	FLYING QUALITY LEVEL
Excellent Highly desirable	Pilot compensation not a factor for desired performance	1	1
Good Negligible deficiencies	Pilot compensation not a factor for desired performance	2	
Fair - Some mildly unpleasant deficiencies	Minimal pilot compensation required for desired performance	3	
Minor but annoying deficiencies	Desired performance requires moderate pilot compensation	4	2
Moderately objectionable deficiencies	Adequate performance requires considerable pilot compensation	5	
Very objectionable but tolerable deficiencies	Adequate performance requires extensive pilot compensation	6	
Major deficiencies	Adequate performance not attainable with maximum tolerable pilot compensation. Controllability not in question.	7	3
Major deficiencies	Considerable pilot compensation is required for control	8	
Major deficiencies	Intense pilot compensation is required to retain control	9	
Major deficiencies	Control will be lost during some portion of required operation	10	

Is it satisfactory without improvement? — Yes / No

No → **Deficiencies warrant improvement**

Is adequate performance attainable with a tolerable workload? — Yes / No

No → **Deficiencies require improvement**

Is it controllable? — Yes / No

No → **Improvement mandatory**

Pilot decisions

*Definition of required operation involves designation of flight phase and/or subphases with accompanying conditions.

Figure 7. Cooper-Harper rating scale and corresponding flying qualities levels.
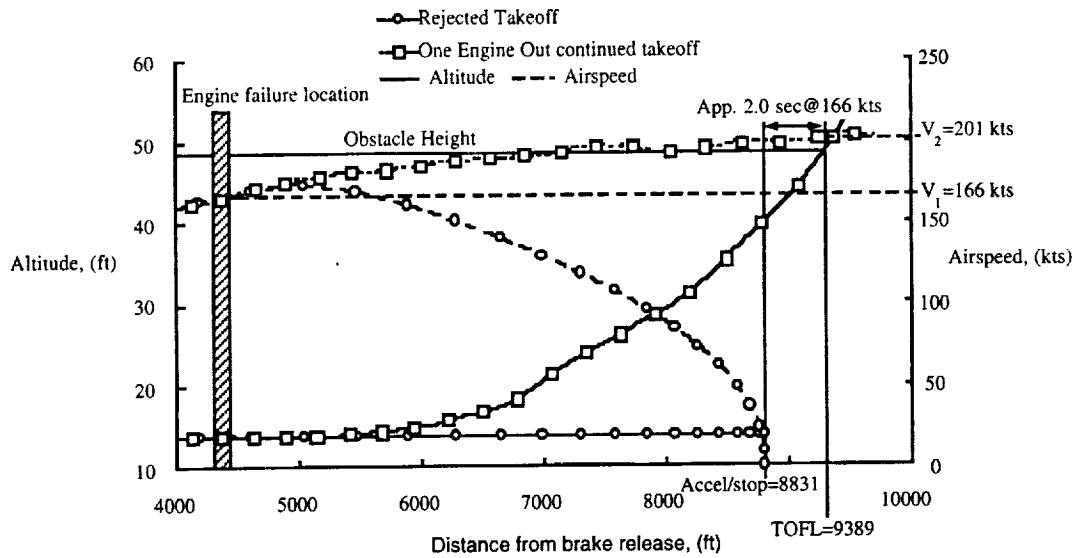
Figure 8. Demonstration of V_1 and V_r speeds. M13 mass case selected. Leading-edge flaps set to 30 degrees, all trailing-edge flap segments set to 10 degrees.
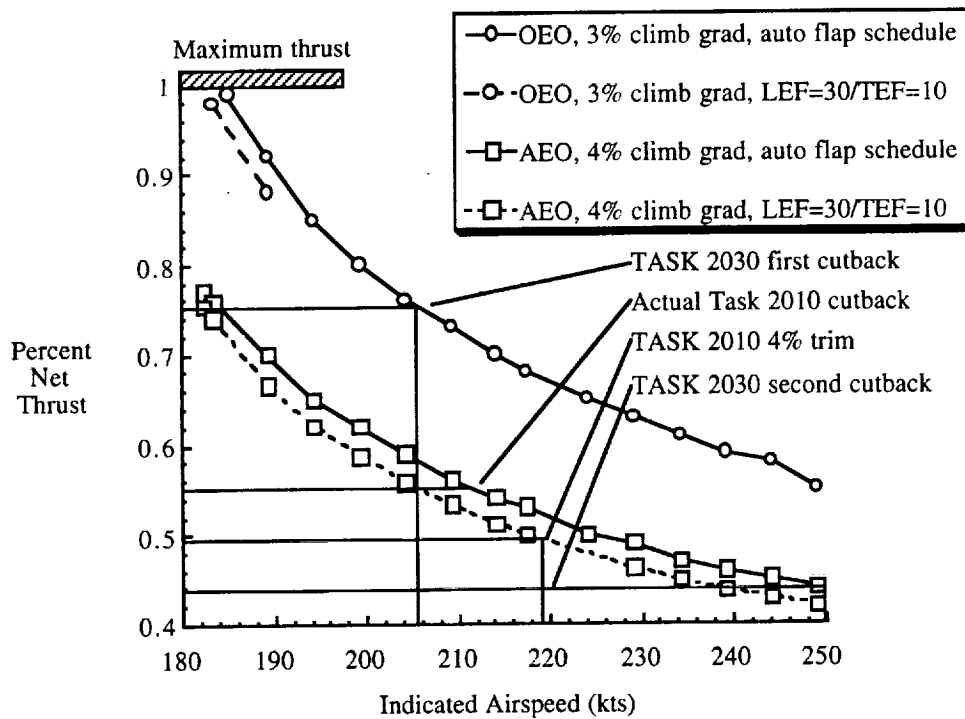
Figure 9. Trim analysis of the Ref.-H vehicle to support rotation speed, climb speed, and level of thrust cutback calculations.

Figure 10 diagram labels:

28
180 GS
0.28 M
1.00 G
7.4 a

Target pitch attitude marker
(desired=+/-0.5, adequate=1.0 degs.)

Pitch rate error brackets
Enlarged reference pitch indicator

4.0 %   4.0% Target climb gradient (PLR maneuver only)

180   000

Pitch rate error pilot metric bounds:

Adequate: +/-1.2 deg/sec

Desired: +/-0.6 deg/sec

Run 001
00:00 ET
12-12-99
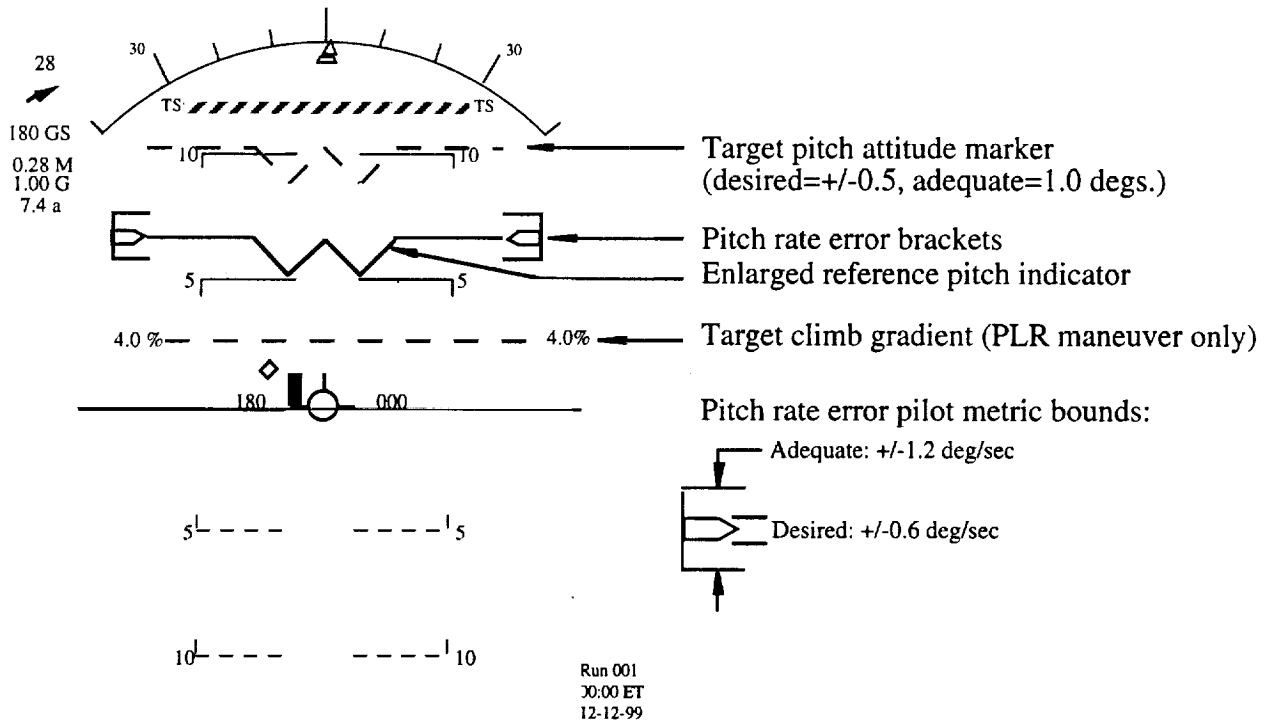
Figure 10. Heads Up Display configuration shown to the pilots during takeoff rotations.

28
258 GS
0.28 M
1.00 G
7.4 a

Normal size pitch reference marker

255   1250
4.0 %   4.0% Velocity vector guidance marker
(lateral and longitudinal guidance)
Target climb gradient (PLR maneuver only)

Velocity vector error pilot metric bounds:

Desired: +/-1 marker width
90% of the time

Marker width=0.85 degrees

Adequate: +/-2 marker widths
90% of the time

Run 001
00:00 ET
12-12-99
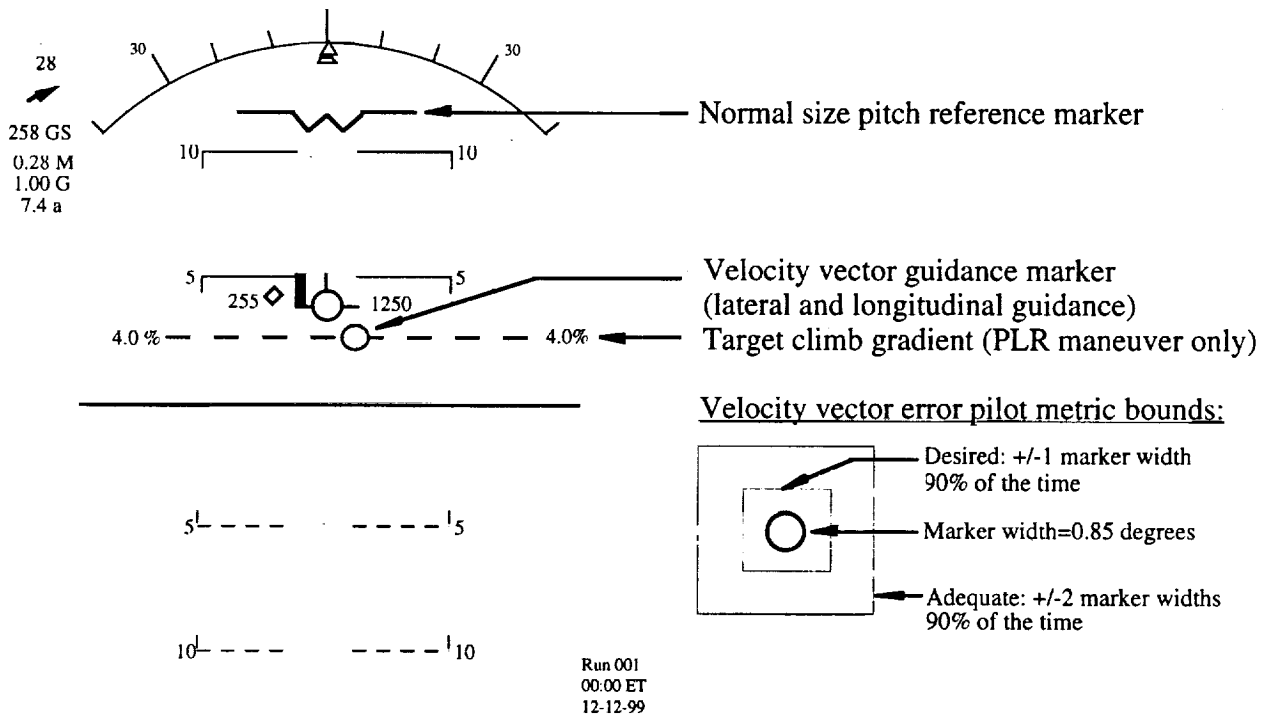
Figure 11. Heads Up Display configuration shown to the pilots during airborne takeoff maneuvers.

41

Centerline point ■

Stage 3 noise
evaluation line.

21325 feet

1476 feet.

Liftoff point.

Brake release.

6562 feet

Approach point ■

42
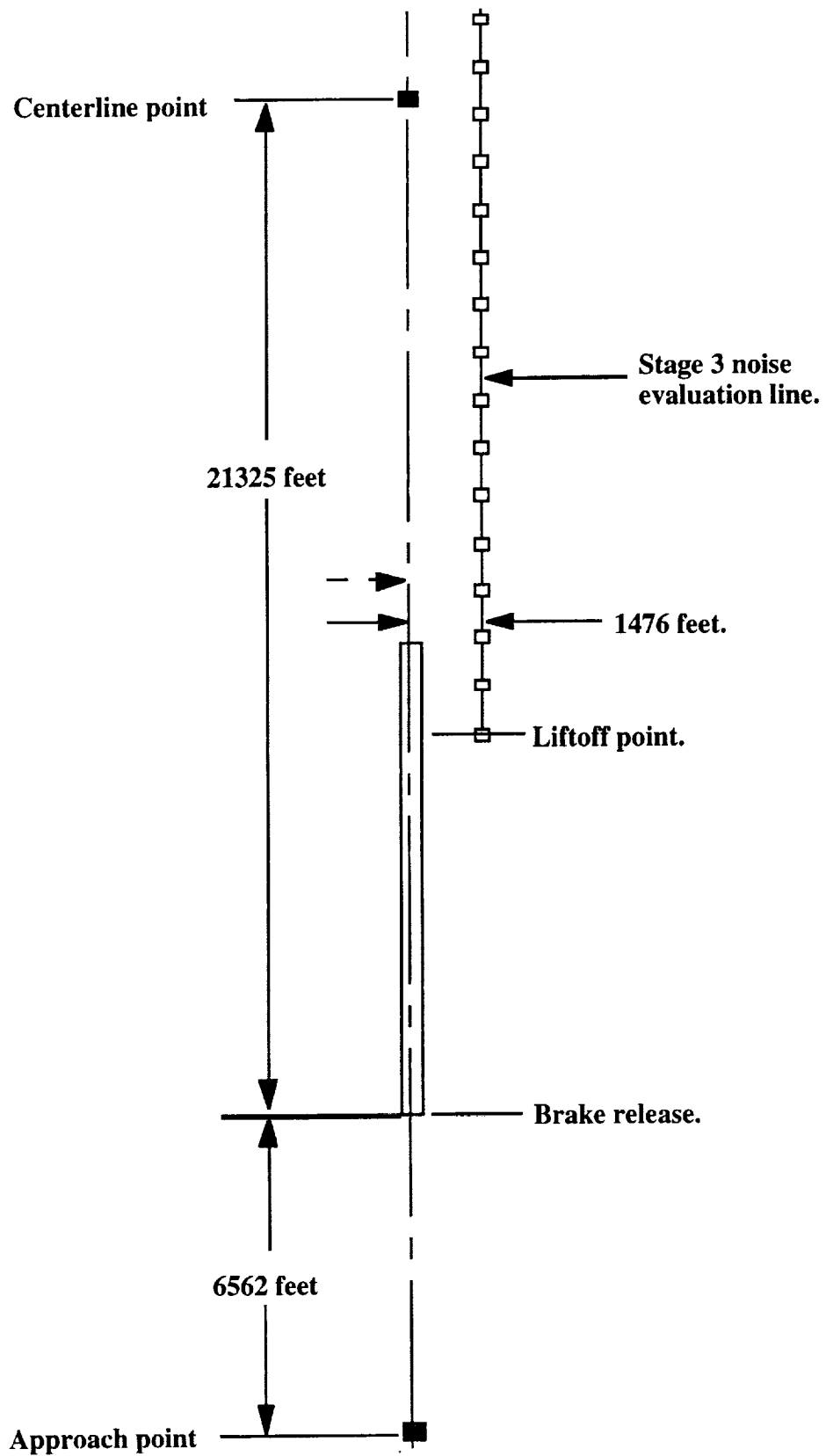
Figure 12. FAR Part 36 noise measurement system layout.
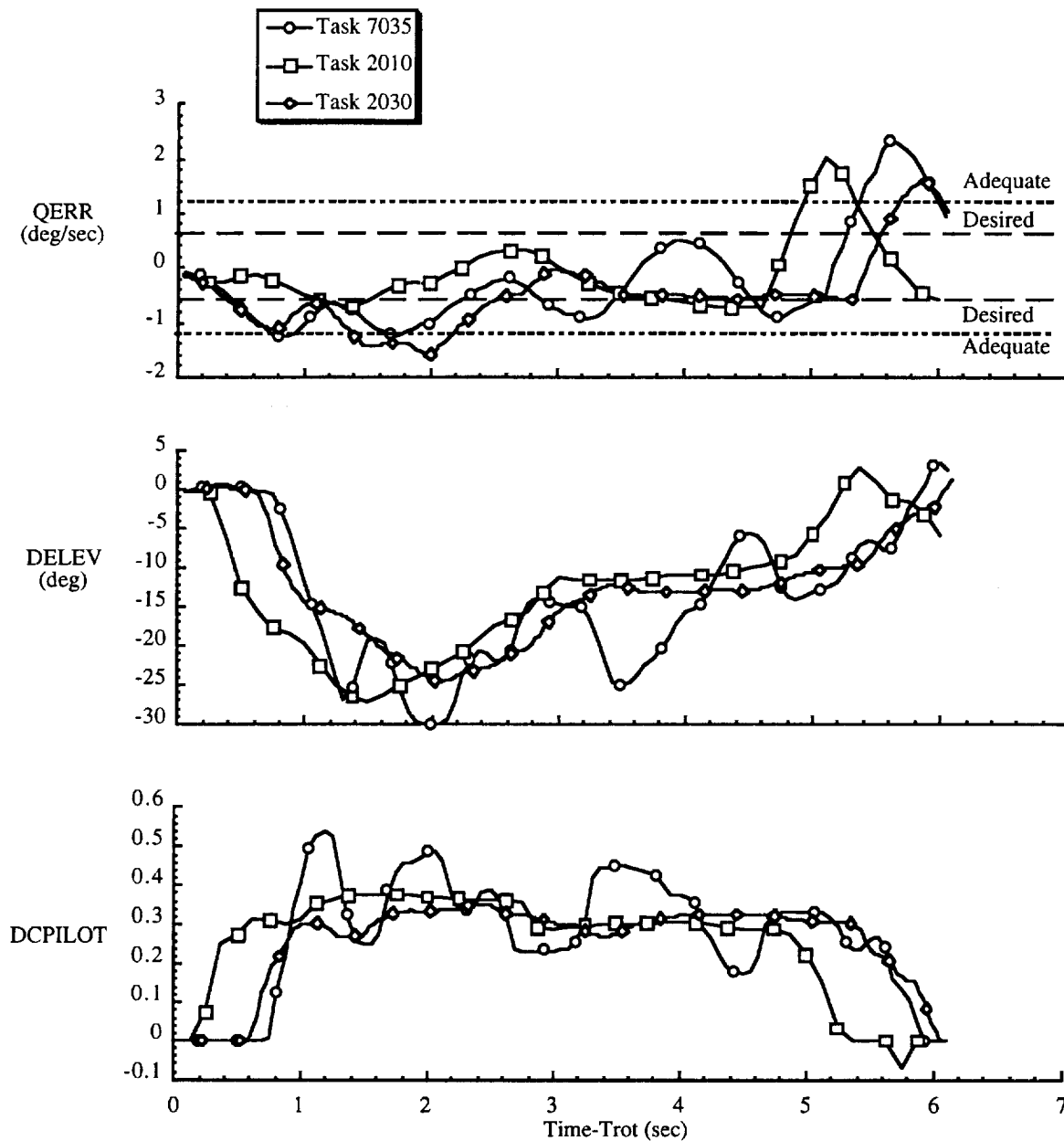
Figure 13. Representative pilot performance during takeoff rotation maneuvers. This figure shows pitch rate error, elevator position, and longitudinal stick pilot inputs as a function of time from rotation initialization.
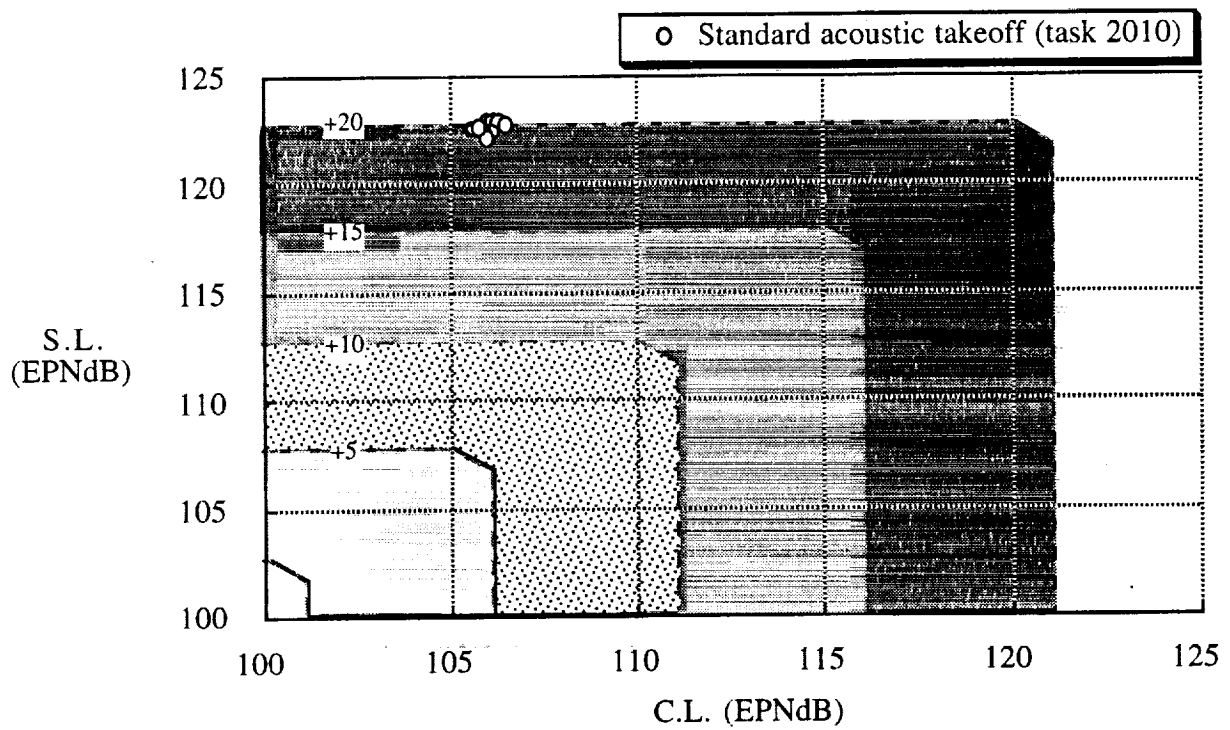
Figure 14. Noise suppression required to meet stage-3 minus 1,5,1 noise levels. Boundaries assume approach noise to be at or below 99.2 EPNdB.
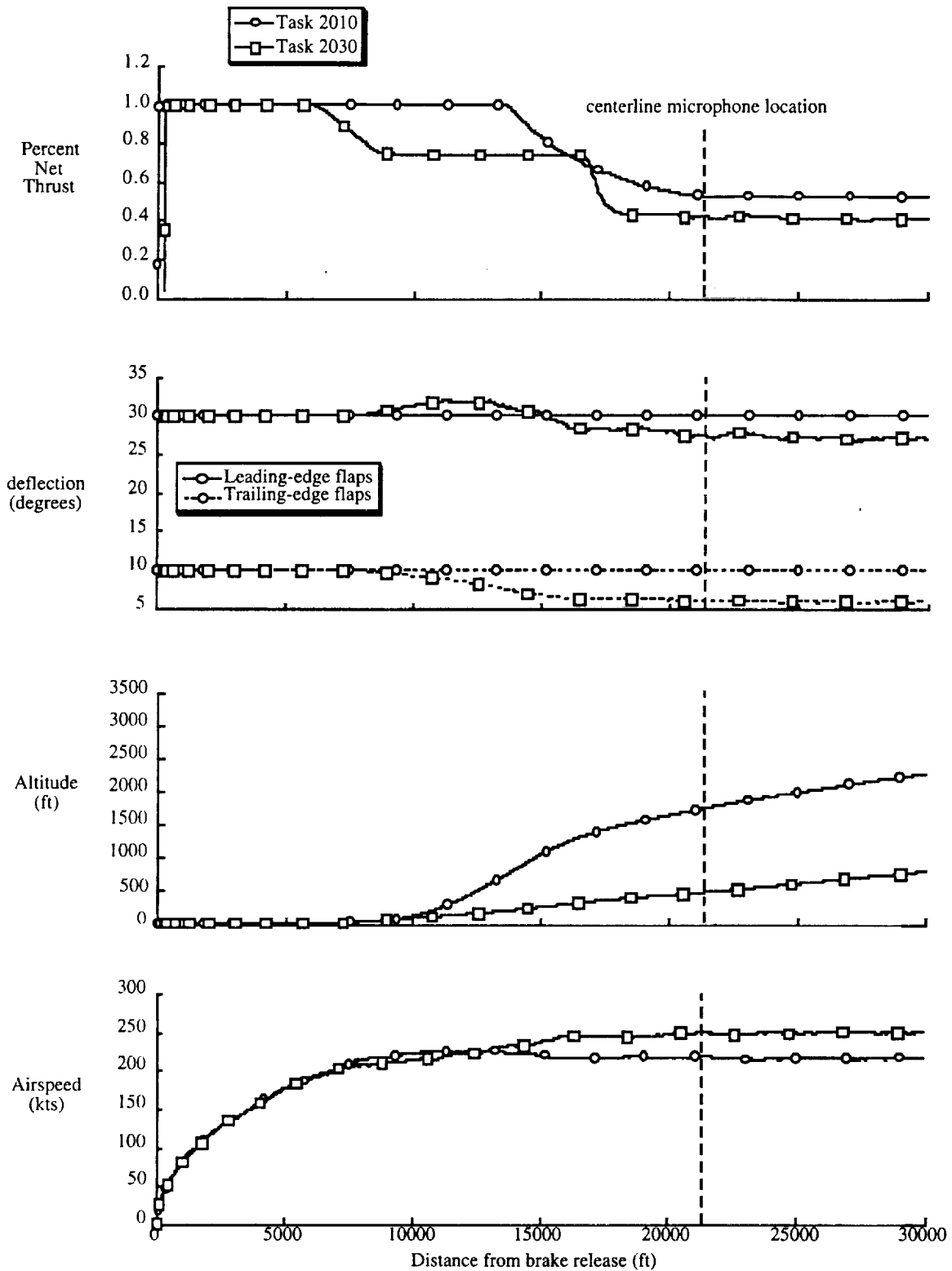
Figure 15. Comparison of thrust, leading- and trailing-edge flap deflections, altitude and airspeed as a function of distance from brake release.
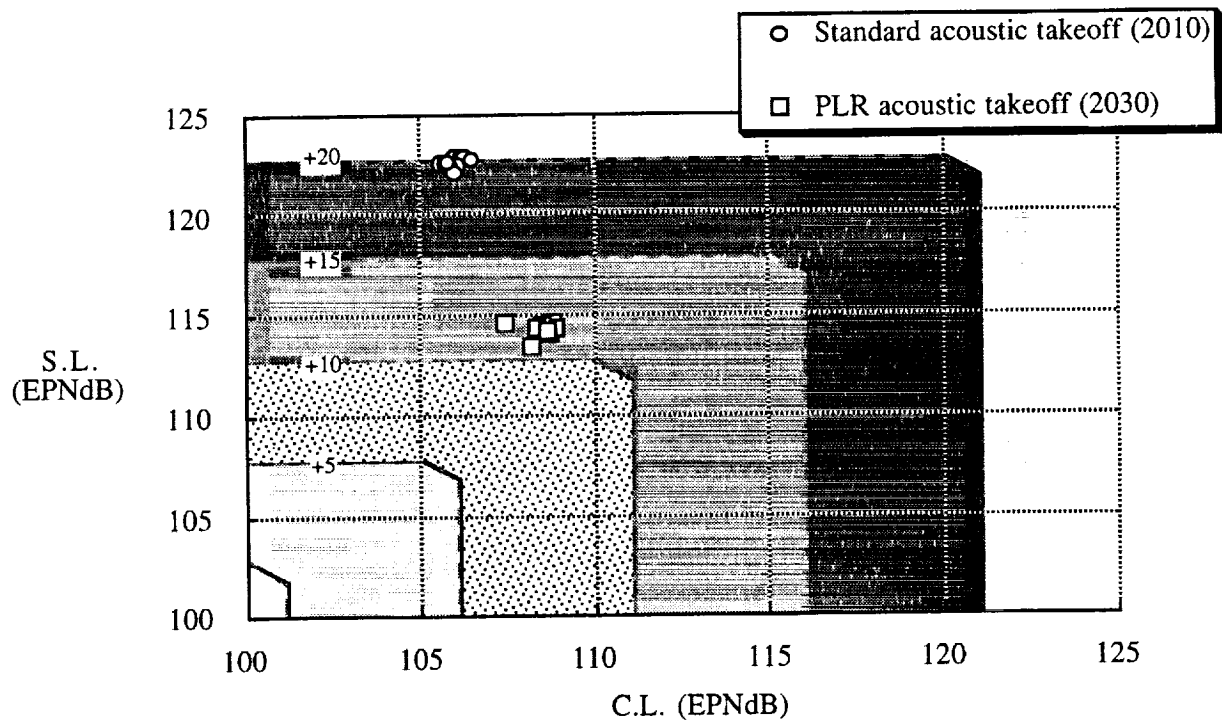
Figure 16. Comparison of noise suppression required to meet stage-3 minus 1,5,1 noise levels for Task 2010 and Task 2030 procedures. Boundaries assume approach noise to be at or below 99.2 EPNdB.
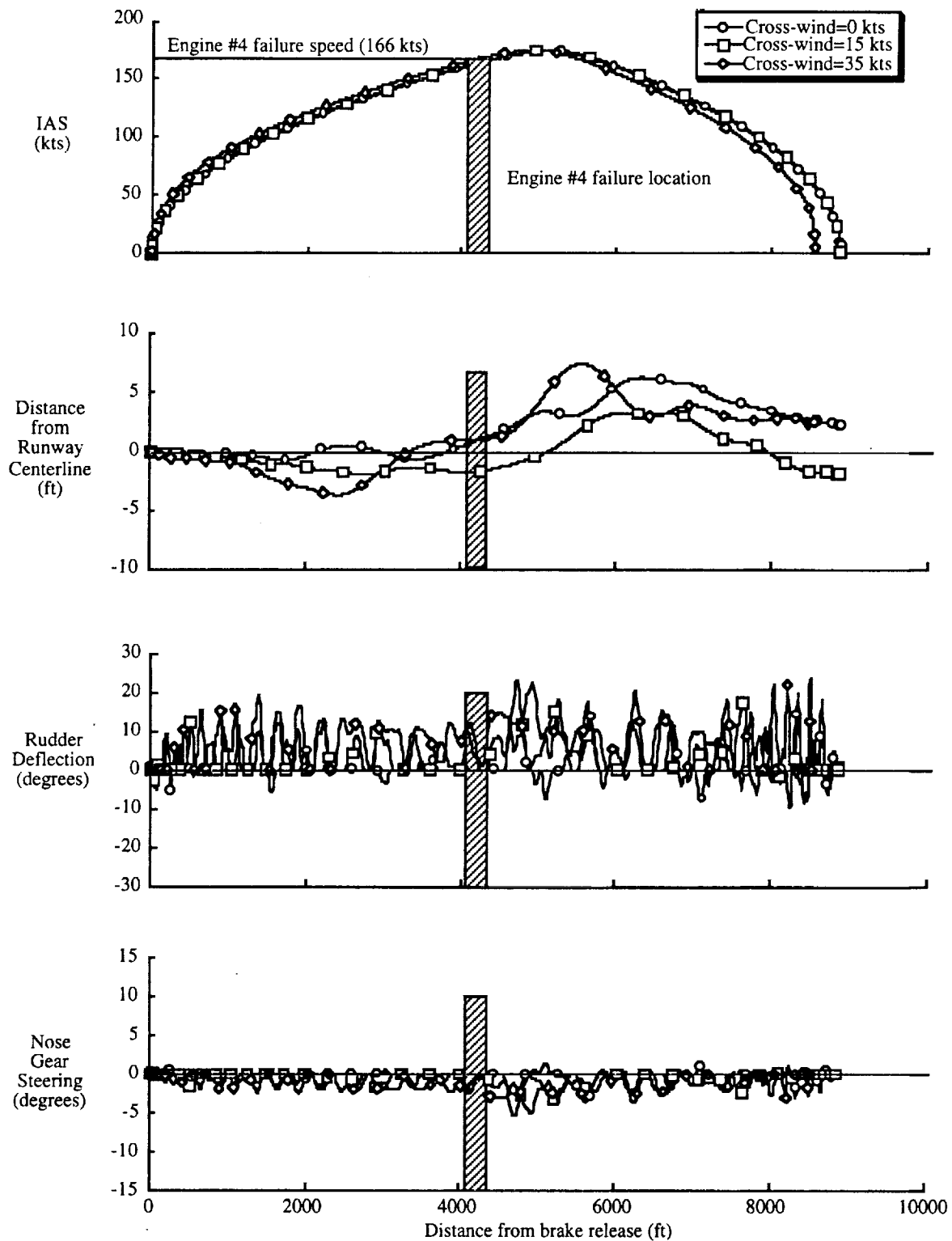
Figure 17. Indicated airspeed, distance from runway centerline, rudder deflection, and nose gear steering angle as a function of distance from brake release for the rejected takeoff maneuver with various cross-winds.

47
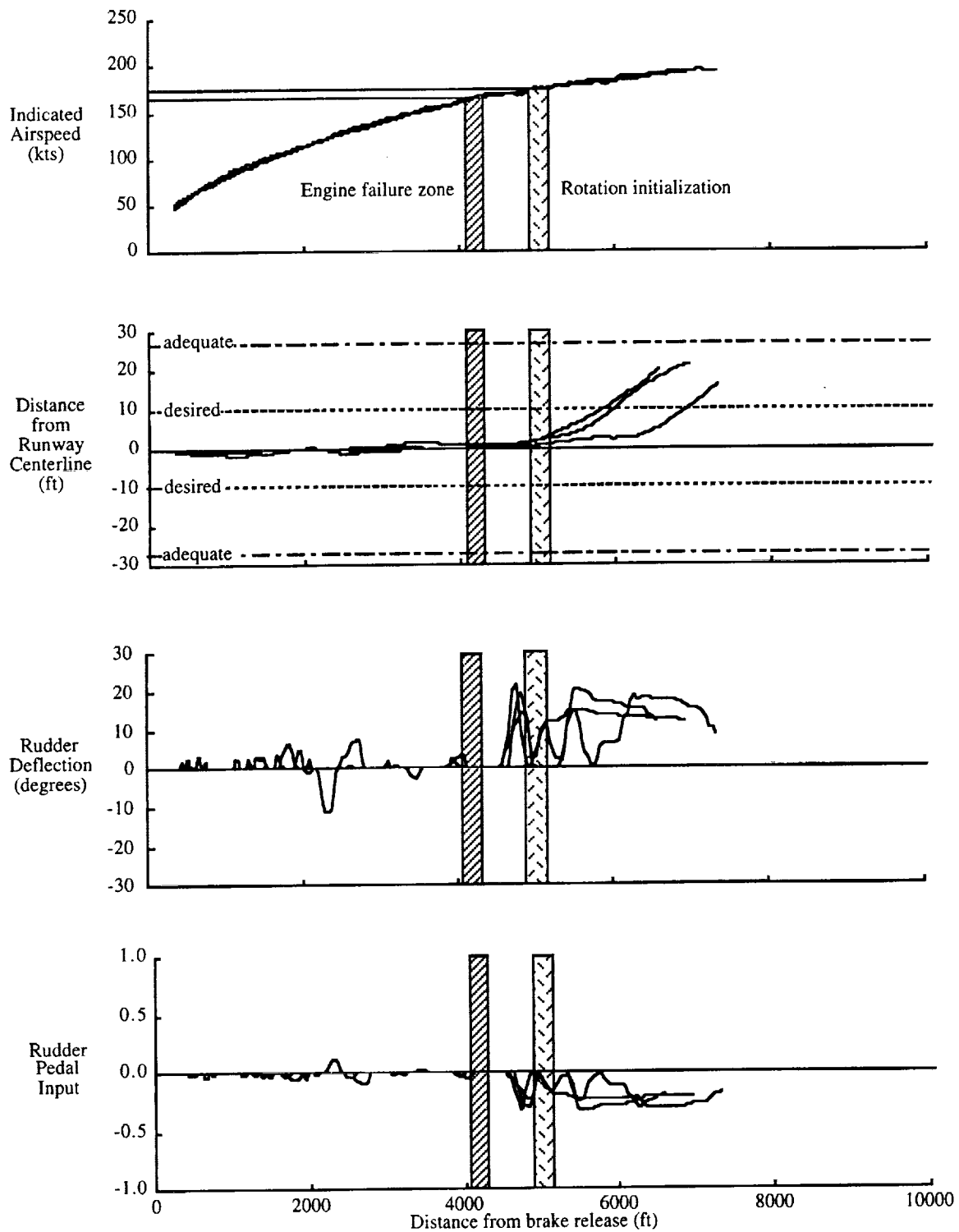
Figure 18. Indicated airspeed, lateral distance from runway centerline, rudder deflection, and pilots rudder pedal inputs as a function of distance from brake release for three different pilots ratable runs for the one-ground portion of the one-engine-out takeoff maneuver.
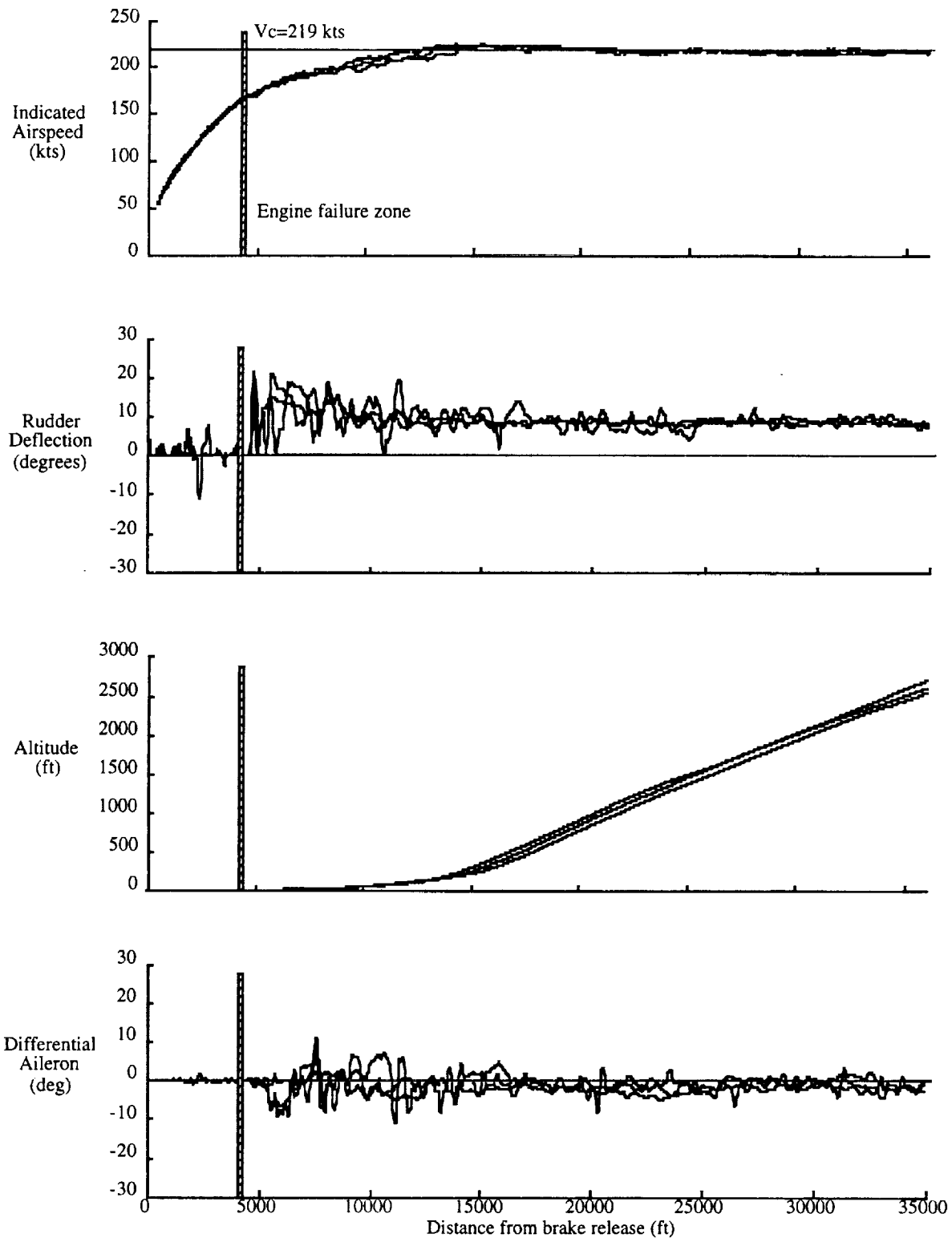
Figure 19. Indicated airspeed, altitude, rudder deflection, and differential aileron deflection for the one-engine-out takeoff maneuvers. Data are shown for three different pilots ratable runs.
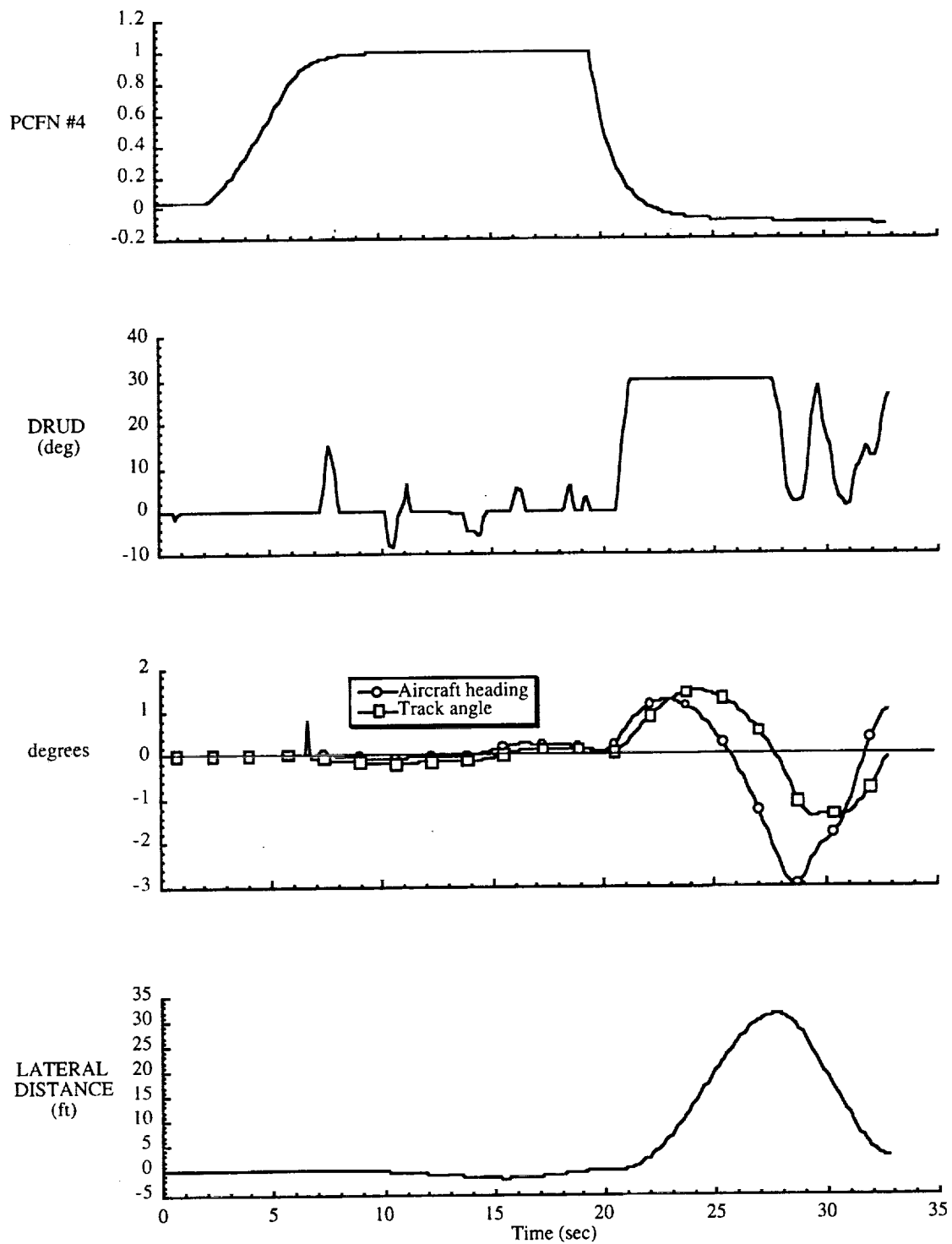
Figure 20. Percent net thrust of engine #4, rudder deflection, aircraft heading and track angle, and lateral distance from runway centerline for a representative V_{MCG} (task 7030) run.
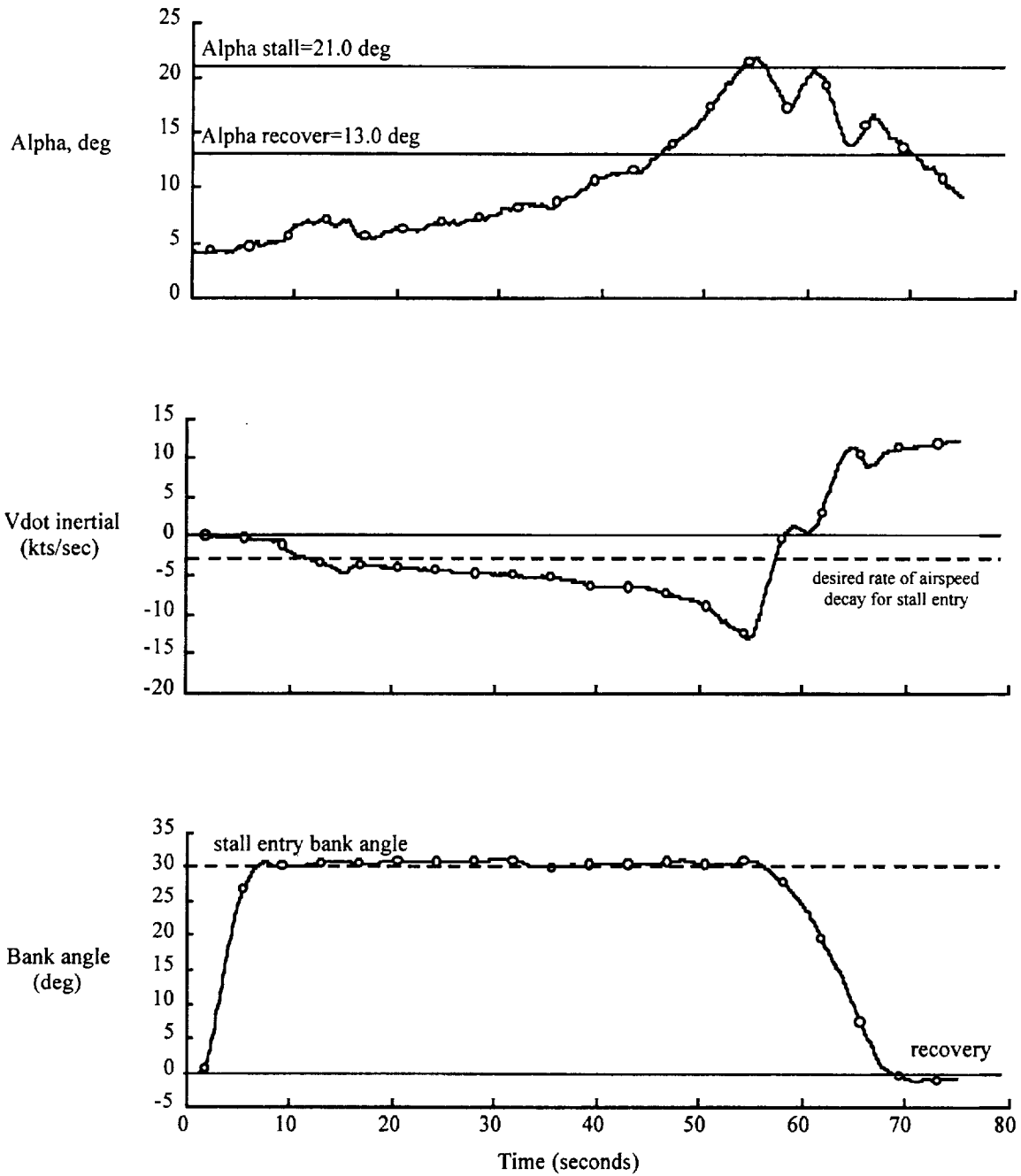
Figure 21. Example of recovery from limit flight data analysis. Data is for task 5040.
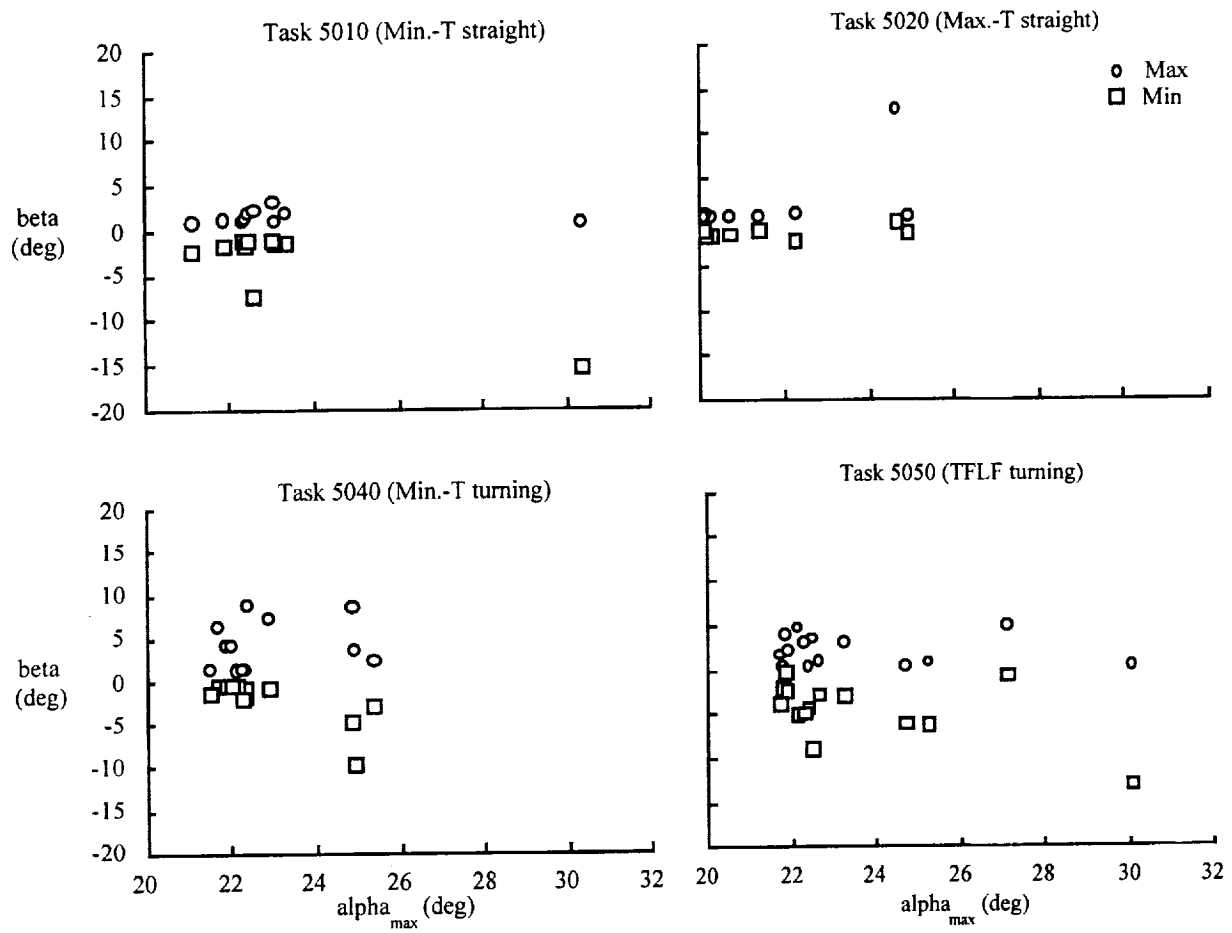
Figure 22. Summary of pilot performance for all of the RFLF maneuvers performed. Maximum and minimum sideslip angle are presented as a function of maximum angle of attack achieved.
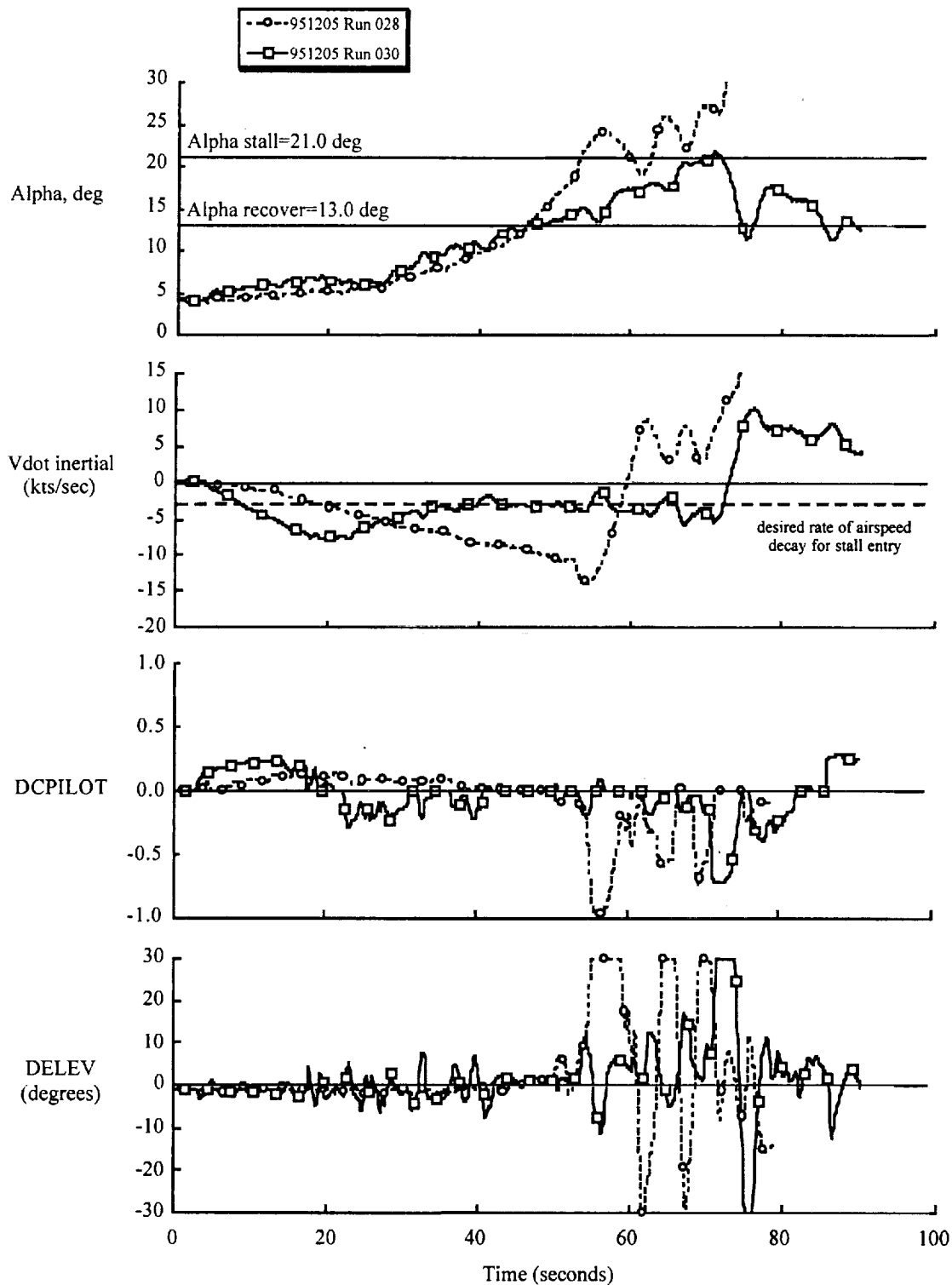
Figure 23. Demonstration of effect of rate of airspeed decay on maximum angle of attack achieved. Angle of attack, inertial rate of airspeed decay, pilot's longitudinal stick input (DCPILOT), and elevator deflection as a function of time for two attempts of task 5010.
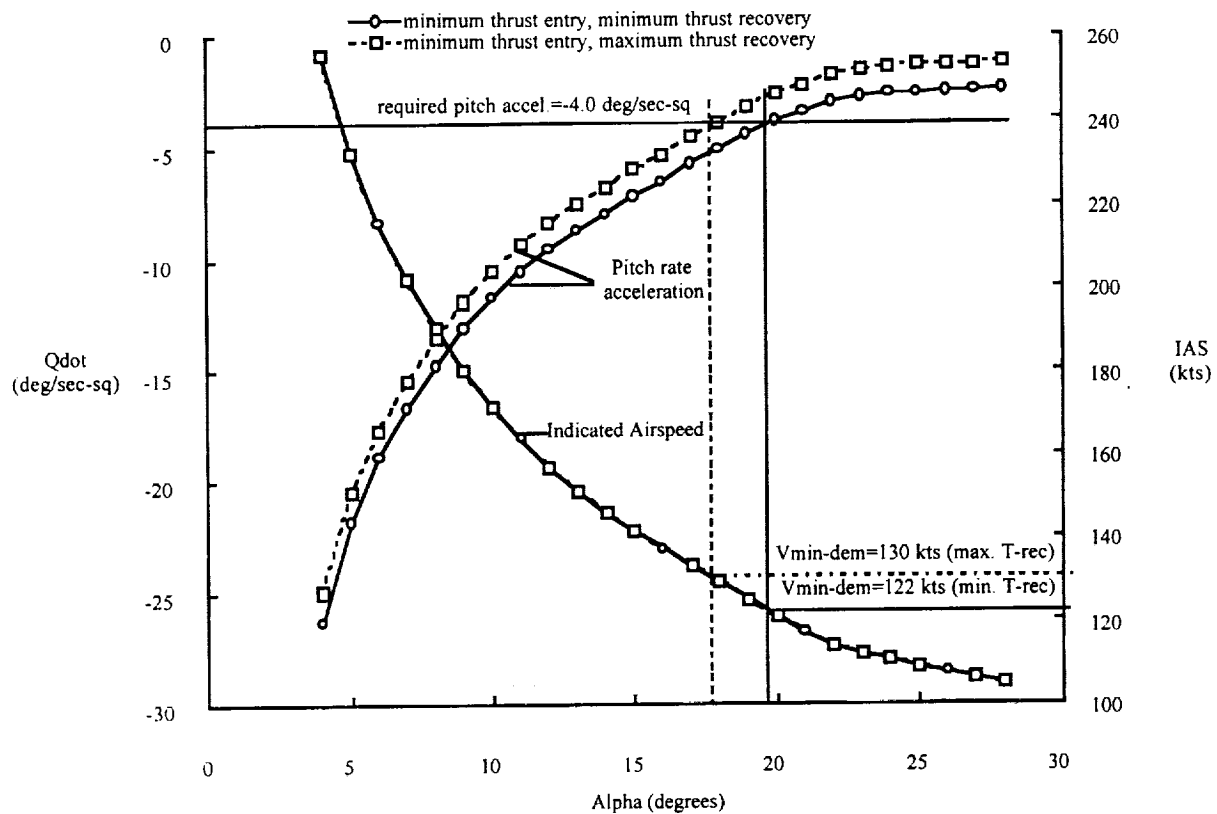
Figure 24. Pitch rate acceleration and indicated airspeed (IAS) as a function of pitch-trimmed angle of attack. Data is presented for a case without thrust effects and one with thrust effects on pitching moment only.
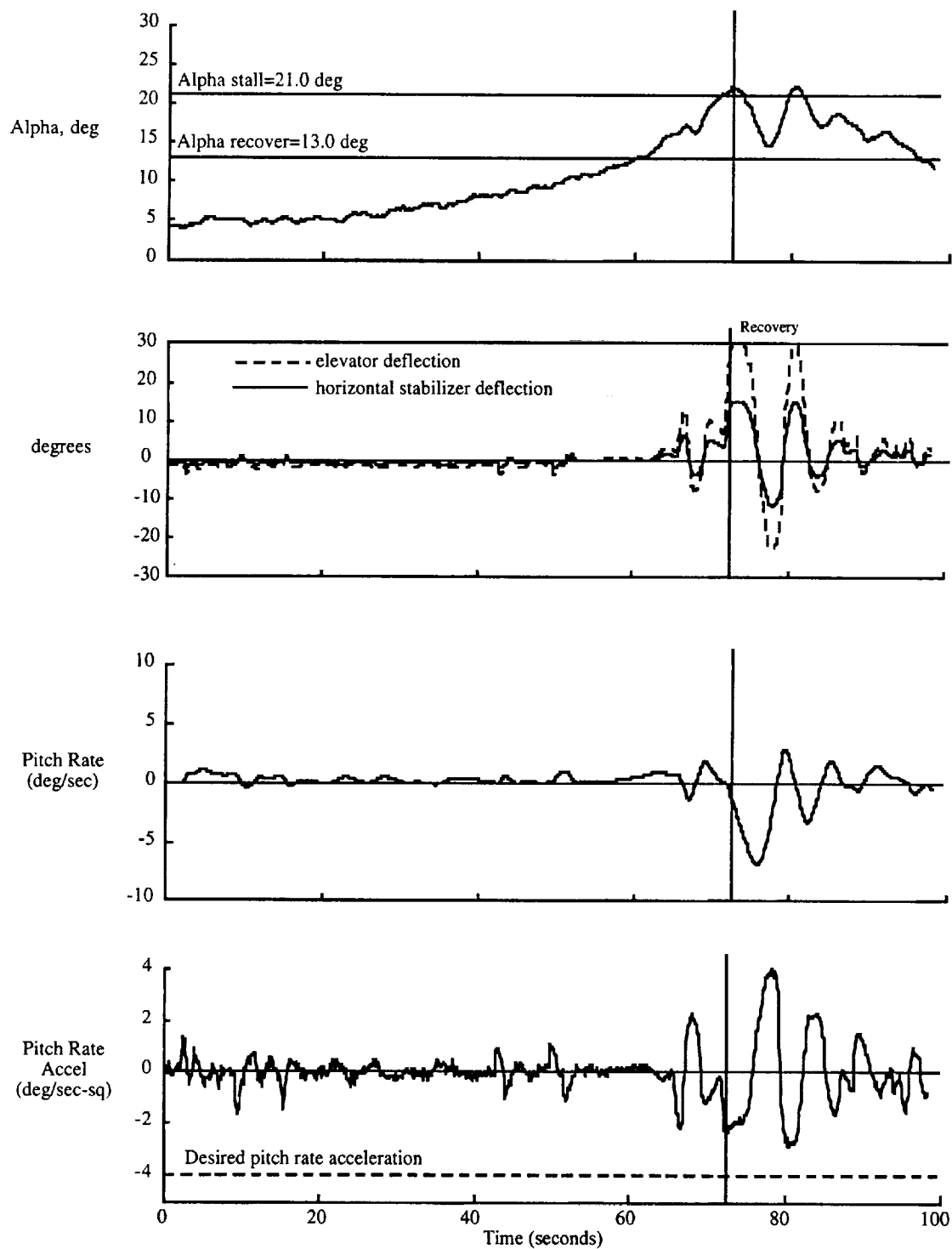
Figure 25. Angle of attack, elevator and horizontal tail positions, pitch rate, and pitch rate acceleration for a representative Task 5010 run.
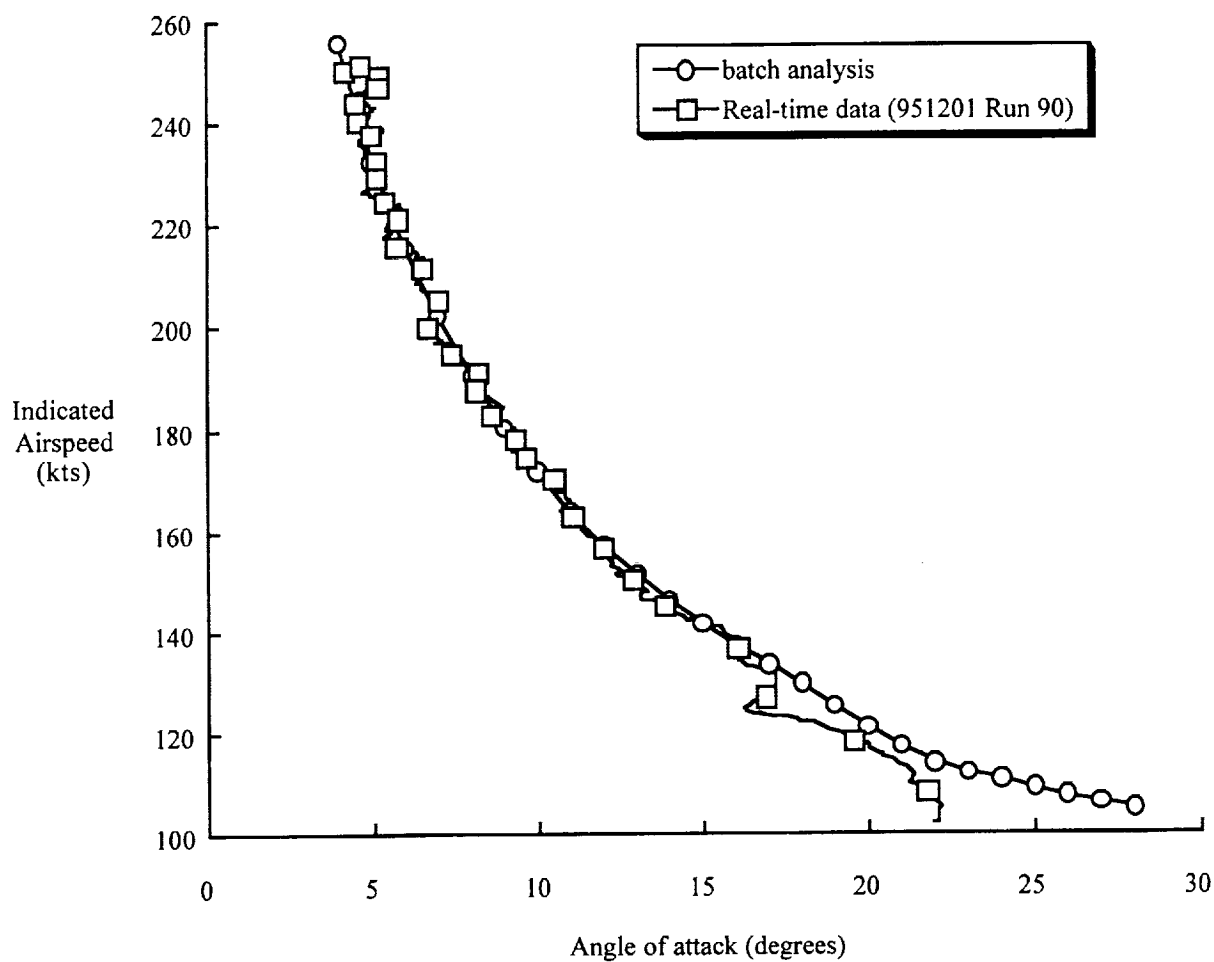
Figure 26. Comparison of indicated airspeed as a function of angle of attack for data from batch analysis and real-time piloted simulation of Task 5010.
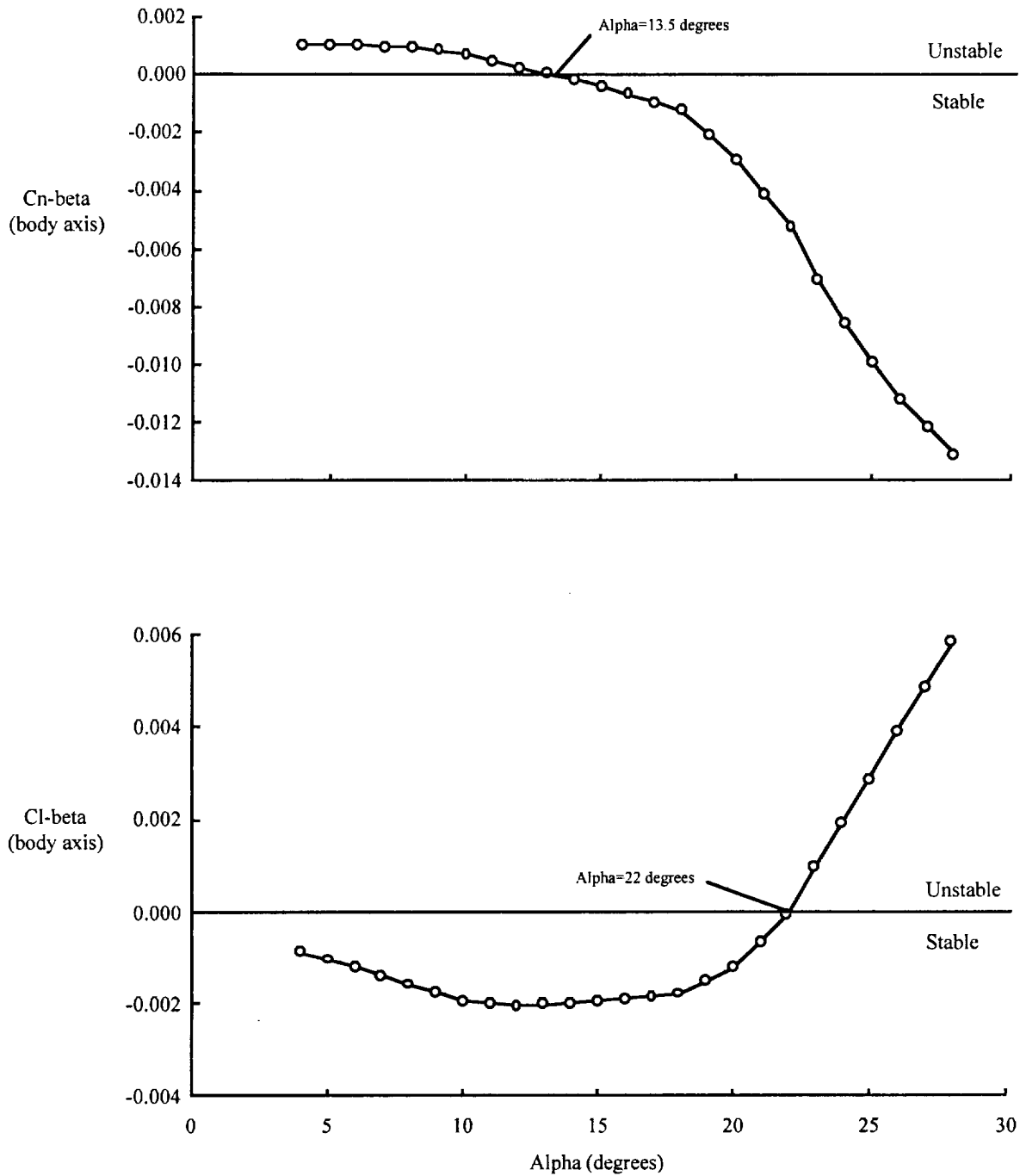
Figure 27. $C_{n\beta}$ and $C_{l\beta}$ as a function of angle of attack for the Ref.-H vehicle. Automatic flaps based on Mach number are included. Mach was calculated from pitch-trimmed C_L. QSE aerodynamics were also selected.
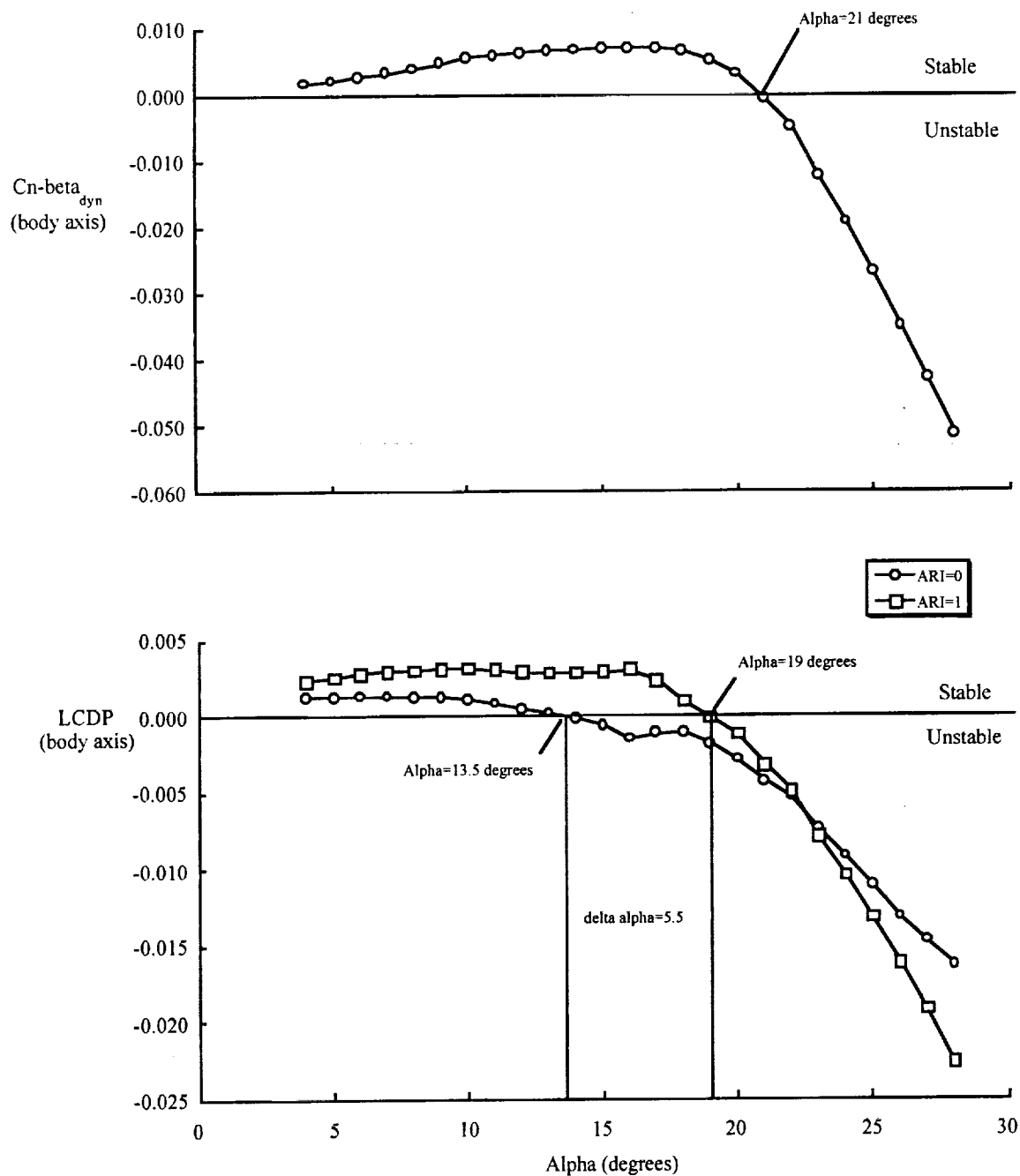
Figure 28. $C_{n\beta}$-dynamic and the lateral control divergence parameter (LCDP) as a function of angle of attack for the Ref.-H vehicle. Automatic flaps based on Mach number are included. Mach was calculated from pitch-trimmed C_L. QSE aerodynamics were also selected.
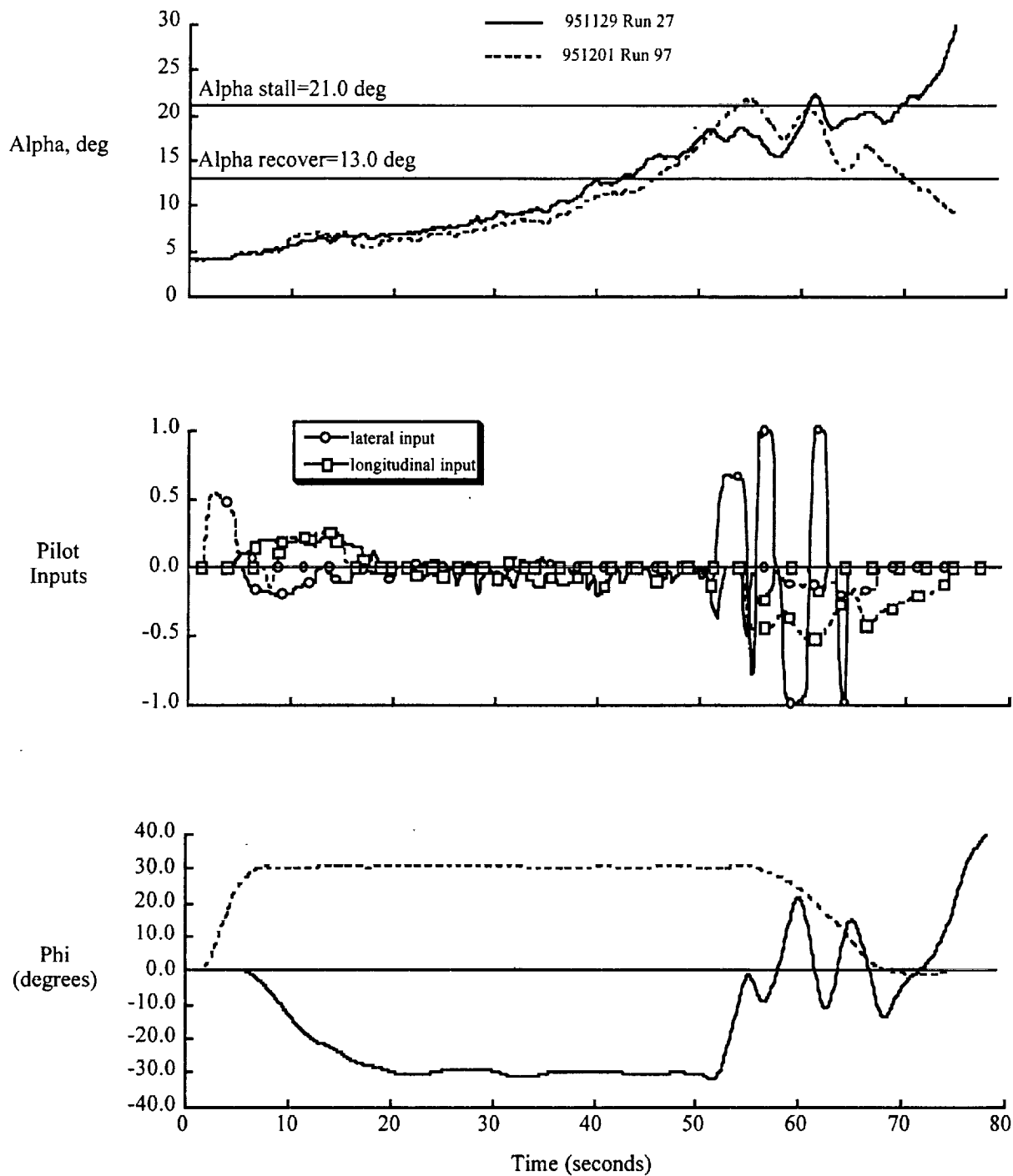
a) Angle of attack , pilot lateral and longitudinal inputs, and bank angle as a function of time.

Figure 29.   Time histories for two attempts of maneuver 5050.
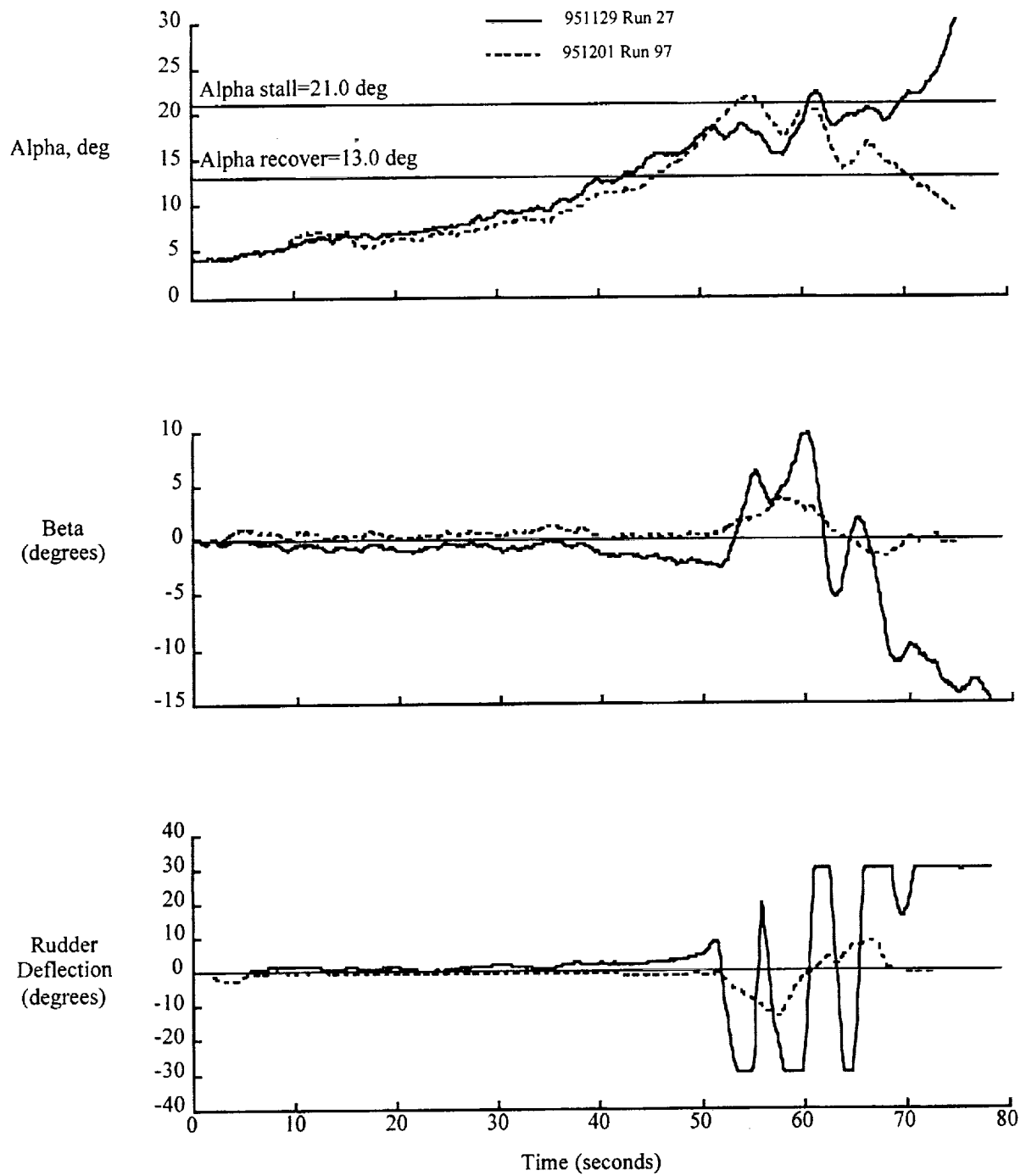
b) Angle of attack , sideslip angle, and rudder deflection as a function of time for two attempts of maneuver 5050.

Figure 29. Concluded.

Appendix A: Guidance algorithms - (Airborne Takeoff Climb Guidance)

Takeoff climb guidance was provided to the pilots to facilitate the generation of consistent takeoff trajectories which were required in order to accurately assess the vehicles noise characteristics. The presentation of the guidance was in the form of a velocity-vector guidance symbol as shown in Figure-A 1. Desired and adequate goals were established for the pilot to gauge his performance. As can be seen in Figure-A 1 the pilot's task was to keep the commanded velocity vector within certain limits of the velocity-vector guidance symbol. This appendix provides details regarding the movement of the velocity-vector symbol.

Lateral Flight Director Description

The lateral displacement of the velocity-vector guidance symbol from the actual flight path marker was defined by the LATGHOST variable.
LATGHOST = VVLAT + LATERR

The variable VVLAT calculates the actual velocity vector movement with the variable LATERR providing an error signal for the pilot to null.

$VVLAT = (1 / (t_{vvlat} * s + 1)) * (TKL180 - PSIL180)$
PSIL180 = Aircraft heading, degs.
TKL180 = Aircraft track angle, degs.
t_{vvlat} = time lag on velocity vector movement. Set to 0.4 seconds.

LATERR = (LATERR1 + LATERR2 + LATERR3 + LATERR4) * GKLATERR
GKLATERR = -0.01

LATERR1 = EPSYRWY * GKSY
EPSYRWY = distance from runway centerline, ft.
GKSY = 1

LATERR2 = (TKL180 - TKLREF) * GKTKL
TKL180 is aircraft actual track angle, degs.
TKLREF should be defined by runway track angle, degs.
GKTKL = 50

LATERR3 = ϕ * GKPHIL
ϕ is aircraft bank angle in degs.
GKPHIL = 5

LATERR4 = PDEG * GKPDEG
PDEG = body axis roll rate in degrees per second.
GKPDEG = -0.5 for initial evaluations.

Limit LATERR to LATLIM
LATLIM = 10 lateral degrees of HUD travel.

Longitudinal Flight Director System

The vertical movement of the velocity-vector guidance symbol was defined depending on what type of takeoff was selected. For PLR takeoffs, the velocity-vector guidance symbol would simply indicate

61

the desired climb gradient as illustrated in Figure-A 1. For all PLR takeoffs performed in support of this study, the commanded climb gradient was 4%. For takeoff tasks which required the pilot to intercept and maintain a specific acceleration and climb speed, such as tasks 2010 and 7035, the vertical movement of the velocity-vector guidance system was based on airspeed error.

The control system used to generate the vertical movement of the velocity-vector guidance symbol with respect to the actual flight path marker is defined below and in Figure-A 2 and Figure-A 3. The velocity flight director system was used to generate a commanded flight path angle adjustment, γ_c, which was added to the normal velocity vector position. Two maneuvers used this system (tasks 2010 and 7035) with the pilot's task to place the commanded velocity vector symbol on top of the velocity-vector guidance symbol.

Gain definition.

$K_{vi} = 0.0$

$K_{DVFD} = 0.20$

$K_{DVDOT} = 0.7$

$\gamma_{BIAS} = 0.0$

Other definition.s

VREF = is the current actual aircraft's complementary filtered indicated airspeed kts.

V_{ct} = is the current commanded airspeed, kts.

Above obstacle heigh.t

$V_{ct} = V_{35} + VDOTC*dt$

Limit V_{ct} to commanded climb speed, V_c, kts

V_{DOTC} = is the current commanded acceleration in kts/sec.

Before intercepting desired climb speed set $V_{DOTC}=V_{DOTC0}$

V_{DOCT0} = nominal rate of acceleration, kts./sec.

$V_{DOT0} = 1.7$ kts/sec

Intercepting desired climb speed.

When the current aircraft indicated airspeed error (VCLIMBER) is less than IASINT, reduce VDOTC using the following definitions: VCLIMBER = | VREF -V_c |

VDOTC = VDOCT0 * (1 - TINT / DELTINT)

IASINT = Airspeed error which identifies desired climb speed interception range (kts.). IASINT = 7.0 kts.

TINT = Elapsed time after reaching intercept speed. TINT = TIME - Time when VCLIMBER initially equals IASINT. Limit TINT to DELTINT.

DELTINT = Length of time to complete airspeed intercept, seconds.

DELTINT = 2 * IASINT / VDOTC0

GCLIM = Limit on climb gradient command. Set lower limit to 3% (1.718 degrees) and upper limit to +15 degrees for initial evaluations.

γ_c = commanded climb angle increment, degrees.

SW1 = Switch to enable integrator path. Set to true for | VREF -V_c | less than 10 kt.

SW2 = Switch to initiate γ_{BIAS}. Set to true for | VREF - CLIMB SPEED | less than 7 kts. Once SW2 becomes true implement so that it remains true for rest of simulated takeoff run.

SW3 = Set to true for ALTLG (landing gear altitude) greater than zero.

Appendix A Figures:

28
258 GS
0.28 M
1.00 G
7.4 a

30   30
10   10

Normal size pitch reference marker

5   5
255 1250
4.0%   4.0%

Velocity vector guidance marker
(lateral and longitudinal guidance)
Target climb gradient (PLR maneuver only)

Velocity vector error pilot metric bounds:

Desired: +/-1 marker width
90% of the time ·

Marker width=0.85 degrees

Adequate: +/-2 marker widths
90% of the time

5   5

10   10

Run 001
00:00 ET
12-12-99

Figure-A 1. Heads Up Display configuration shown to the pilots during the airborne part of the takeoff maneuvers.

g BIAS

Integrator
control limit

Limiter

SW2
F.

VREF
+
−
SW1
F.
DVi
$\frac{Kvi}{s}$
Li

1/(tBs + 1)

Vct

SW3 F.
KDVFD
+
+
+
+
+
GCLIM
gc

Limiter

VDOTI
+
−
SW3 F.
KDVDOT
VDOTC
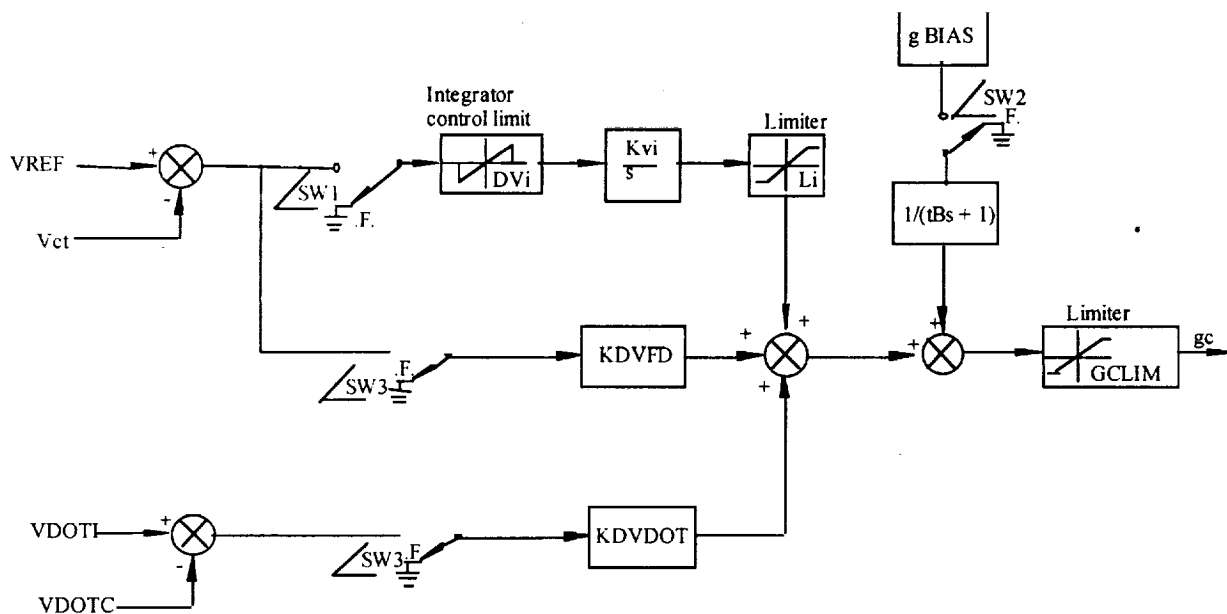
Figure-A 2. Velocity flight director command system used for tasks 2010 and 7035.

63

Filter time constants
tv comp	5.0
tαcomp	0.5
tβcomp	0.5
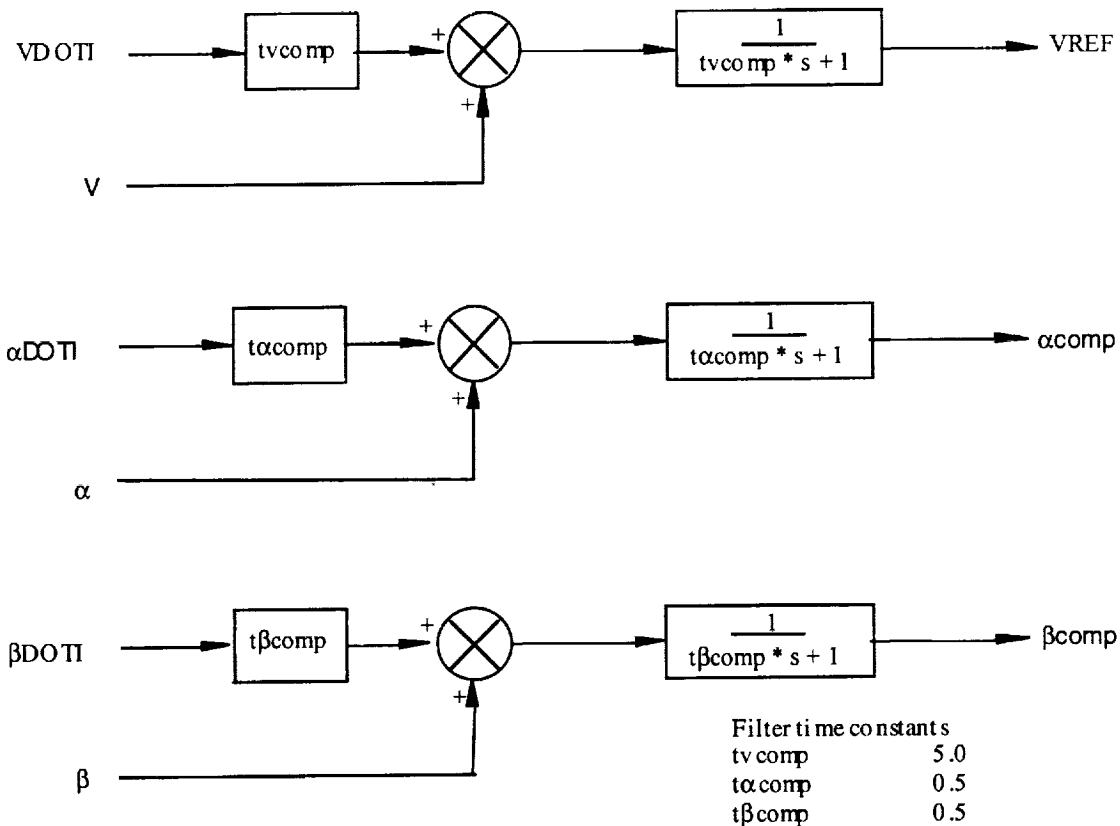
Defining equations for the complementary filter:

$$\alpha DOTI = -57.3 * (g / VTLIM) * (Nzcg * \cos(\alpha comp) + Nxcg * \sin(\alpha comp) - \cos(\theta) * \cos(\phi) * \cos(\alpha comp) - \sin(\theta) * \sin(\alpha comp)) + Q$$

$$\beta DOTI = 57.3 * (g / VTLIM) * (Nycg + \cos(\theta) * \sin(\phi)) - R * \cos(\alpha comp) + P * \sin(\alpha comp)$$

$$VDOTIFPS = g (Nxcg * \cos(\alpha comp) - Nzcg * \sin(\alpha comp) + Nycg * \sin(\beta comp) - \sin(\theta) * \cos(\alpha comp) + \cos(\theta) * \cos(\phi) * \sin(\alpha comp) + \cos(\theta) * \sin(\phi) * \sin(\beta comp))$$

$$VDOTIKTS = VDOTIFPS / 1.6878$$

$$VDOTI = VDOTIKTS * RHOFAC$$

Where RHOFAC = SQRT (RHORAT), with RHORAT defined as the ratio of the current ambient air density divided by the air density at sea level for a standard day.

VTLIM = 200, VT less than or equal to 200 ft/sec

P, Q, R = body-axis angular rates (deg/sec)

θ, φ, = aircraft euler angles

Nxcg, Nycg, Nzcg = body-axis accelerations, q's

VTLIM = VT, VT > 200 ft/ sec

Figure-A 3. Application of a complementary filter to generate V_{REF} and V_{DOTI} be used in the velocity flight director command system.

Appendix B: Description of Cockpit Control Inceptors and Control Laws

Description of Control Inceptors

The pilot's controls consisted of a two-axis side-stick controller for longitudinal and lateral control inputs, rudder pedals for directional control inputs, and a four-lever throttle quadrant. For this portion of the 1995 NASA LaRC Ref.-H assessment, the PF only manipulated the side-stick and rudder pedals with the PNF providing thrust changes, except for the rejected takeoff tasks where the PF was required to reduce thrust when commencing the braking portion of the maneuver. No manual flap changes were required for this study.

Figure B 1 provides a detailed description of the force characteristics of the side-stick controller and rudder pedals are illustrated in. In this figure a detailed description of the relationship between control inceptor forces and resulting displacements is provided. Figure B2 describes the resulting control system inputs, as a function of pilot inceptor displacements, for a range of flight conditions. Note that he breakout force listed in Figure B 1 are only the force needed to create a displacement of the control inceptor. The subsequent application of software deadbands to the control system inputs had the effect of simulating a higher breakout force to the pilot. To calculate the effective breakout force, multiply the controller deadband in Figure B2 by the appropriate force gradient in Figure B 1 and then add to the breakout force listed in Figure B 1

Longitudinal Control Laws

The longitudinal control law used for this investigation was basically described in the August 18, 1995 release of the Boeing $\dot{\gamma} / V$ control document entitled, "Flight Control System for NASA Simulation", reference B 1. The main block diagram of the $\dot{\gamma} / V$ control system is shown in Figure B3. Several minor modifications to the control law were implemented as described in the following paragraphs.

Provisions for weight-on-wheels mode.

1) Modifications to the ITGA integrator path to implement the weight-on-wheels mode are shown in Figure B4. The ITGA integrator is set to zero when the simulation is initialized at the beginning of every takeoff run. Logic is incorporated to keep the integrator value at zero during takeoff runs before the aircraft is airborne, and also to drive integrator output to zero when the vehicle is operating on the ground after touchdown. The value of KWIND was set at -2.0. The sw_ongrnd switch is implemented such that when there is weight on any of the landing gear units it is true, and remains true if momentary weight is reapplied to any landing gear unit during the takeoff roll. Once the aircraft is airborne (i.e. no weight on any gear units) the sw_ongrnd switch is set to false. For landings, sw_ongrnd remains false until weight is applied to any landing gear unit. In the event that the aircraft becomes momentarily airborne during the landing rollout, sw_ongrnd remains true.

2) Modification to Ksp path are shown in Figure B5. This fader modification removes the vdthat feed-in to the stabilizer command when weight is on the wheels.

3) Modification to kspd path are shown in Figure B6. This fader modification removes the gamma error feed-in to the stabilizer command when weight is on the wheels.

The FADER control system block element is defined as a linear ramp where the output from this element is zero when there is weight on any of the aircraft's landing gear units and equal to 1.0 when time (t) is greater than TOSW+DELTFD, as shown in Figure B7. The parameter, TOSW, is defined as the time when weight was removed from the landing gear system. When t is between these two points, a linear interpolation is provided between 0 and 1.0. In addition, once the condition for TOSW has been met, the function of the FADER is not affected if weight is momentarily placed back on the landing gear units. When in landing mode, similar logic is used to ramp the output from the FADER block to

zero once weight is initially indicated on any of the landing gear units. The value of DELTFD was set to 1.5 seconds.

A new sw_ongrnd condition must persist for SWCON seconds before switch transition occurs, where SWCON is defined as the length of time the switch condition must exist for switching to occur. The value of SWCON was set to 0.5 seconds.

Low-pass Filter on vdhat Signal.

A filter was added to the vdhat signal path where it feeds into the stab command to reduce the bandwidth of the signal coming from the outer loop guidance function to the inner loop stability augmentation. The time constant in this filter, τ_{vdhat}, is scheduled with Mach Number as indicated in Figure B8.

Vortex Fence Actuation for Takeoff.

During takeoff the vortex fence was deployed to aid in the initiation of the rotation maneuver. Figure B9 shows the signal flow diagram used to control deployment of the vortex fence device. The vortex fence was always operated in automatic mode. As a result its operation was transparent to the pilot. During takeoff maneuvers the vortex fence was locked in its fully retracted position until the pilot initiated rotation for lift-off. If the pilot attempted to rotate before Vr then the vortex fence would not deploy until the aircraft's speed reached V_r. Once the vortex fence deployed it was commanded to follow a deflection schedule which was inversely proportional to the pitch attitude of the vehicle. The deflection schedule commanded 100% vortex fence deflection (90 degrees) when the aircraft was in the pre-rotation pitch attitude and 0% (0 degrees) when the aircraft reached the target rotation pitch attitude (10.5 degrees). If the vortex fence was still open once the vehicle left the ground the vortex fence was commanded to close at its rate limit. The block diagram and logic below describe the details of its intended operation for takeoff maneuvers.

The following equations and definitions were employed along with the signal flow shown in Figure B9 to generate the vortex fence commanded deflections when the aircraft is configured for takeoff.

$$\Delta \theta 0 = \theta_{(rot - targ)} - \theta_{vr}$$

θ_{vr} is the aircraft's pitch rotation attitude when the aircraft reaches the rotation speed, Vr.

$\theta_{(rot - targ)}$ is the target pitch rotation attitude currently being generated, degrees.

$\theta_{(degs)}$ is the current aircraft's pitch attitude, degrees.

VTFCOM is the commanded vortex fence deflection and is the input to the actuator model.

Switching logic:
Switch 1 is initialized to true and set to false when landing gear altitude is greater than 0.50 feet.
Switch 2 is set to true when the complementary filtered airspeed is greater than Vr.
Switch 3 is set to true and remains true when DCPILOT (pilot's pitch stick input) becomes greater than zero after the aircraft has reached Vr.

Actual Vortex Fence Operation In Takeoff mode.

As a result of a last minute change to the landing mode operation of the vortex fence, the takeoff mode operation of the vortex fence was inadvertently and severely affected. Basically, an incorrect mode logic statement produced an error which rendered the vortex fence almost useless during takeoff rotations. The actual operation of the vortex fence was very similar to the intended operation, except during the deployment phase of the vortex fence when the aircraft was on the ground during rotation initiation. Instead of deploying at the surface actuator deflection rate of 90 degrees/seconds the rate of deflection of the vortex fence was only 5 degrees per second. The result of this error was that it could only deflect to approximately 20 degrees before being commanded to start retracting based on the aircraft's pitch attitude closure with the target pitch attitude. Once the aircraft became airborne, the

higher rate limit was reinstated resulting in the vortex fence retracting normally. The fact that the vortex fence wasn't operating properly went unnoticed during the piloted assessment runs as a result of it passing checkout very late in the development phase of the simulation and the fact that the elevator and stab were not being position limited. Since the aircraft behaved nominally, it is believed that the CHR ratings would not have been affected the vortex fence anomaly.

Lateral/ Directional Control Laws

The lateral/ directional control laws used in this investigation are basically those described in the August release of the McDonnell Douglas p/β control document entitled, "Description of Lateral-Directional SCAS Control Laws for Ref. H Assessment", reference B 2. Several modifications were made to the control laws based on the October 21 release of a revised set of lateral-directional control document entitled, "Candidate Lateral-Directional Control Laws", but insufficient time was available to implement and check out the complete set of revisions prior to the start of the experiment. Therefore, the control laws used in this investigation basically conform to those described in the August 1995 documentation, with the exception of several minor modifications as described in the following paragraphs.

Provisions for weight-on-wheels mode.

1) Weight-on-wheels modifications to Douglas roll control laws are shown in Figure B11. The constant, KWIND, is defined the same way KWIND is defined and used with the Boeing $\dot{\gamma}/V$ control law modification. The value of this constant was -2.0 sec.

2) Weight-on-wheels modifications to Douglas directional control laws are shown in Figure B12. The modifications to the directional control law involve implementing the FADER function to remove complementary filtered beta from the control system and also replacing inertial beta-dot with body-axis yaw rate when transitioning between airborne and on-ground phases of flight. These modifications also assist takeoff maneuvers which require complementary filtered beta and inertial beta-dot instead of body axis yaw rate. The operation of the FADER control system block element is the same as that defined earlier in Figure B7.

Other Modifications to the Directional Control Law.

1) The constant, taubeta, in the sideslip complementary filter in the p/β lateral/directional control law was set to 3.0. (Originally it was set to 0.005).

2) The beta-dot inertial signal for the complementary filter in the Douglas lateral/directional control law was computed using the following equation:

$$\beta \text{ dot I} = 57.3 \text{*}(g/VTLIM)\text{*}(Nycg+ \cos\theta \text{ * } \sin\phi)\text{-r * } \cos \alpha_{comp} + p \text{ * } \sin \alpha_{comp}$$

3) The beta-dot feedback signal in the p/β lateral/directional control law was replaced with the beta-dot inertial quantity calculated using the above equation.

Control Mixer and Control Allocation

This document describes the control allocation strategy employed for the NASA LaRC 1995 piloted Ref.-H assessment project. Elements described are the horizontal tail, elevator, leading- and trailing-edge flaps, rudder, and vortex fence operations. The logic employed was similar to that previously outlined by Brett Churchill and Karl Bilimoria in references B3 and B4. No provisions were made for Spoiler Slot Deflectors (SSD's) or Speed Brakes for this version of the Ref.-H simulation.

Horizontal Tail.

The elevator has two segments (left and right); each segment is assumed to have three actuators. The stabilizer has one segment and is assumed to have four actuators. Although the horizontal stabilizer and elevators are defined as being actuated independently, the elevators are electronically slaved to the horizontal stabilizer in a 2:1 ratio. The elevator and stabilizer control deflection signals are fed to each unit in the appropriate ratio.

Leading- and Trailing-edge flaps.

Trailing-edge flap segments 1,3 and 6,8 were used as flaperons and employed high-rate actuators. Segments 2, 4, 5, and 7 were only flaps and assumed low-rate actuators. For a definition of leading- and trailing-edge flap segments refer to Figure 3.

Symmetric deflection schedules for leading- and trailing-edge flaps were defined as functions of angle attack and Mach number in Figure B13 and Figure B14, respectively. The minimum symmetric automatic flap deflections followed the minimum leading- and trailing-edge flap schedule based on angle of attack shown in Figure B14. The outboard and inboard flap commands ($\delta fOcmd$ and $\delta ficmd$) are from the autoflap schedules presented in reference B 3. Deflections are positive trailing edge down.

Flap transition logic for the takeoff mode was designed such that the flap transition from the initial flap setting (LEF=30/TEF=10) to the automatic flap schedule would initiate once the aircraft's landing gear height reached 35'. Commanded transition would occur over a 18 second interval. During landing approaches the transition to the touch-down flap setting (LEF=0/TEF=30) would initiate at 390 feet. A linear ramp based on time was used to define the flap deflections during transition. The length of time used for the transition was 18 seconds which permitted the automatic flap system to complete the flap reconfiguration by the time the aircraft descended to approximately 130 ft while following a standard ILS approach. This length of time also provided the smoothest transition possible given the fact that the flap reconfiguration could not commence until the aircraft was sufficiently passed the approach noise measurement microphone location, which was located at 6,562 feet from the runway threshold, and also be completed before touch-down flare initiation. During landing abort/go around maneuvers the transition from touch-down flap deflections back to the automatic flap schedule occurred over 18 seconds once the TOGA switch was selected by the pilot. The block diagram of the autoflap command generation system is shown in Figure B15.

Flaperon Control Mixers.

The Boeing mixer architecture used for the piloted assessment is shown in Figure B16. It involved a simple summation of aileron and flap commands for trailing edge devices 1, 3, 6, and 8, which acted as flaperons. Surfaces 2, 4, 5, and 7 functioned as flaps only.

Control surface lockout strategy.

The control surface lockout strategy for trailing edge surfaces 1, 2, 7, and 8 is shown in Figure B17. The lockout signal varies between 0 and 1 as illustrated in the figure. This signal multiplies the aileron command to trailing edge surfaces 1 and 8. The lockout signal also multiplied the command to the upper rudder segment, δ R1, as shown in Figure B18.

Appendix B references

B 1   Coleman, Edward E.; Duffy, Keith S.; Kraft, Raymond H.: "Flight Control System for NASA Simulation." Boeing documents HSCT-BE49B-L95-011,012,013,014, 1995.

B 2   Williams, T.M.; Griffith, M.J.; Rossitto, K.F.: "Candidate Lateral-Directional Control Laws -- Milestone Report." McDonnell Douglas Aerospace, Long Beach, CA; CRAD-9408-TR-0977, NASA Contract NAS1-20220, October 21, 1995.

B 3   Churchill, B.J., "Definition of Control Surface Allocation," Boeing document AERO-B1B8B-C95-029, July 11, 1995.

B 4   Bilimoria, Karl D.: "Control Surface Issues: Oct-Nov '95 VMS Simulation (Draft III)"

Appendix B figures

Lateral and longitudinal trim button

7-5/8"

Hand controller details
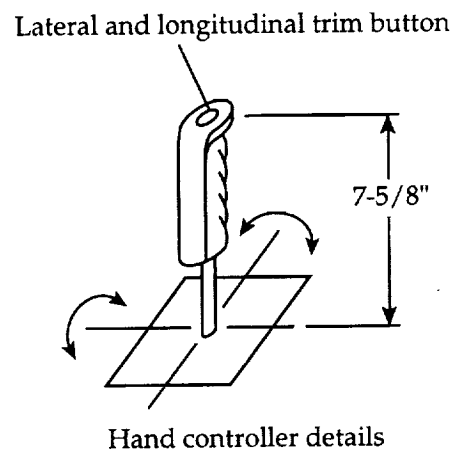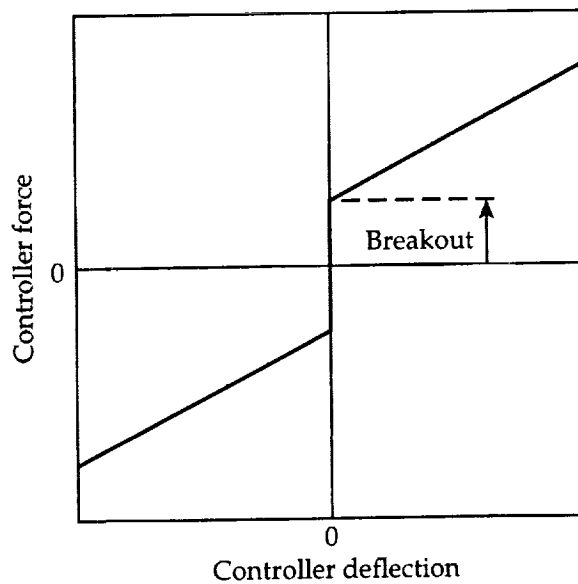
Pilot Control Device	Axis	Breakout, lbs	Force gradient	Neutral position	Max. deflection
Side stick	Pitch	+/-0.86	0.815 lbs/deg	10° forward	+/-12.27°
Side stick	Roll	+/-0.87	0.479 lbs/deg	20° inboard	+/-12.27
Rudder pedals	Yaw	+/-13.5	32.5 lbs/in	0 in	+/-3.75"

Figure B 1. Force displacement characteristics of the side-stick and rudder pedal control inceptors.

Figure B2. Definition of control system inputs for longitudinal, lateral, and directional axes as a function of pilot's control displacements.
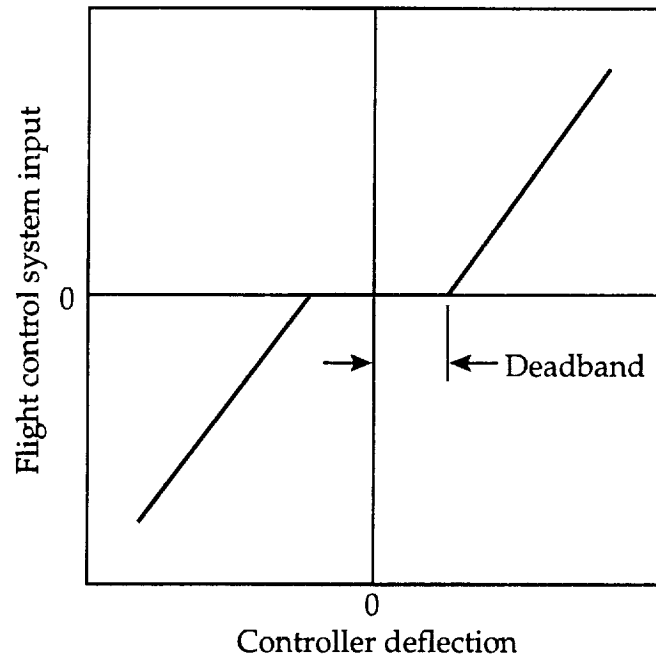
Pilot control device	Axis	Controller deadband	Control system input	Gradient	Maximum control system input
Side stick	Pitch	0.96°	gdcws	0.763 deg/sec/deg@FC1 0.255 deg/sec/deg@FC2	+/-8.60 deg/sec@FC1 +/-2.87 deg/sec@FC2
Side stick	Roll	0.29°	δ_{cw}	1.96 deg/sec/deg@FC3 2.90 deg/sec/deg@FC4	+/-21.5 deg/sec@FC3 +/-31.8 deg/sec@FC4
Rudder pedals	Yaw	+/-0.125″	δ_{rp}	11.8 deg/in@FC5 1.5 deg/in@FC6 0.55 deg/in@FC6	+/-42.6 deg@FC5 +/-5.3 deg@FC6 +/-2.0 deg@FC7

Flight condition	Definition
FC1	200 kts true airspeed
FC2	1,4209 kts true airspeed
FC3	Mach number less than 0.9, with aircraft's wings level
FC4	Mach number equal to 2.4, with aircraft's wings level
FC5	Mach number less than or equal to 0.3
FC6	Mach number equal to 0.9
FC7	Mach number equal to 2.4

Figure B2. Definition of control system inputs for longitudinal, lateral, and directional axes as a function of pilot's control displacements.

Figure B3. Main block diagram of the $\dot{\gamma}\,/\,V$ control system.

Figure B4. Modification to ITGA integrator path for weight-on-wheels mode.

Original control system element
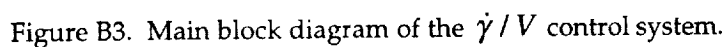
Modified control system element
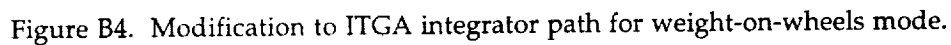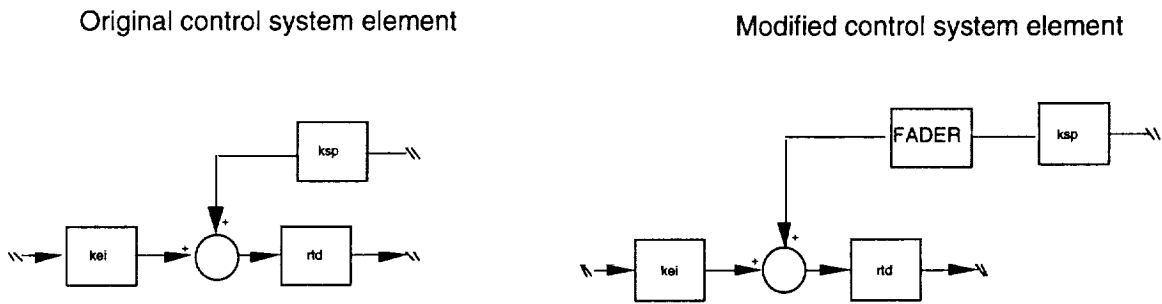
Figure B5. Modification to Ksp gain path for weight-on-wheels mode.

Original control system element

Modified control system element
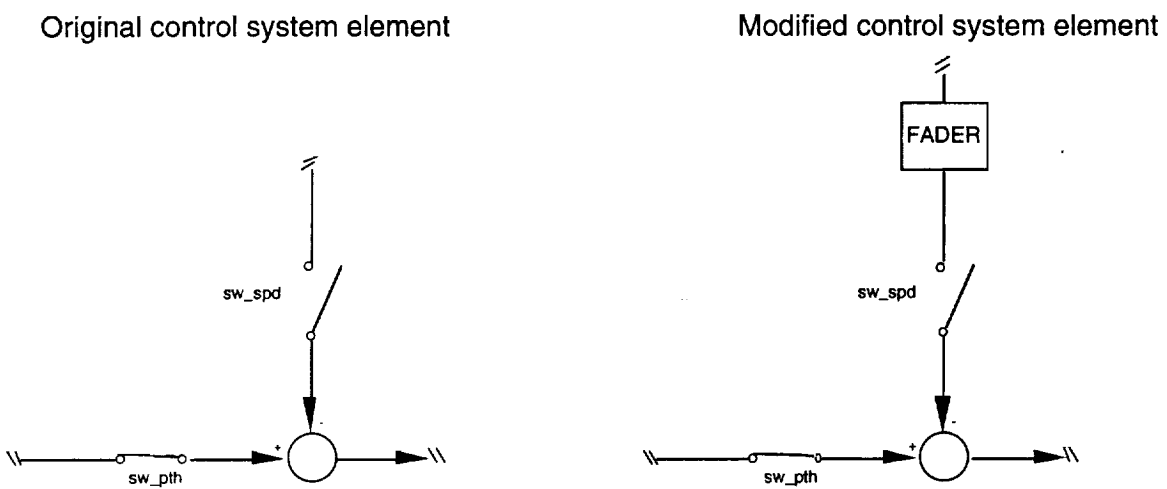
Figure B6. Modification to Kspd gain path for weight-on-wheels mode.

FADER takeoff element

1.0

0.0

time t=TOSW   time t=TOSW+DELTFD
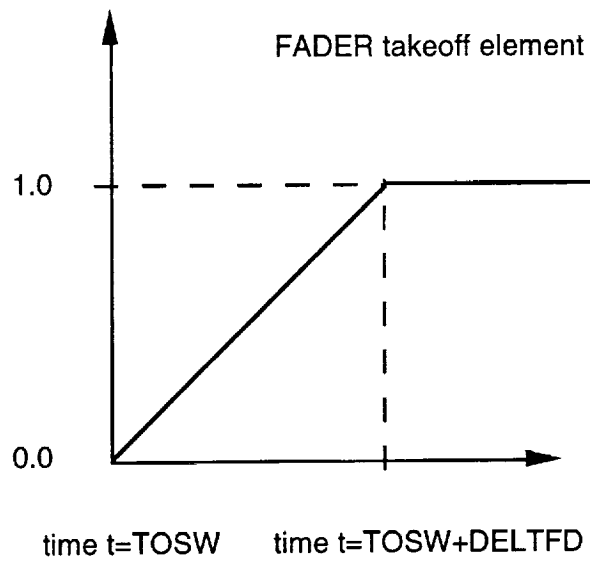
Figure B7. Operation of FADER takeoff element

vdthat $\longrightarrow$ $\boxed{\dfrac{1}{\tau_{vdthat}\, s + 1}}$ $\longrightarrow$ to stab command path
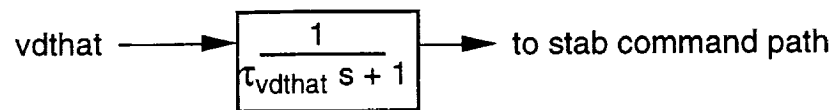
Mach < 0.3 : $\tau_{vdhat} = 10$ sec

0.3 < Mach < 0.9 :   Linear Interpolation

Mach > 0.9 : $\tau_{vdhat} = 2$ sec

Figure B8. Low-pass filter and time-constant schedule applied to vdthat signal.

90

$$\frac{1}{\Delta\theta_0}$$

.F.

SW1

VTFMCOM

θ (rot-targ)

+

−

θ (degs)

VTFMCOM

.F.

SW2

.F.

SW3

VTFCOM
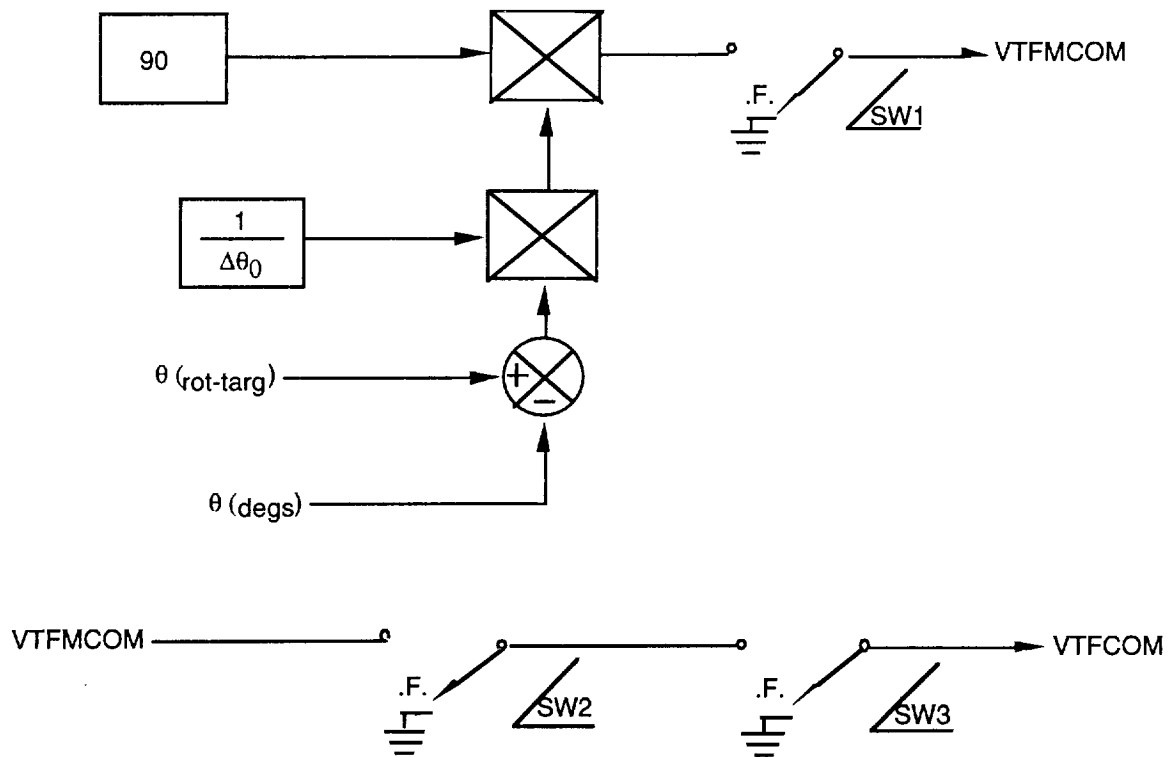
Figure B9. Deployment of vortex fence to aid takeoff rotation.
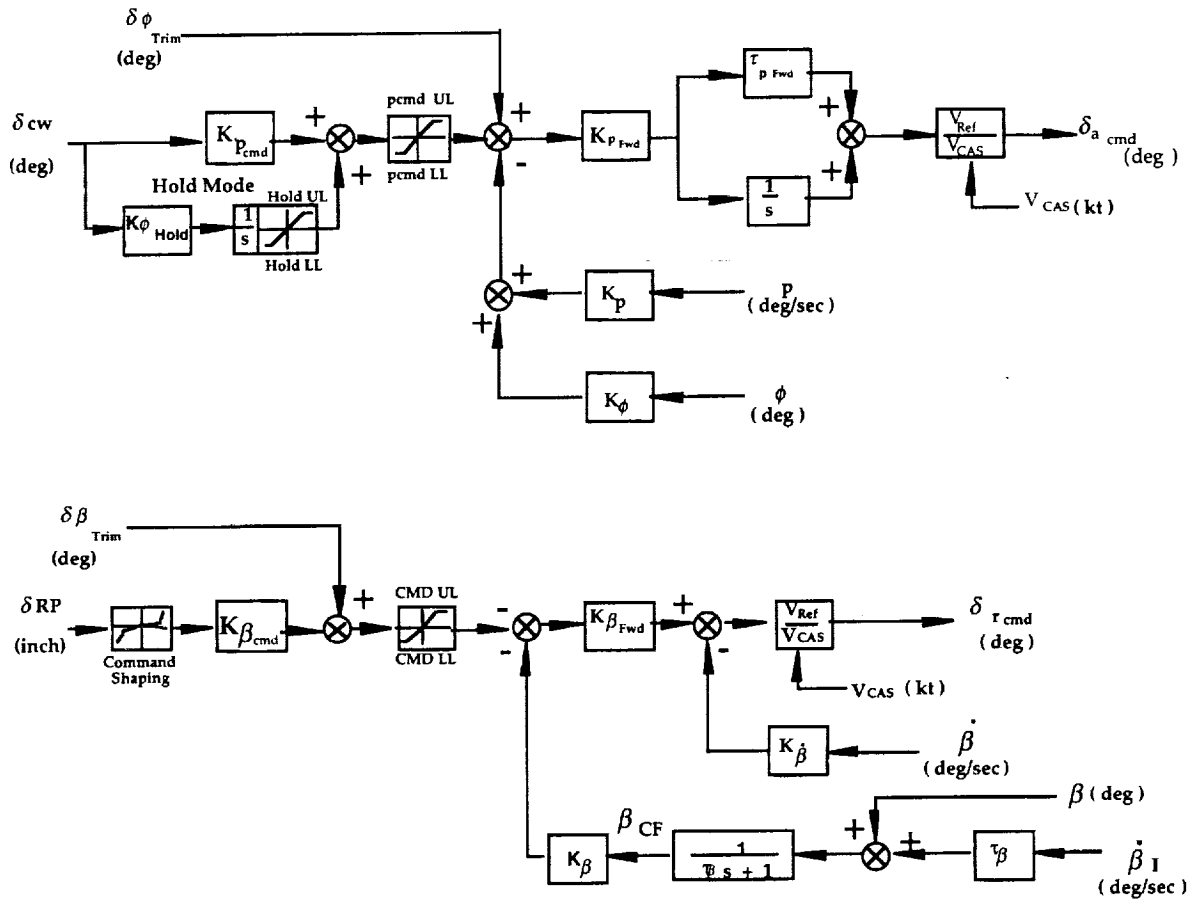
Figure B10. Main block diagrams of the lateral/directional p / β control system employed.

76
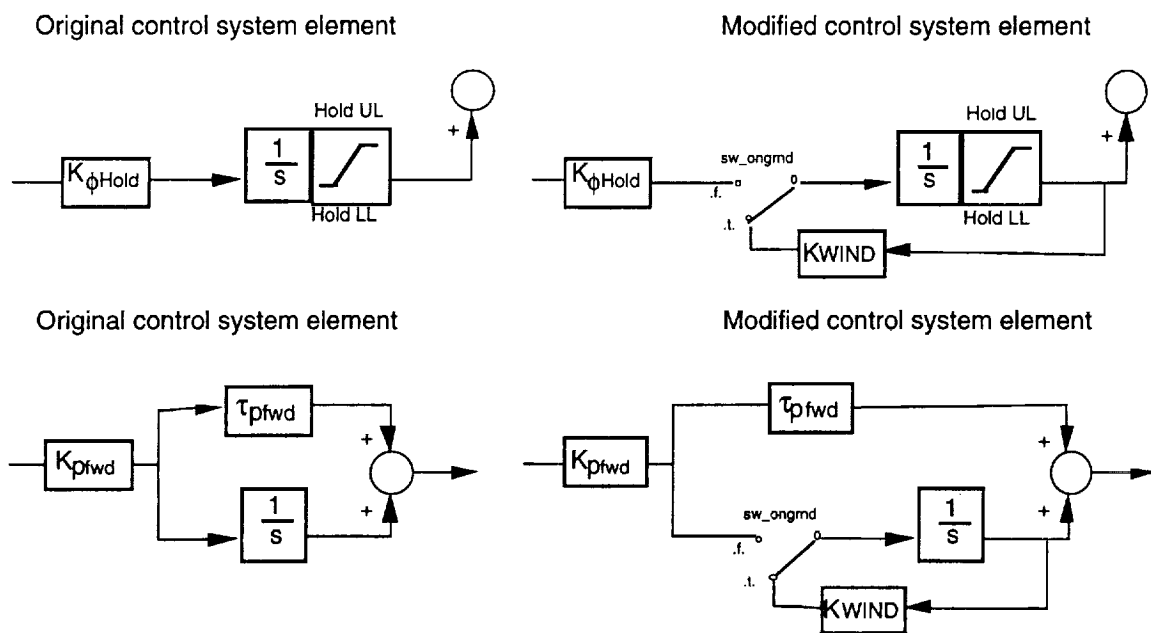
Figure B11. Modifications to p/β roll control laws for weight-on-wheels mode.
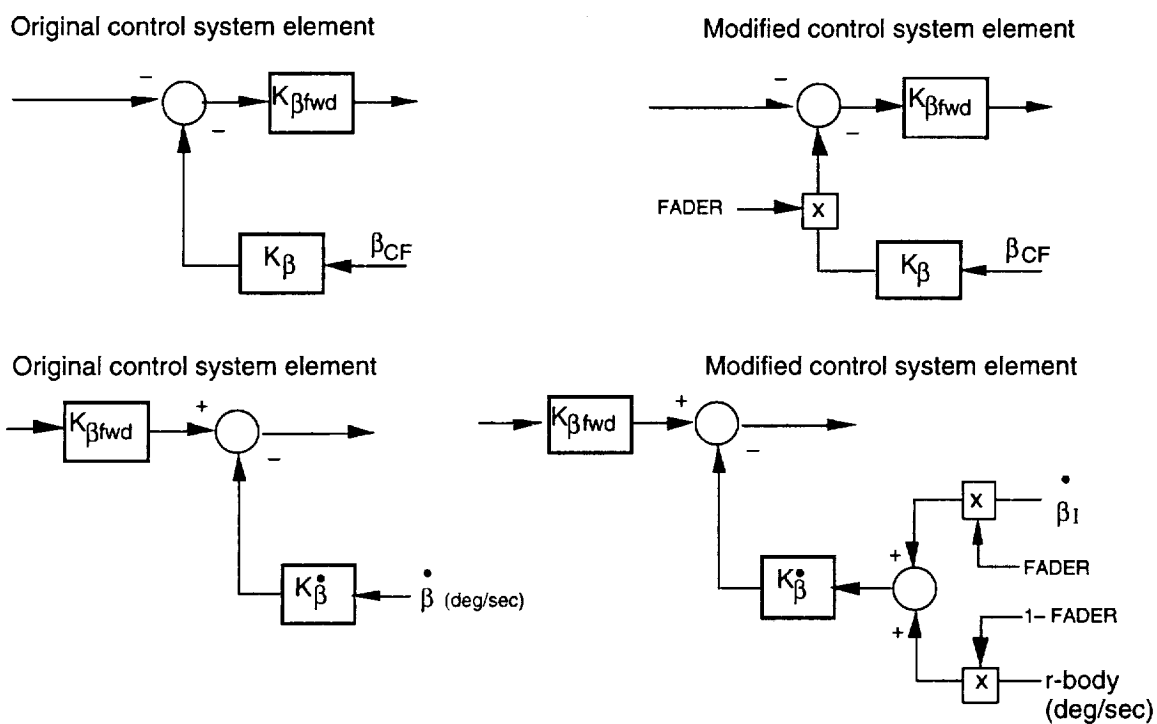
Figure B12. Modifications to p/β yaw control laws for weight-on-wheels mode.

77

Outboard flap segments

Inboard flap segments
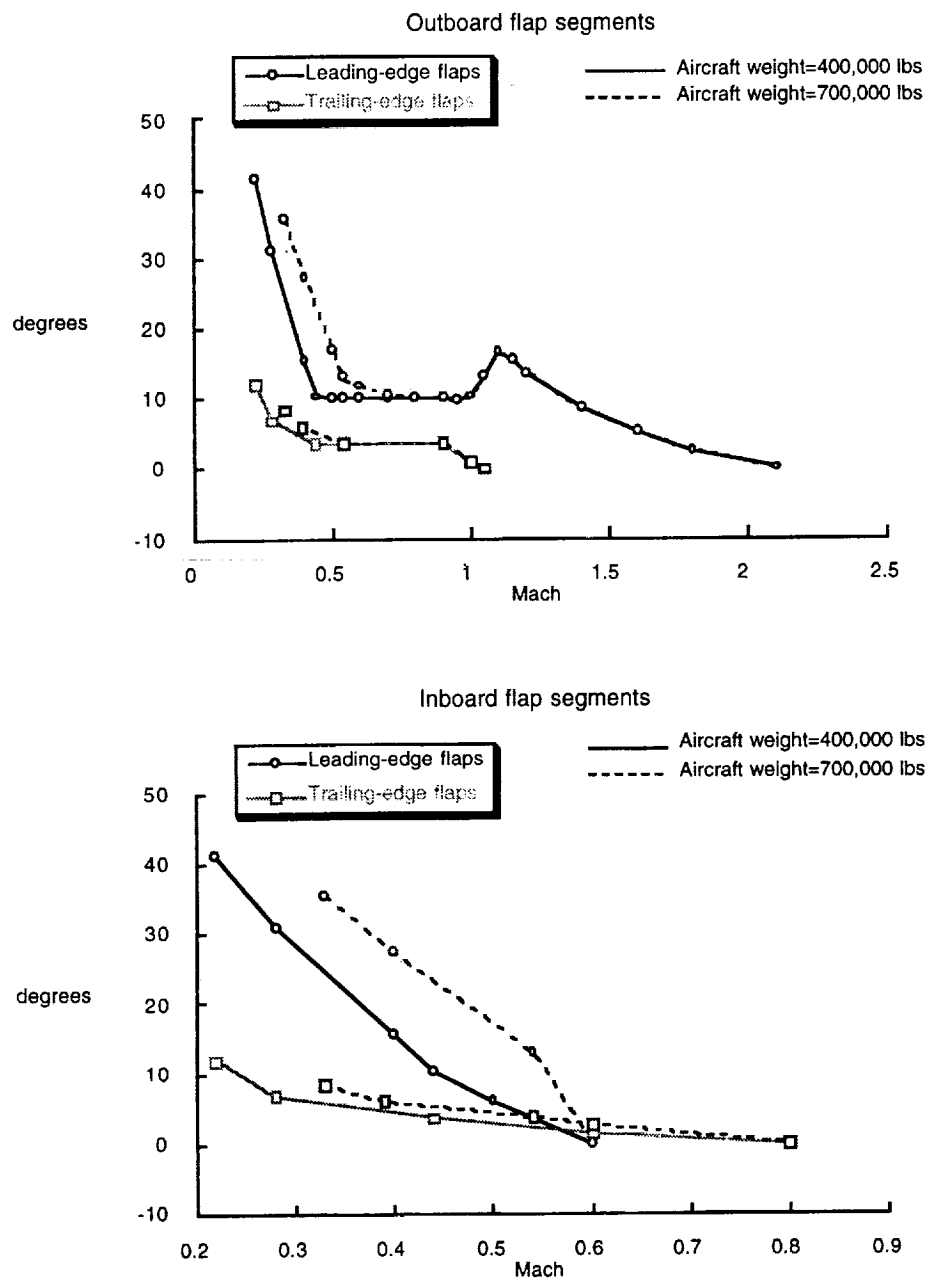
Figure B13. Symmetric leading- and trailing-edge flap deflection as a function of Mach number.

78

Minimum leading- and trailing-edge flap deflections
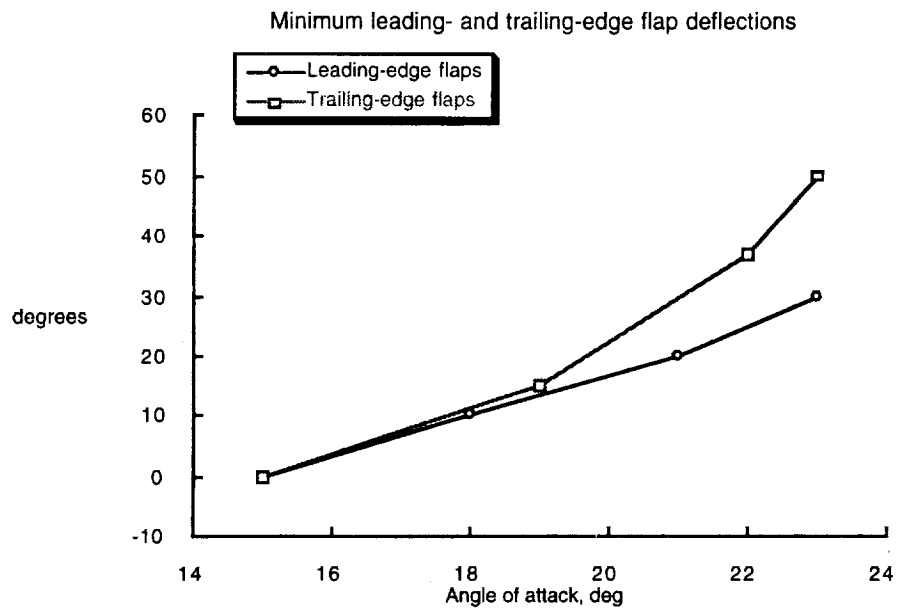
Figure B14. Minimum symmetric leading- and trailing-edge flap deflection as a function of angle of attack.

Trailing Edge Devices:

SW1 — True / False switch, Rate Limit (Δsw_{max}), 1, 10, *, ⊗

Table 1TE
Mach →
Weight →
Data
Interpolation

Table 2TE
α → min
Position Limit
→ Reference Flap Command (to mixer)

SW2 — True / False, Rate Limit (Δsw_{max}), 1, 30

DTE3, DTE6, DTE4, DTE5 (δf_{cmd}):
use inboard trailing edge schedules for Table 1TE

DTE1, DTE8, DTE2, DTE7 (δf_{cmd}):
use outboard trailing edge schedules for Table 1TE
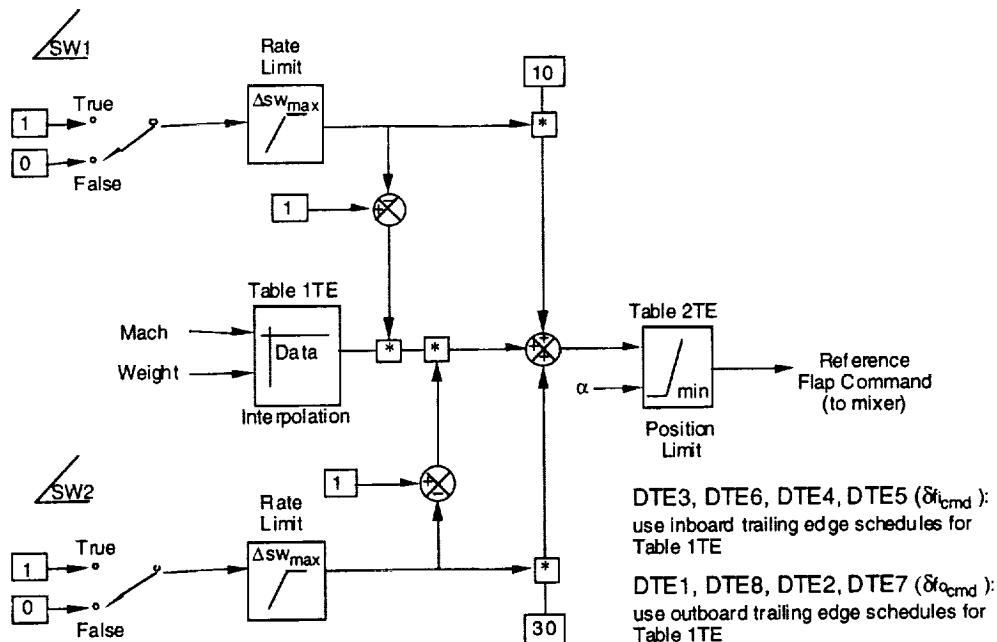
SW1: Iff h < 35 ft and Mode = Takeoff, then SW1 = True
SW2: Iff h < 394 ft and Mode = Landing, then SW2 = True

Pilot's Take-Off/ Go-Around (TOGA) Switch:
If TOGA switch has been depressed, then Mode = Takeoff;
Else Mode = Mode $_{(n-1)}$;
Nominally, mode is set at task initialization.

Leading Edge Devices:

SW1 — True / False switch, Rate Limit (Δsw_{max}), 1, 30, *, ⊗

Table 1LE
Mach →
Weight →
Data
Interpolation

Table 2LE
α → min
Position Limit
→ Leading Edge Device Command (to actuators)

SW2 — True / False, Rate Limit (Δsw_{max}), 1, 0

DLE1 and DLE4: use outboard leading edge schedules for Table 1LE

DLE2 and DLE3: use inboard leading edge schedules for Table 1LE
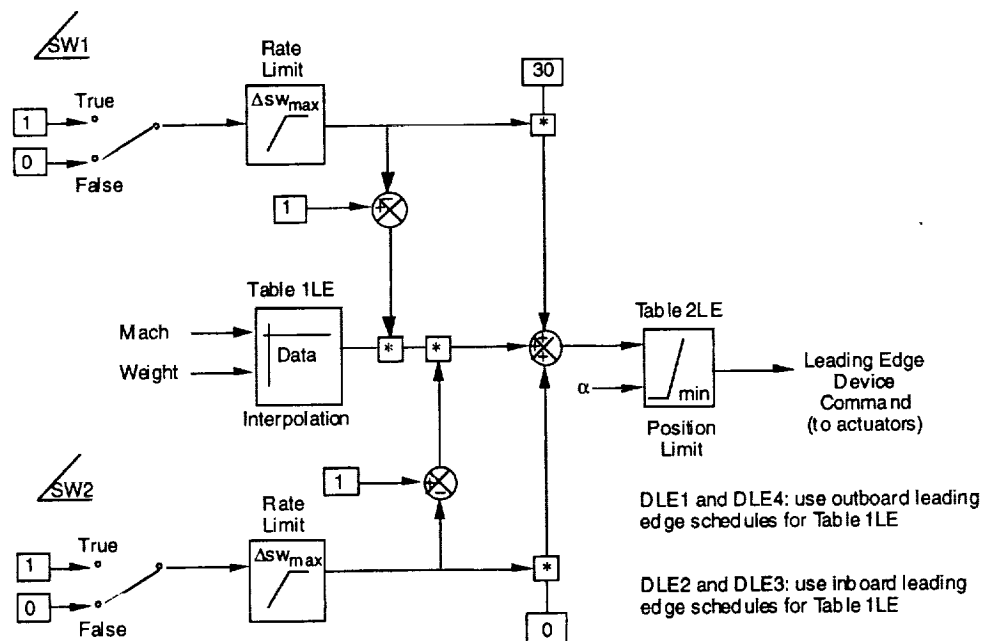
(Switching Logic is Identical to Trailing Edge Devices)

(Set Δsw_{max} = 0.3 /sec)

Figure B15. Automatic command generation system for leading- and trailing-edge flaps.

80
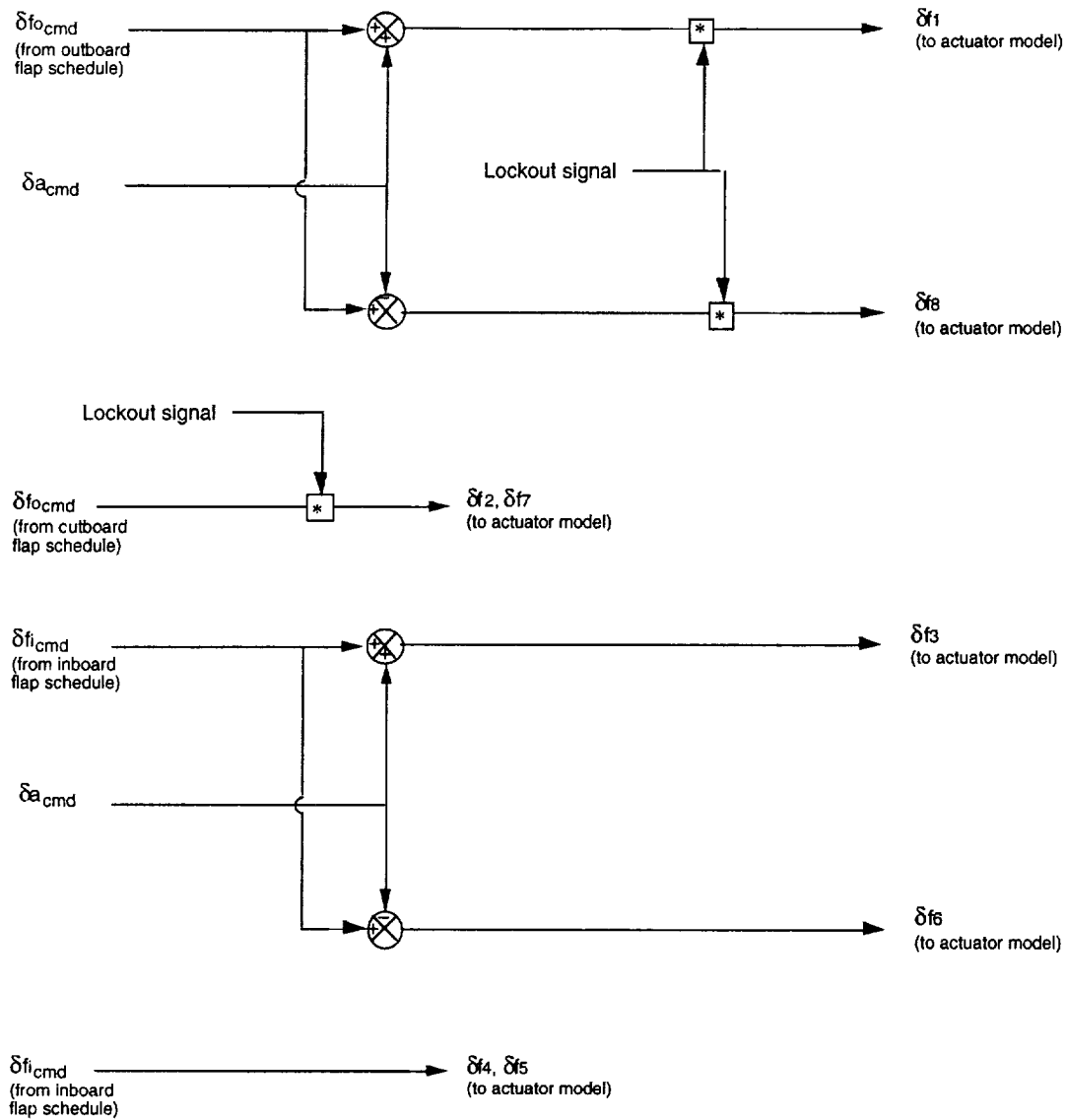
Figure B16. Diagram of Boeing control mixer used in piloted Ref.-H assessment.
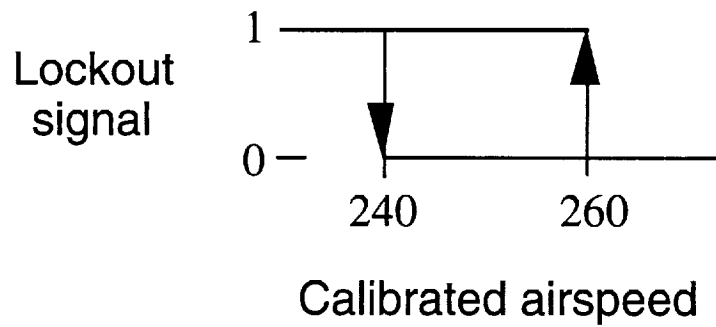
Figure B17. Diagram of lockout schedule for trailing edge flaps 1 and 8.

δr_c
(from
yaw
control)

δ R3
(to actuator model)

δ R2
(to actuator model)

*

δ R1
(to actuator model)
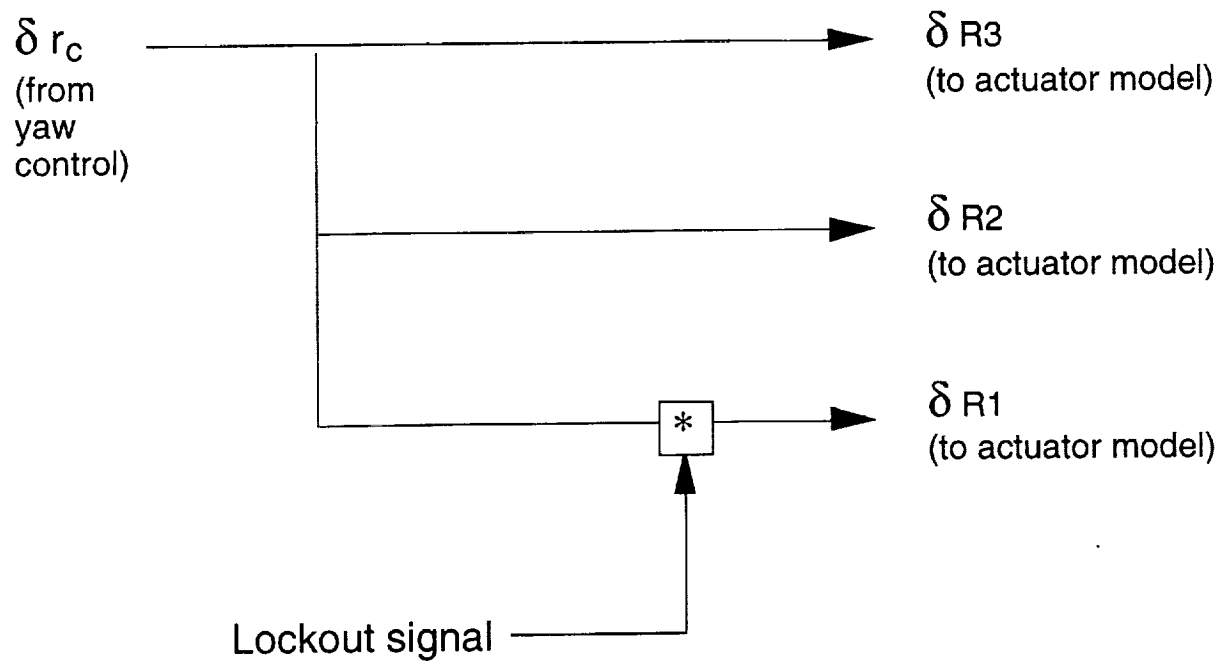
Lockout signal

Figure B18. Use of control lockout signal for uppermost rudder segment.

Appendix C: Block-1 maneuver set flight cards

Appendix C contains all of the Block-1 maneuver flight cards. They are included in this document to define the various tasks employed for this study by illustrating exactly what each research pilot was tasked to perform. Each flight card had an identification number located in the upper right hand corner. The identification number was used to rapidly reconfigure the simulation for the different tasks through the use of initial condition (I.C.) files. Pilot's tasks and rating criteria, aircraft configuration, control system options, and tasks initialization points were defined in each flight card. The test engineer, who served as the PNF, had copies of the flight cards included in this appendix. The research pilot was provided portions of the flight cards in the cockpit which highlighted the pilot's task and rating criteria and facilitated the maneuver rating process.

Symbol and Abbreviation list

A/P	Autopilot
A/T	Autothrottle
ALT	Initial altitude, ft.
BGV	Boeing $\dot{\gamma}/V$ longitudinal control system
C.G.	Center of gravity, percent cbar.
DME	Distance measuring equipment. Employed in this study to measure distance from brake release, nautical miles
DPB	Douglas p/β lateral/directional control system
EPR	Engine pressure ratio
F/D	Flight director
Grad1	Initial climb gradient for the PLR procedure, percent
Grad2	Secondary climb gradient for the PLR procedure, percent
G.W.	Gross weight, lbs
HUD	Heads up display
i_H	Initial horizontal tail deflection
LEF	Initial leading-edge flap deflection, positive down, degrees
M13	Mass case for maximum takeoff weight
MTE	Mission Task Element
PF	Pilot flying
PLR	Program Lapse Rate takeoff procedure
PNF	Pilot not flying
PSCAS	Pitch-axis stability and control system
R/C	Rate of climb
rot.	Rotation

RSCAS	Roll and yaw axis stability and control system
RWY	Runway
SDB	Structural Dynamics Branch developed landing gear cornering model
T0	Initial thrust level, percent net thrust
T1	First cutback thrust level for the PLR procedure, percent net thrust
T.O.	Takeoff
TEF	Initial trailing-edge flaps, positive down, degrees
V_1	Takeoff decision speed, kts.
V_2	One engine failed safety speed, kts.
V_2+10	Climb speed for non-PLR tasks.
V_{climb}	Climb speed for PLR task
VCUT	Speed at which first thrust cutback is performed for the PLR procedure
V_{ef}	Engine failure speed, kts.
V_{LO}	Estimated lift-off speed, kts.
V_{min}	Minimum speed to maintain a 3% climb gradient with one engine failed
V_r	Takeoff rotation speed, kts.

Flight Phase	MTE	Weather State	Failures	Loading
2A. Takeoff	5. Rejected Takeoff	0. None	0. None	3. M13

ALT Field	V_1	: 166	PSCAS BGV	ABNORMALS/EXCEPTIONS:
GW 649,914	V_r	: 174	RSCAS DPB	Select SDB cornering model
C.G. 48.1	V_{LO}	: 197	A/T OFF	
GEAR DOWN	V_2	: 209	HUD ON	
LEF/TEF 30/10	V_2+10	: 219	F/D OFF	
	V_{min}	: 181	A/P OFF	

Rwy Hdg	Wind Speed / Dir	Ceiling	Visibility	Rwy Surface	Initial Position
360	0 / 000	Unlimited	Unlimited, Daylight	Dry, Grooved	End of Rwy, On Centerline

Procedure–Evaluation Pilot (PF):

1.   Set brakes after going into operate mode.
2.   Advance throttles to takeoff EPR.
3.   Release the brakes and maintain centerline during ground roll. PNF will make airspeed call-outs, and monitors engine performance.
4.   When PNF calls "Abort," immediately retard throttles to idle and apply maximum braking. Maintain runway centerline.
5.   Terminate the maneuver when the aircraft is stopped.

Procedure–Test Engineer / Pilot Not Flying (PNF):

1.   Reset simulator to noted conditions.
2.   Make airspeed callout at 100 knots.
3.   Immediately before reaching V_1, call "Engine# Failed, Abort." .

Date: _____ Pilot: _____ Runs: _____

Evaluation Segment:	Runway Centerline Tracking	Long CHR	Lat / Dir CHR
Start Evaluation:	Stopped on Runway		
End Evaluation:	Stopped on Runway	N/A	

Evaluation Basis: The pilot is to evaluate the ease of tracking the runway centerline with rudder pedals alone as the aircraft accelerates and rudder pedals combined with differential braking as the aircraft decelerates during the takeoff roll.

Performance Standards	Target	Desired	Adequate
Runway Centerline Deviation (feet)	0	±10	±27

Flight Phase	MTE	Weather State	Failures	Loading
2A. Takeoff	5. Rejected Takeoff	0. 15 kts. cross-wind	0. None	3. M13

ALT Field	V_1	: 166	PSCAS BGV	ABNORMALS/EXCEPTIONS:
GW 649,914	V_r ·	: 174	RSCAS DPB	Select SDB cornering model
C.G. 48.1	V_{LO}	: 197	A/T OFF	
GEAR DOWN	V_2	: 209	HUD ON	
LEF/TEF 30/10	V_2+10	: 219	F/D OFF	
	Vmin	: 181	A/P OFF	

Rwy Hdg	Wind Speed / Dir	Ceiling	Visibility	Rwy Surface	Initial Position
360	0 / 000	Unlimited	Unlimited, Daylight	Dry, Grooved	End of Rwy, On Centerline

Procedure–Evaluation Pilot (PF):

1. Set brakes after going into operate mode.
2. Advance throttles to takeoff EPR.
3. Release the brakes and maintain centerline during ground roll. PNF will make airspeed call-outs, and monitors engine performance.
4. When PNF calls "Abort," immediately retard throttles to idle and apply maximum braking. Maintain runway centerline.
5. Terminate the maneuver when the aircraft is stopped.

Procedure–Test Engineer / Pilot Not Flying (PNF):

1. Reset simulator to noted conditions.
2. Make airspeed callout at 100 knots.
3. Immediately before reaching V_1, call "Engine# Failed, Abort." .

Date: _____ Pilot: _____ Runs: _____

Evaluation Segment:	Runway Centerline Tracking	Long CHR	Lat / Dir CHR
Start Evaluation: End Evaluation:	Stopped on Runway Stopped on Runway	N/A	

Evaluation Basis: The pilot is to evaluate the ease of tracking the runway centerline with rudder pedals alone as the aircraft accelerates and rudder pedals combined with differential braking as the aircraft decelerates during the takeoff roll.

Performance Standards	Target	Desired	Adequate
Runway Centerline Deviation (feet)	0	±10	±27

Flight Phase	MTE	Weather State	Failures	Loading
2A. Takeoff	5. Rejected Takeoff	0. 35 kts. cross-wind	0. None	3. M13

ALT Field	V_1	: 166	PSCAS BGV	ABNORMALS/EXCEPTIONS:
GW 649,914	V_r	: 174	RSCAS DPB	Select SDB cornering model
C.G. 48.1	V_{LO}	: 197	A/T OFF	
GEAR DOWN	V_2	: 209	HUD ON	
LEF/TEF 30/10	V_2+10	: 219	F/D OFF	
	Vmin	: 181	A/P OFF	

Rwy Hdg	Wind Speed / Dir	Ceiling	Visibility	Rwy Surface	Initial Position
360	0 / 000	Unlimited	Unlimited, Daylight	Dry, Grooved	End of Rwy, On Centerline

Procedure–Evaluation Pilot (PF):
1.   Set brakes after going into operate mode.
2.   Advance throttles to takeoff EPR.
3.   Release the brakes and maintain centerline during ground roll. PNF will make airspeed call-outs, and monitors engine performance.
4.   When **PNF** calls "**Abort**," immediately retard throttles to idle and apply maximum braking. Maintain runway centerline.
5.   Terminate the maneuver when the aircraft is stopped.

Procedure–Test Engineer / Pilot Not Flying (PNF):
1.   Reset simulator to noted conditions.
2.   Make airspeed callout at 100 knots.
3.   Immediately before reaching V_1, call "**Engine# Failed, Abort.**" .

Date: _____ Pilot: _____ Runs: _____

Evaluation Segment:	Runway Centerline Tracking	Long CHR	Lat / Dir CHR
Start Evaluation:	Stopped on Runway		
End Evaluation:	Stopped on Runway	N/A	

Evaluation Basis: The pilot is to evaluate the ease of tracking the runway centerline with rudder pedals alone as the aircraft accelerates and rudder pedals combined with differential braking as the aircraft decelerates during the takeoff roll.

Performance Standards	Target	Desired	Adequate
Runway Centerline Deviation (feet)	0	±10	±27

Flight Phase	MTE	Weather State	Failures	Loading
2A. Takeoff	100. Acoustic Profile Takeoff	1. Light Turbulence	0. None	3. M13

ALT Field	V_1 : 166	PSCAS BGV	ABNORMALS/EXCEPTIONS:
GW 649,914	V_r : 174	RSCAS DPB	NONE
C.G. 48.1	V_{LO} : 198	A/T OFF	Lift off pitch attitude=10.5 degs
GEAR DOWN	V_2 : 209	HUD ON	rot. pitch accel/decel=1.5/2.5 degs/sec sq
LEF/TEF 30/10	V_2+10 : 219	F/D ON	rot. steady state pitch rate=3.0 degs/sec
	V_{min} : 181	A/P OFF	Takeoff EPR: Max Cutback EPR: 52% Max

Rwy Hdg	Wind Speed / Dir	Ceiling	Visibility	Rwy Surface	Initial Position
360	0 / 000	Unlimited	Unlimited	Dry, Grooved	End of Rwy, On Centerline

Procedure–Evaluation Pilot (PF):

1.   Set brakes after going into operate mode.
2.   Advance throttles to takeoff EPR (100%).
3.   Release the brakes and maintain centerline during ground roll. PNF will make airspeed call-outs, and monitors engine performance.
4.   At rotation speed (Vr), initiate rotation to follow rotation rate pitch guidance indicators and maneuver the aircraft to intercept the lift-off rotation pitch attitude. After liftoff, resume pitch rotation to capture and follow velocity vector guidance symbol.
5.   At positive climb-rate, call "**gear-up**".
6.   When established at V2+10, PNF takes control of the throttles.
7.   Maintain target climb airspeed and runway heading throughout cutback maneuver.
8.   Terminate maneuver at 8.0 DME to record enough data for acoustic calculations.

Procedure–Test Engineer / Pilot Not Flying (PNF):

1.   Reset simulator to noted conditions.
2.   Make airspeed call-outs at 100 knots, V1, and Vr.
3.   Move gear handle to gear-up position, when requested by **PF**.
4.   Monitor gear retraction and automatic Vortex Fence extension and retraction.
5.   Make altitude call-outs at 500, and 600 feet. At 700 feet, call "**cutback**", and manually retard throttles to cutback EPR without causing excessive pitch-rate to maintain climb-speed (Vc) and exceed low-g limit (0.8) during pushover.
6.   Maintain cutback condition until 8.0 DME to gather sufficient information for acoustic calculations.

Notes on maneuver: This maneuver is to be performed with the leading- and trailing-edge flaps fixed to 30/10 degrees.

Date: _____ Pilot: _____ Runs: _____

Evaluation Segment:	Runway Centerline Tracking	Long CHR	Lat / Dir CHR
Start Evaluation:	Stopped on Runway	NA	
End Evaluation:	Liftoff		

Evaluation Basis: The pilot is to evaluate the ease of tracking the runway centerline with rudder pedals alone as the aircraft accelerates during the takeoff roll.

Performance Standards	Target	Desired	Adequate
Runway Centerline Deviation (feet)	0	±10	±27

Evaluation Segment:	Takeoff Rotation	Long CHR	Lat / Dir CHR
Start Evaluation:	V_1		
End Evaluation:	Liftoff		

Evaluation Basis: The pilot is to evaluate the promptness of the rotation, ease of tracking pitch rate guidance indicators, establishing lift-off pitch attitude, and ability to maintain runway centerline tracking during this maneuver sub-phase. Tail strike should not occur during this maneuver.

Performance Standards	Target	Desired	Adequate
Liftoff Pitch Rate Control (deg)	generated	<±.5 bracket 90% of time	<±1 bracket 90% of time
Climb Pitch Attitude Control (deg)	10.5	±.5	±1
Runway Centerline Deviation (feet)	0	±10	±27

Evaluation Segment:	Climb with Configuration Changes	Long CHR	Lat / Dir CHR
Start Evaluation:	Liftoff		
End Evaluation:	8.0 DME from brake release		

Evaluation Basis: The pilot is to check the handling qualities in climb during reconfiguration for noise abatement while following the velocity vector guidance symbol. Check for objectionable transients in airplane response during thrust changes encountered during manual thrust cutback. Monitor airspeed control during climbout. Climb speed, Vc, is 219 kts.

Performance Standards	Target	Desired	Adequate
Longitudinal velocity vector control (deg)	generated	<±1 V-vector height 90% of time	<±2 V-vector height 90% of time
Lateral velocity vector control (deg)	generated	<±1 V-vector width 90% of time	<±2 V-vector width 90% of time

Flight Phase	MTE	Weather State	Failures	Loading
2A. Takeoff	102. PLR Takeoff	1. Light turbulence	0. None	3. M13

ALT 0	V_1	166	PSCAS :BGV	ABNORMALS/EXCEPTIONS:
GW 649,914	V_r	174	RSCAS :DPB	Takeoff EPR (T0) : Max
C.G. 48.1	V_{LO}	197	A/T :ON	First cutback speed (VCUT1) : 187
GEAR DOWN	V_2	209	HUD :ON	Delta time first cutback : 7 seconds
LEF/TEF 30/10- auto	V_{climb}	250	F/D :TO mode	First cutback thrust level (T1) : 75%
	V_{min}	181	A/P :OFF	rot. pitch acc/decc=1.5/2.5 degs/sec-sq
			grad1/2 :4%/4%	rot. steady state pitch rate=3.0 degs/sec

Rwy Hdg	Wind	Ceiling	Visibility	Rwy Surface	Initial Position
360	0/000	Unlimited	Unlimited	Dry, Grooved	End of RWY, On Centerline

Procedure–Evaluation Pilot (PF):
1. Engage autothrottle, verify initial and secondary climb gradients (grad1, grad2), and confirm proper EPR (as set by the autothrottle system) and flap position (as set by the autoflap system).
2. Release the brakes and maintain centerline during ground roll.
3. At rotation speed (Vr), initiate rotation to follow rotation rate pitch guidance indicators and maneuver the aircraft to intercept the lift-off rotation pitch attitude. After liftoff, resume pitch rotation to capture and follow velocity vector guidance symbol.
4. At positive climb-rate, call **"gear-up"**.
5. Maneuver the aircraft to follow velocity vector guidance to maintain the extended runway centerline and desired climb gradient.
6. At approximately 3.0 DME and 250 kts, intercept and maintain secondary target climb gradient (if different than the initial climb gradient).

Procedure–Test Engineer / Pilot Not Flying (PNF):
1. Reset simulator to noted conditions.
2. Make airspeed call-outs at 100 knots, V1, and Vr.
3. Raise landing gear upon PF call.
4. Monitor progress of first automatic thrust reduction to first cutback thrust level (T1).
5. Once first thrust reduction is complete call out **"T1 thrust"**.
6. At approximately 3.0 DME and 250 knots, monitor the autothrottle system transition to airspeed hold mode as it completes the second thrust cutback.
7. Continue the maneuver to at least 8.0 DME to record sufficient data for acoustic calculations.

Evaluation Segment:	Runway Centerline Tracking	Long CHR	Lat / Dir CHR
Start Evaluation:	Stopped on Runway	N/A	
End Evaluation:	Liftoff		

Evaluation Basis: The pilot is to evaluate the ease of tracking the runway centerline with rudder pedals alone as the aircraft accelerates during the takeoff roll.

Performance Standards	Target	Desired	Adequate
Deviation from Runway Centerline (ft)	0	±10	±27

Evaluation Segment:	Takeoff Rotation	Long CHR	Lat / Dir CHR
Start Evaluation:	V_1		
End Evaluation:	Liftoff		

Evaluation Basis: The pilot is to evaluate the promptness of the rotation, ease of establishing the lift-off pitch attitude, and ability to maintain runway centerline tracking during this maneuver sub-phase. Tail strike should not occur during this maneuver.

Performance Standards	Target	Desired	Adequate
Lift-Off Pitch Rate Control (deg)	generated	<±.5 bracket 90% of time	<±1 bracket 90% of time
Climb Pitch Attitude Control (deg)	10.5	±.5	±1
Runway Centerline Deviation (feet)	0	±10	±27

Evaluation Segment:	Climb with Auto Configuration Changes	Long CHR	Lat / Dir CHR
Start Evaluation:	Liftoff		
End Evaluation:	8.0 DME		

Evaluation Basis: The pilot is to check the handling qualities in climb during the highly automated noise abatement procedure. Check for objectionable transients in airplane response during airspeed change, automatic thrust and flap reconfiguration. Evaluate ease of following velocity vector guidance to maintain desired climb gradient and ground track. Comment on possible safety of flight issues regarding this type of procedure.

Performance Standards	Target	Desired	Adequate
Longitudinal velocity vector control (deg)	Grad1 or Grad2	<±1 V-vector height 90% of time	<±2 V-vector height 90% of time
Lateral velocity vector control (deg)	generated	<±1 V-vector width 90% of time	<±2 V-vector width 90% of time

Flight Phase	MTE	Weather State	Failures	Loading
13A. TCA Descent	400. Stall - Idle Power	1. Light Turbulence	0. None	7. MFC- Final Cruise, Aft C.G.

ALT :10,000 GW :384,862 C.G. .53.2 GEAR :UP TEF/LEF :Auto i_H :Trim	KCAS 250 EPR Idle R/C Trim	PSCAS :BGV RSCAS :DPB A/T :OFF HUD :ON F/D :OFF A/P :OFF	ABNORMALS/EXCEPTIONS: NONE

Rwy Hdg	Wind Speed / Dir	Ceiling	Visibility	Rwy Surface	Initial Position
360	/	Unlimited	Unlimited	N/A	N/A

Procedure–Evaluation Pilot (PF):
1.   Establish straight descending flight at 250 knots on a cardinal heading with idle thrust.
2.   Using flight path gradient, establish and maintain a smooth deceleration of approximately 3 knots per second.
3.   Decelerate to a speed which produces approximately 21 degrees angle of attack (app. 110 knots).
4.   Apply forward column until positive recovery is assured.
5.   Terminate maneuver when recovery is assured (i.e. wings level with aoa less than 13 degrees and decreasing). NO THROTTLE ADJUSTMENTS ARE ALLOWED.

Procedure–Test Engineer / Pilot Not Flying (PNF):
1.   Reset simulator to noted conditions.
2.   Monitor deceleration and call out deviations from the target rate. Verify flaps are automatically extending on schedule.
3.   Call out "**Recover**" when angle of attack reaches 21 degrees (app. 110 knots).
4.   Verify flaps retract during recovery.
5.   Terminate maneuver when recovery is assured (i.e. wings level with aoa less than 13 degrees and decreasing).

Date: _____ Pilot: _____ Runs: _____

Evaluation Segment:	Stall–Idle Power	Long CHR	Lat / Dir CHR
Start Evaluation: End Evaluation:	Wings level Wings level at recovered angle of attack condition (i.e. aoa less than 13 degrees and decreasing)	·	

Evaluation Basis: Maneuver possible without exceptional piloting strength or skill. No control reversals or PIO.

Performance Standards	Target	Desired	Adequate
Maximum bank angle (deg)	0	±5	±10

Flight Phase	MTE	Weather State	Failures	Loading
3B. TCA Climb	400. Stall - Max Takeoff Power	1. Light Turbulence	0. None	3. M13-MTOW, Fwd C.G.

ALT 5,000 GW 649,914 C.G. 48.1 GEAR UP TEF/LEF Auto i_H Trim	KCAS 186 EPR TOGA R/C Trim	PSCAS BGV RSCAS DPB A/T OFF HUD ON F/D OFF A/P OFF	ABNORMALS/EXCEPTIONS: NONE

Rwy Hdg	Wind Speed / Dir	Ceiling	Visibility	Rwy Surface	Initial Position
360	0 / 000	Unlimited	Unlimited	N/A	N/A

Procedure–Evaluation Pilot (PF):
1.   Establish straight climbing flight at 186 knots on a cardinal heading with maximum takeoff thrust.
2.   Using flight path gradient, establish and maintain a smooth deceleration of approximately 3 knots per second.
3.   Decelerate to a speed which produces approximately 21 degrees angle of attack (app. 156 knots).
4.   Apply forward column until positive recovery is assured.
5.   Terminate maneuver when recovery is assured (i.e. wings level with aoa less than 13 degrees and decreasing)..

Procedure–Test Engineer / Pilot Not Flying (PNF):
1.   Reset simulator to noted conditions.
2.   Monitor deceleration and call out deviations from the target rate. Verify flaps are automatically extending on schedule.
3   Call out "**Recover**" when angle of attack reaches 21 degrees (app. 156 knots).
4.   Verify flaps retract during recovery.
5.   Terminate maneuver when recovery is assured (i.e. wings level with aoa less than 13 degrees and decreasing).

Date: _____ Pilot: _____ Runs: _____

Evaluation Segment:	Stall–Max Takeoff Power	Long CHR	Lat / Dir CHR
Start Evaluation: End Evaluation:	Wings Level Wings level at recovered angle of attack condition (i.e. aoa less than 13 degrees and decreasing)		

Evaluation Basis: Maneuver possible without exceptional piloting strength or skill. No control reversals or PIO.

Performance Standards	Target	Desired	Adequate
Maximum bank angle (deg)	0	±5	±10

Flight Phase	MTE	Weather State	Failures	Loading
13A.　TCA Descent	403.　Turning Stall - Idle Power	1.　Light Turbulence	0.　None	7.　MCF- Final Cruise, Aft C.G.

ALT :10,000 GW :384,862 C.G. :53.2 GEAR :UP TEF/LEF :Auto i$_H$:Trim	KCAS　250 EPR　Idle R/C　Trim	PSCAS :BGV RSCAS :DPB A/T :OFF HUD :ON F/D :OFF A/P :OFF	ABNORMALS/EXCEPTIONS: NONE

Rwy Hdg	Wind Speed / Dir	Ceiling	Visibility	Rwy Surface	Initial Position
360	0 / 000	Unlimited	Unlimited	N/A	N/A

Procedure–Evaluation Pilot (PF):

1. Establish a 30 degree banked turn with idle thrust.
2. Using flight path gradient, establish and maintain a smooth deceleration of approximately 3 knots per second.
3. Decelerate to a speed which produces approximately 21 degrees angle of attack (app. 113 knots) before initiating recovery.
4. Apply forward column and roll wings level until positive recovery is assured.
5. Terminate maneuver when recovery is assured (i.e. aoa less than 13 degrees and decreasing). NO THROTTLE ADJUSTMENTS ARE ALLOWED.

Procedure–Test Engineer / Pilot Not Flying (PNF):

1. Reset simulator to noted conditions.
2. Monitor deceleration and call out deviations from the target rate. Verify flaps are automatically extending on schedule.
3. Call out "Recover" when angle of attack reaches 21 degrees (app. 113 knots).
4. Verify flaps retract during recovery.
5. Terminate maneuver when recovery is assured (i.e. wings level with aoa less than 13 degrees and decreasing). NO THROTTLE ADJUSTMENTS ARE ALLOWED.

Date: _____ Pilot: _____ Runs: _____

Evaluation Segment:	Turning Stall–Idle Power	Long CHR	Lat / Dir CHR
Start Evaluation: End Evaluation:	30 degree banked turn, idle thrust Wings level at recovered angle of attack condition (i.e. AOA less than 13 degrees and decreasing).		

Evaluation Basis: Maneuver possible without exceptional piloting strength or skill. No control reversals or PIO.

Performance Standards	Target	Desired	Adequate
Wings level bank angle (deg)	0	+/-5	+/-10

Flight Phase	MTE	Weather State	Failures	Loading
13A. TCA Descent	404. Turning Stall - TFLF	1. Light Turbulence	0. None	7. MCF- Final Cruise, Aft C.G.

ALT :10,000 GW :384,862 C.G. :53.2 GEAR :UP TEF/LEF :Auto i$_H$:Trim	KCAS 250 EPR Idle R/C Trim	PSCAS :BGV RSCAS :DPB A/T :OFF HUD :ON F/D :OFF A/P :OFF	ABNORMALS/EXCEPTIONS: NONE

Rwy Hdg	Wind Speed / Dir	Ceiling	Visibility	Rwy Surface	Initial Position
360	0 / 000	Unlimited	Unlimited	N/A	N/A

Procedure–Evaluation Pilot (PF):

1.   Establish straight and level flight at the noted conditions.
2.   Establish a 30 degree banked turn without adjusting the throttles.
3.   Using flight path gradient, establish and maintain a smooth deceleration of approximately 3 knots per second.
4.   Decelerate to a speed which produces approximately 21 degrees angle of attack (app. 113 knots) before initiating recovery.
5.   Apply forward column and roll wings level until positive recovery is assured.
6.   Terminate maneuver when recovery is assured (i.e. aoa less than 13 degrees and decreasing). NO THROTTLE ADJUSTMENTS ARE ALLOWED.

Procedure–Test Engineer / Pilot Not Flying (PNF):

1.   Reset simulator to noted conditions.
2.   Monitor deceleration and call out deviations from the target rate. Verify flaps are automatically extending on schedule.
3.   Call out "**Recover**" when angle of attack reaches 21 degrees (app. 113 knots).
4.   Verify flaps retract during recovery.
5.   Terminate maneuver when recovery is assured (i.e. wings level with aoa less than 13 degrees and decreasing). NO THROTTLE ADJUSTMENTS ARE ALLOWED.

Date: _____ Pilot: _____ Runs: _____

Evaluation Segment:	Turning Stall–Thrust for Level Flight	Long CHR	Lat / Dir CHR
Start Evaluation: End Evaluation:	30 degree banked turn, thrust for level flight. Wings level at recovered angle of attack condition (i.e. AOA less than 13 degrees and decreasing).		

Evaluation Basis: Maneuver possible without exceptional piloting strength or skill. No control reversals or PIO.

Performance Standards	Target	Desired	Adequate
Wing level bank angle (deg)	0	+/-5	+/-10

Flight Phase	MTE	Weather State	Failures	Loading
2A. Takeoff	100. OEO continued Takeoff	1. Light Turbulence	0. None	3. M13

ALT Field	V_1 : 166	PSCAS BGV	ABNORMALS/EXCEPTIONS:	
GW 649,914	V_r : 174	RSCAS DPB	NONE	
C.G. 48.1	V_{LO} : 192	A/T OFF	Lift off pitch attitude=10.5 degs	
GEAR DOWN	V_2 : 209	HUD ON	rot. pitch accel/decel=1.5/2.5 degs/sec sq	
LEF/TEF 30/10	V_2+10 : 219	F/D OFF	rot. steady state pitch rate=3.0 degs/sec	
	V_{min} : 181	A/P OFF	Takeoff EPR: Max	

Rwy Hdg	Wind Speed / Dir	Ceiling	Visibility	Rwy Surface	Initial Position
360	0 / 000	Unlimited	Unlimited	Dry, Grooved	End of Rwy, On Centerline

Procedure–Evaluation Pilot (PF):
1. Set brakes after going into operate mode.
2. Advance throttles to takeoff EPR (100%).
3. Release the brakes and maintain centerline during ground roll. PNF will make airspeed call-outs, and monitors engine performance.
4. At V1 continue takeoff and accelerate aircraft to Vr.
5. At rotation speed (Vr), initiate rotation to follow rotation rate pitch guidance indicators and maneuver the aircraft to intercept the lift-off rotation pitch attitude. After liftoff, resume pitch rotation to capture and follow velocity vector guidance symbol.
6. At positive climb-rate, call "**gear-up**".
7. Terminate maneuver at 6.0 DME. Data is not needed for acoustic calculations.

Procedure–Test Engineer / Pilot Not Flying (PNF):
1. Reset simulator to noted conditions.
2. Make airspeed call-outs at 100 knots, and V1.
3. When engine failure is observed, call out "**engine # failed, continue takeoff**".
4. Make airspeed call-out at Vr.
5. Move gear handle to gear-up position, when requested by PF.
6. Monitor gear retraction and automatic Vortex Fence extension and retraction.
7. Terminate maneuver at 6.0 DME. Data is not needed for acoustic calculations.

Notes on maneuver: This maneuver is to be performed with the leading- and trailing-edge flaps fixed to 30/10 degrees.

Evaluation Segment:	Runway Centerline Tracking	Long CHR	Lat / Dir CHR
Start Evaluation:	Stopped on Runway	NA	
End Evaluation:	Liftoff		

Evaluation Basis: The pilot is to evaluate the ease of tracking the runway centerline with rudder pedals alone as the aircraft accelerates during the takeoff roll.

Performance Standards	Target	Desired	Adequate
Runway Centerline Deviation (feet)	0	±10	±27

Evaluation Segment:	Takeoff Rotation	Long CHR	Lat / Dir CHR
Start Evaluation:	V_1		
End Evaluation:	Liftoff		

Evaluation Basis: The pilot is to evaluate the promptness of the rotation, ease of tracking pitch rate guidance indicators, establishing lift-off pitch attitude, and ability to maintain runway centerline tracking during this maneuver sub-phase. Tail strike should not occur during this maneuver.

Performance Standards	Target	Desired	Adequate
Liftoff Pitch Rate Control (deg)	generated	<±.5 bracket 90% of time	<±1 bracket 90% of time
Climb Pitch Attitude Control (deg)	10.5	±.5	±1
Runway Centerline Deviation (feet)	0	±10	±27

Evaluation Segment:	Climb with Configuration Changes	Long CHR	Lat / Dir CHR
Start Evaluation:	Liftoff		
End Evaluation:	6.0 DME from brake release		

Evaluation Basis: The pilot is to check the handling qualities in climb while following the velocity vector guidance symbol. Check for objectionable transients in airplane response during maneuver. Monitor airspeed control during climbout. Climb speed, Vc, is 219 kts.

Performance Standards	Target	Desired	Adequate
Longitudinal velocity vector control (deg)	generated	<±1 V-vector height 90% of time	<±2 V-vector height 90% of time
Lateral velocity vector control (deg)	generated	<±1 V-vector width 90% of time	<±2 V-vector width 90% of time

Flight Phase	MTE	Weather State	Failures	Loading
2A. Takeoff	602. VMCG	1. None	60. Single Engine Failed	7. MCF- Final Cruise, Aft C.G.

ALT Field	SPEED	Static	PSCAS BGV	ABNORMALS/EXCEPTIONS:
GW 384,862	EPR	Max	RSCAS DPB	NONE
C.G. 53.2	R/C	0 :	A/T OFF	
GEAR DOWN	Vef	127 kts	HUD ON	No nosewheel cornering force above 80 knots.
TEF/LEF 30/10			F/D OFF	Fail #4 engine at 127 kts.
iH 0			A/P OFF	

Rwy Hdg	Wind Speed / Dir	Ceiling	Visibility	Rwy Surface	Initial Position
360	0 / 000	Unlimited	Unlimited	N/A	End of runway, on centerline

Sim Note: Position freeze may be used up to TBD knots to prevent runway overrun.

Procedure–Evaluation Pilot (PF):
1.   Set brakes.
2.   Advance throttles to takeoff EPR.
3.   Release the brakes and maintain centerline during ground roll. PNF will make airspeed call-outs, and monitors engine performance.
4.   When engine fails, maintain runway centerline with rudder control only, minimizing deviation.
5.   Terminate maneuver after recovery from maximum centerline deviation has been accomplished.

Procedure–Test Engineer / Pilot Not Flying (PNF):
1.   Reset simulator to noted conditions.
2.   Remove nose gear cornering forces at approximately 80 kts.
3.   At VMCG (127 knots), fail an outboard engine and call out "**Engine X Failed**".
4.   Note maximum centerline deviation.

Date: _____ Pilot: _____ Runs: _____

Evaluation Segment:	Minimum Control Speed - Ground	Long CHR	Lat / Dir CHR
Start Evaluation:	At Vmcg on runway centerline		
End Evaluation:	After recovery from maximum deviation from runway centerline has been accomplished.		
Evaluation Basis: Evaluate maximum runway centerline deviation.			

Performance Standards	Target	Desired	Adequate
Maximum runway centerline deviation (ft)	<30	<30	<30

Appendix D: Pilot Biographies

Pilot A had a Bachelor of Science from the University of Washington where he attended a flight test course. Pilot A served as Engineering Test Pilot for two General Aviation manufacturers and accumulated time as a test pilot on 30 different general aviation fixed wing aircraft, before joining an HSR program industry partner as a research project pilot. He is a graduate of a company-run flight test school. Pilot A holds an Airline Transport Pilot Certificate with type ratings in 7 transport aircraft, and has over 16,000 hours flight time, of which nearly 10,000 hours have been in flight tests. Pilot A is a certificated flight instructor in both GA and transport aircraft with 3000 hours of instruction given.

Pilot B was trained as a Naval Aviator and graduated from the U.S. Naval Test Pilot School, Patuxent River, Maryland. Pilot B has a Ph.D. in Hypersonic Flight Dynamics from the University of Southern California. He is employed by an HSR program industry partner as the chief pilot for the High Speed Civil Transport and as a project experimental test pilot in a number of aircraft programs. He holds an Airline Transport Pilot Certificate, and has First Pilot time in over 50 aircraft, including the Grumman F-14A and several transport aircraft.

Pilot C is a graduate of the Air Force Test Pilot School and holds a Masters of Science from the Air Force Institute of Technology. Pilot C was a combat fighter pilot for the United States Air Force with 2000 hours combat experience in A-10, F-4, F-5, and F-100 aircraft. He is employed by Calspan corporation and has extensive experience in variable stability aircraft and in in-flight simulation studies involving a wide variety of simulated aircraft, including fighters, bombers, and transport designs. He has over 1000 hours of flight time given demonstration to military test pilot students in the Variable Stability Learjet owned and operated by Calspan.

Pilot D served with the United States Marine Corps from 1953 to 1962 as a single engine Fighter-Bomber pilot. He has been a research pilot with NASA since 1962 and has accumulated more than 10,000 total hours in a wide variety of aircraft including helicopter, VTOL, STOL, and light and heavy fixed wing aircraft. He has an Airline Transport Pilot Certificate with type ratings in the Convair 990 and the Douglas DC-8.

Pilot E was trained as a Naval Aviator and flew Vought F-8s in both active and reserve duty. Pilot E flew with a major airline for four years in Boeing 727 aircraft before joining NASA as an Instructor Pilot in the Shuttle Training Aircraft before becoming a Research Pilot at a NASA Research Center. As a NASA pilot, Pilot E has flown a number of research aircraft in addition to research simulations of other vehicles. Pilot E holds a Bachelor of Science from the University of North Carolina at Chapel Hill and a Masters degree in Aerospace Engineering from the University of Virginia. Pilot E has accumulated over 10,000 flying hours in over 45 different aircraft including F-8, F-18, F-16, F-15, F-5, A-4, B-727, B-737, Gulfstream II/STA, T-38, OV-10, and LR-28 aircraft and a number of general aviation types.

REPORT DOCUMENTATION PAGE

1. AGENCY USE ONLY (Leave blank)	2. REPORT DATE	3. REPORT TYPE AND DATES COVERED
	December 1999	Contractor Report

4. TITLE AND SUBTITLE
Initial Piloted Simulation Evaluation of the Reference-H High-Speed Civil Transport Design During Takeoff and Recovery From Limit Flight Conditions

5. FUNDING NUMBERS
C NAS1-19000
WU 573-07-24
WBS 4.3.5

6. AUTHOR(S)
Louis J. Glaab

7. PERFORMING ORGANIZATION NAME(S) AND ADDRESS(ES)
Lockheed Martin Engineering & Sciences Company
Hampton, Va 23681

8. PERFORMING ORGANIZATION REPORT NUMBER

9. SPONSORING/MONITORING AGENCY NAME(S) AND ADDRESS(ES)
National Aeronautics and Space Administration
Langley Research Center
Hampton, VA 23681-2199

10. SPONSORING/MONITORING AGENCY REPORT NUMBER
NASA/CR-1999-209523

11. SUPPLEMENTARY NOTES
Langley Technical Monitor: Carey S. Buttrill

12a. DISTRIBUTION/AVAILABILITY STATEMENT
Unclassified–Unlimited
Subject Category 08   Distribution: Nonstandard
Availability: NASA CASI (301) 621-0390

12b. DISTRIBUTION CODE

13. ABSTRACT (Maximum 200 words)

An initial assessment of a proposed High-Speed Civil Transport (HSCT) was conducted in the fall of 1995 at the NASA Langley Research Center. This configuration, known as the Industry Reference-H (Ref.-H), was designed by the Boeing Aircraft Company as part of their work in the High Speed Research program. It included a conventional tail, a cranked-arrow wing, four mixed-flow turbofan engines, and capacity for transporting approximately 300 passengers. The purpose of this assessment was to evaluate and quantify operational aspects of the Reference-H configuration from a pilot's perspective with the additional goal of identifying design strengths as well as any potential configuration deficiencies. This study was aimed at evaluating the Ref.-H configuration at many points of the aircraft's envelope to determine the suitability of the vehicle to accomplish typical mission profiles as well as emergency or envelope-limit conditions. Pilot-provided Cooper-Harper ratings and comments constituted the primary vehicle evaluation metric. The analysis included simulated real-time piloted evaluations, performed in a 6 degree of freedom motion base NASA Langley Visual-Motion Simulator, combined with extensive bath analysis. The assessment was performed using the third major release of the simulation data base (known as Ref.-H cycle 2B).

14. SUBJECT TERMS	15. NUMBER OF PAGES
High Speed Research; High Speed Civil Transport; Reference H	113
	16. PRICE CODE A06

17. SECURITY CLASSIFICATION OF REPORT	18. SECURITY CLASSIFICATION OF THIS PAGE	19. SECURITY CLASSIFICATION OF ABSTRACT	20. LIMITATION OF ABSTRACT
Unclassified	Unclassified	Unclassified	UL